PROJECT ADMINISTRATION DATA SHEET

1 Cost of 4 pgs

GEORGIA INSTITUTE OF TECHNOLOGY
OFFICE OF RESEARCH ADMINISTRATION

RESEARCH PROJECT INITIATION

Date: January 13, 1975

Project Title: Deformation Mechanisms in Beta Titanium Alloys

Project No: E-19-632

Principal Investigator Dr. E. A. Starke

Sponsor: Office of Naval Research; Arlington, Va. 22217

Agreement Period: From 7/1/74 Until ~~6/31/75~~ 3/31/82

Type Agreement: Contract N00014-75-C-0349

Amount: $38,000.00

Reports Required: Progress Reports at least annually; Final Technical Report

Sponsor Contact Person (s):

Technical Matters
(Scientific Officer)
Director - Metallurgy Programs
Material Sciences Div.
Office of Naval Research
Department of the Navy
800 North Quincy Street
Arlington, Va. 22217

Contractual Matters
(thru ORA)
Mr. R. J. Whitcomb (ACO)
ONR Resident Representative
Campus

Assigned to: Chemical Engineering

COPIES TO:

- Principal Investigator
- School Director
- Dean of the College
- Director, Research Administration
- Director, Financial Affairs (2)
- Security-Reports-Property Office ✓
- Patent Coordinator
- Library
- Rich Electronic Computer Center
- Photographic Laboratory
- Project File
- Other

RA-3 (6-71)

EORGIA INSTITUTE OF TECHNOLOGY OFFICE OF CONTRACT ADMINISTRATION

SPONSORED PROJECT TERMINATION/CLOSEOUT SHEET

Date November 29, 1983

oject No. E-19-632 School/~~KXX~~ ChE

cludes Subproject No.(s)

oject Director(s) Dr. S.B. Chakrabortty ~~XXXXX~~ / GIT

ponsor Office of Naval Research

tle "Deformation Mechanisms in Beta Titanium Alloys"

fective Completion Date: 3/31/82 (Performance) 5/31/82 (Reports)

rant/Contract Closeout Actions Remaining:

- [ ] None
- [ ] Final Invoice or Final Fiscal Report
- [X] Closing Documents
- [X] Final Report of Inventions
- [X] Govt. Property Inventory & Related Certificate
- [ ] Classified Material Certificate
- [ ] Other

ntinues Project No. Continued by Project No.

OPIES TO:

oject Director
esearch Administrative Network
esearch Property Management
ccounting
ocurement/EES Supply Services
esearch Security Services
eports Coordinator (OCA)
gal Services
Library
GTRI
Research Communications (2)
Project File
Other

OCA 60-1028

E-14 998 filed in PSR-posted SKB

Status Report

Deformation Mechanisms in Beta Titanium Alloys
ONR Task Order No. N00014-75-C-0349

November 1, 1976

Introduction

The general goal of this research is to obtain an understanding of the influence of microstructural features on the monotonic and cyclic deformation behavior of titanium alloys. Traditional methods of analysis, (S-N data, crack growth studies) have failed to establish guidelines for improving fatigue properties by alloy design. The experimental part of this program is designed to provide quantitative property-microstructure relationships by correlating both cyclic stress-strain response (CSSR) and crack propagation data with microstructure and deformation mode. Previous work on this contract has shown that the deformation mode (planar slip, multiple slip, coarse twinning, and fine twinning) and ductility of Ti-V alloys can be controlled to a large extent by controlling the solute content and volume fraction of omega. Consequently, the system is a unique one for studies directed at establishing the effect of microstructure and deformation mode on the fatigue performance of titanium alloys.

Current Progress

Monotonic Tension Tests: In order to select the strain amplitude range for the low-cycle fatigue tests, tensile test data were obtained on the commerically prepared Ti-24% V, 28% V, and 36% V alloys. As expected, deformation twins with audible clicks were only observed for the 24% V alloy. The twins were observed as large bands on the surface and as small micro-twins by transmission microscopy. Scanning micrographs of the deformed 36% V alloy showed uniformly spaced deformation bands and planar slip. Significant grain rotation, consistent with restricted slip, was observed. Herringbone-type slip steps, indicative of multiple slip, were present only in the necked region, and a very small strain hardening exponent, n, consistent with these observations, was observed, Figure 1. The 24% V alloy, which deformes by coarse twinning and slip, had a higher n value, and a surprisingly larger reduction in area prior to failure, when compared to the 36% V alloy. All fractures were ductile and due to microvoid coalescence.

Low Cycle Fatigue Tests: Strain-controlled low cycle fatigue tests are being used to measure the cyclic stress strain response of the various Ti-V alloys heat treated to produce various microstructures having different deformation modes. Since the fatigue performance of materials is very sensitive to the reversibility of the deformation mode, the Bauschinger effect is being quantitatively measured in the LCF tests. This is accomplished by measuring the parameters β^1 and $\Delta\sigma_b$, defined in Figure 2. Figure 3 shows the first have cycle of the cyclic stress-strain curves of the as-quenched Ti-24% V alloy, which have a significant Bauschinger effect due to untwinning

in the reverse quarter cycle. The corresponding $2\beta^1/\varepsilon p$ and Δc values are plotted versus the tensile plastic strain in Figure 4. Both these values increase with decreasing ε_p, suggesting that the hardening mechanisms under tension result in residual stresses which resist "untwinning" strains.

Figure 5 shows examples of stress amplitude-cycles curves for the as-quenched alloys. The 36% V alloy cyclic softens at small strain amplitudes. All other alloys cyclic harden. The extent of this behavior is clearly demonstrated by the cyclic stress-strain curves of Figure 6. The softening of the 36% V alloy at low strain amplitudes can be explained by the fact that the stress necessary to activate dislocation sources and generate slip dislocations is larger than the stress necessary to move them. However, as the strain amplitude is increased, the effect disappears due to the increased probability of slip dislocation — forrest dislocation interaction. The softening observed in the first few cycles of the very low strain amplitude tests of the 24% V alloy was probably due to the reduced reversed stress required for untwinning. However, matrix dislocation interactions become more important with accumulated strain, and hardening predominates. Hardening is maximum for the 24% V alloy because the twin interfaces and omega precipitates act as barriers to deformation and increase the denisty of geometrically necessary dislocations. The 28% V alloy contains some twins but almost no omega, and the 36% V alloys, which shows the minimum hardening, deforms by planar slip and contains no omega.

Figure 7 shows the Coffin-Manson plate for 24%V, 28% V, and 36% V alloys in the as-quenched condition. The slopes of these plots are shown in Figure 8, along with the twin fault probability as a function of vanadium content. The fatigue performance appears to be better for the alloys with higher vanadium content and lower twin fault probability. A discontinuity is observed in the slope of the 24% V alloy; and this may be related to the twinning mode dominating at low strain amplitudes. Twin interface are likely nucleation and propagation sites for fatigue cracks, however, the effect of twinning on the cyclic-stress strain response has not been firmly established at this time.

The average energy absorbed per cycle is plotted as a function of cycles to crack initiation in Figure 9. The slopes of these curves are similar to those of their respective Coffin-Manson plots, and an energy analysis of fatigue life prediction is now being considered. Figure 10 shows the total energy absorbed prior to crack initiation as a function of strain amplitude. Deformation twinning is the prominent deformation mode for the 24% V alloy at low strain amplitudes and the total energy absorbed is very low. However, for higher strain amplitudes, as might be present in the plastic zone of a propagating crack, the energy absorbed is larger than for the 36% V alloy. The decrease in ΔEi for smaller $\Delta\varepsilon_p/2$ values for the 36% V alloy is probably related to the fatigue softening effect. The decrease at large values of $\Delta\varepsilon_p/2$ is not clear at the moment and extensive work is underway to try and elucidate this phenomenon.

Deformation twinning may effect the fatigue response in two ways:
1) it can reduce the fatigue life by providing twin interfaces for fatigue

crack initiation, and 2) it can reduce the accumulation of fatigue damage by making the deformation more reversable due to untwinning and increase the fatigue life. The results presented above seems to indicate that for the beta Ti-V alloys the effect of the former overwhelms the effect of the latter at least for LCF and/or crack initiation. These experiments, however, are by no means complete. Further LCF studies are now being conducted on these and other aging treatments which produce different microstructures. Crack propagation measurements, now being made, should aid in our analysis of microstructural effects on fatigue performance.

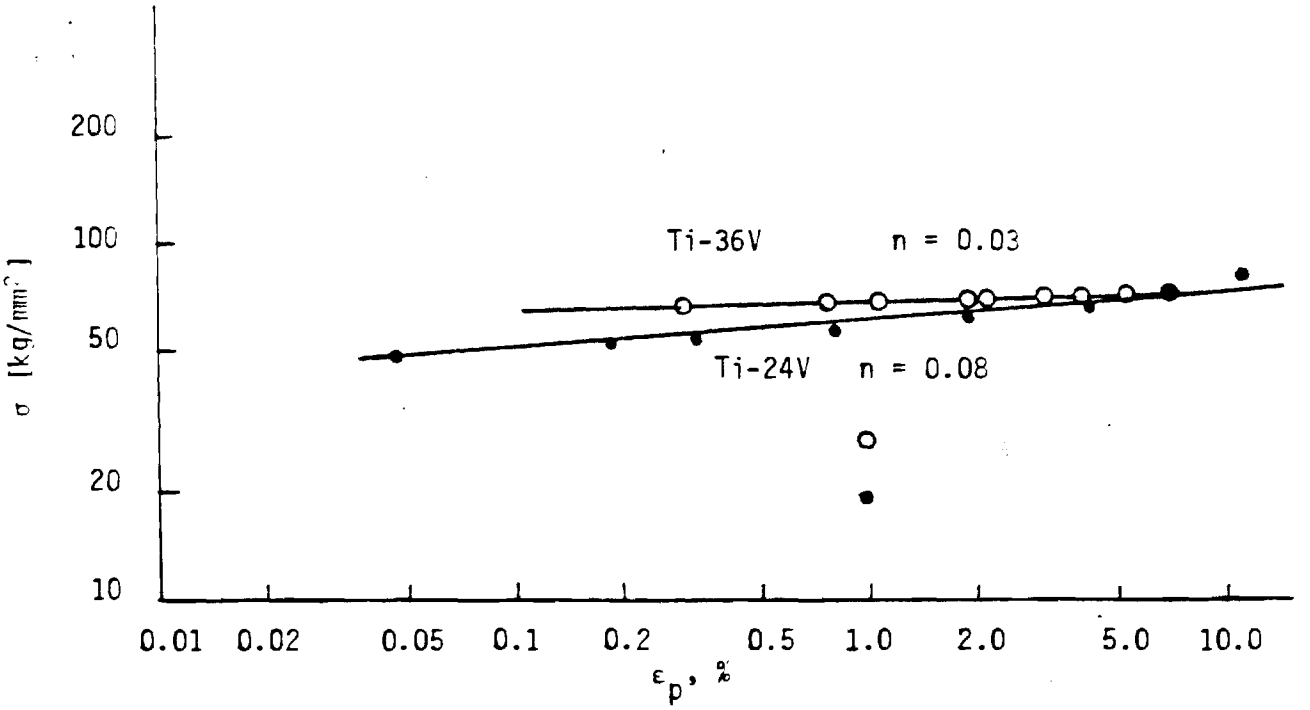

Figure 1. Monotonic stress (σ) versus strain (ε_p) curves for Ti-24V and -36V alloys under as quenched condition.

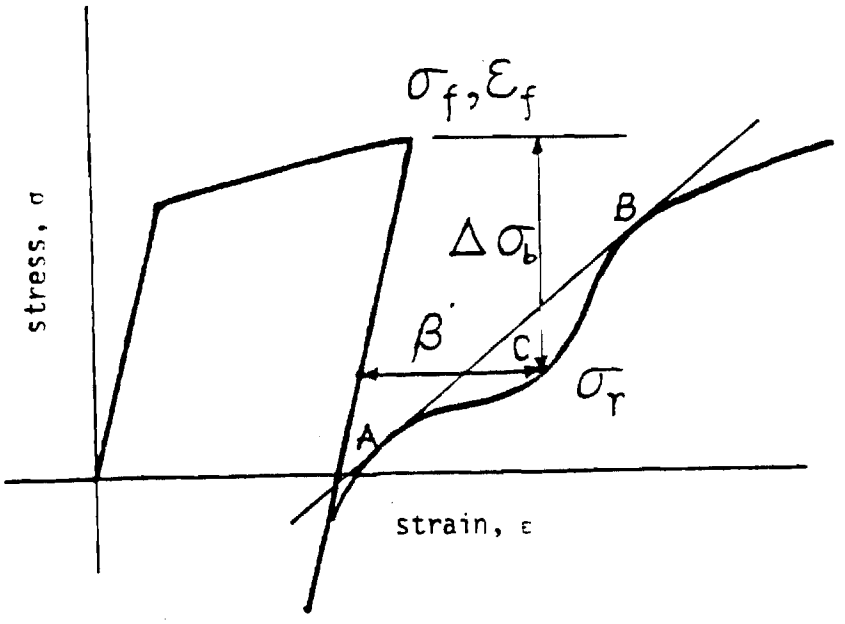

Figure 2. Graphical construction for measurement of the Bauschinger effect. AB is the tangent to both sides of the reversed flow curve. C is the point on the curve with maximum deviation from AB.

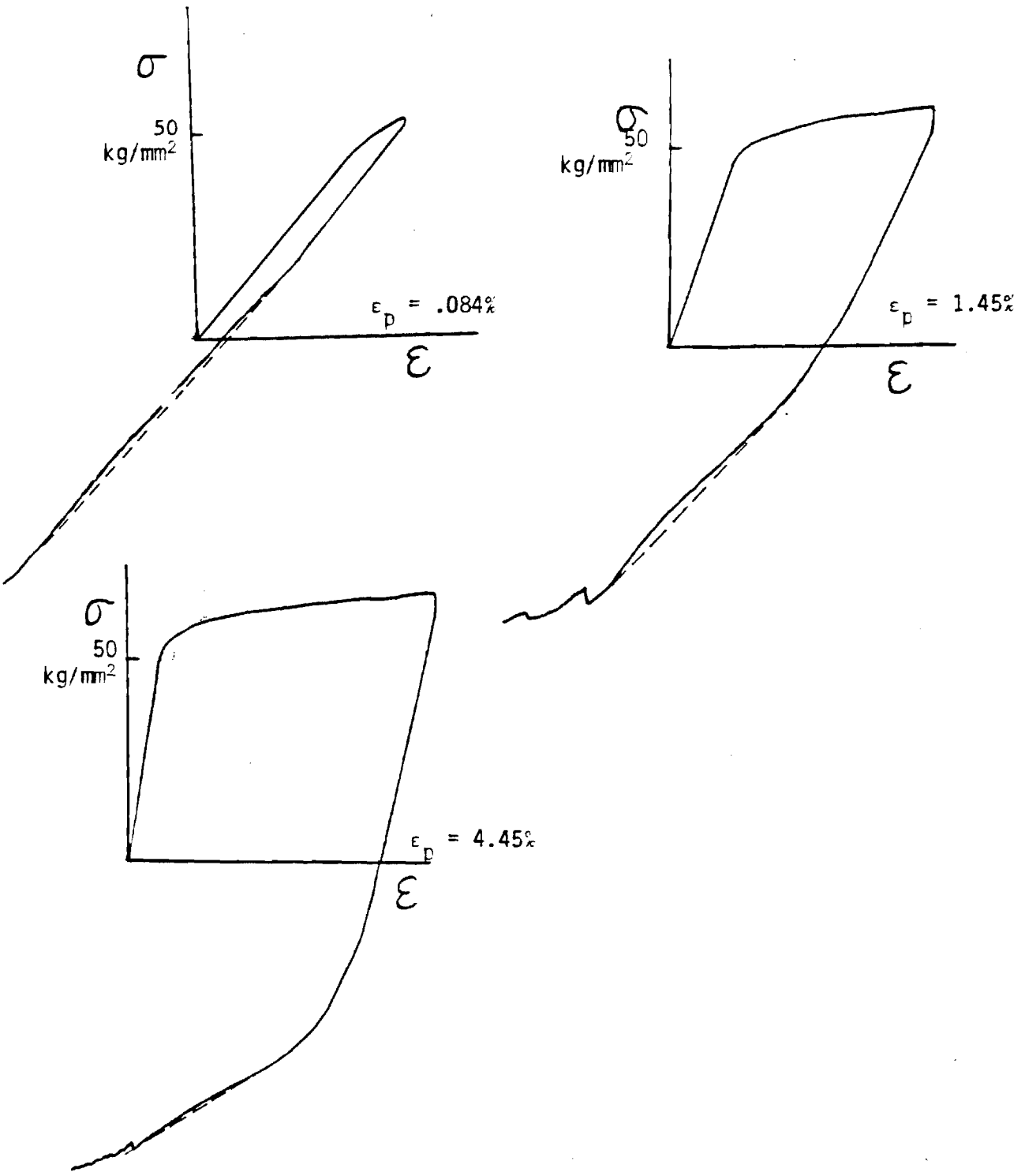

Figure 2. Stress-strain curves for the first half cycle for various forward plastic strains (ε_p) for Ti-24V alloy in the as quenched condition.

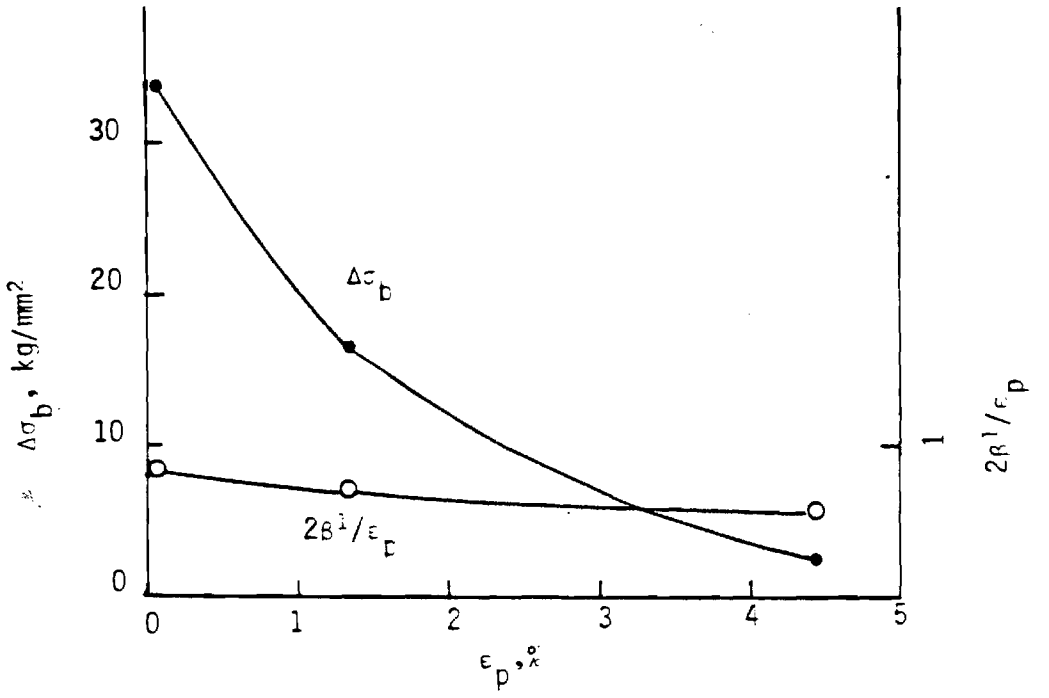

Figure 4. $2\beta^1/\varepsilon_p$ and $\Delta\sigma_b$ values for the first strain reversal versus ε_p, the plastic strain in the forward direction, for the Ti-24V alloy under as quenched condition.

Figure 5A
Ti-24%V

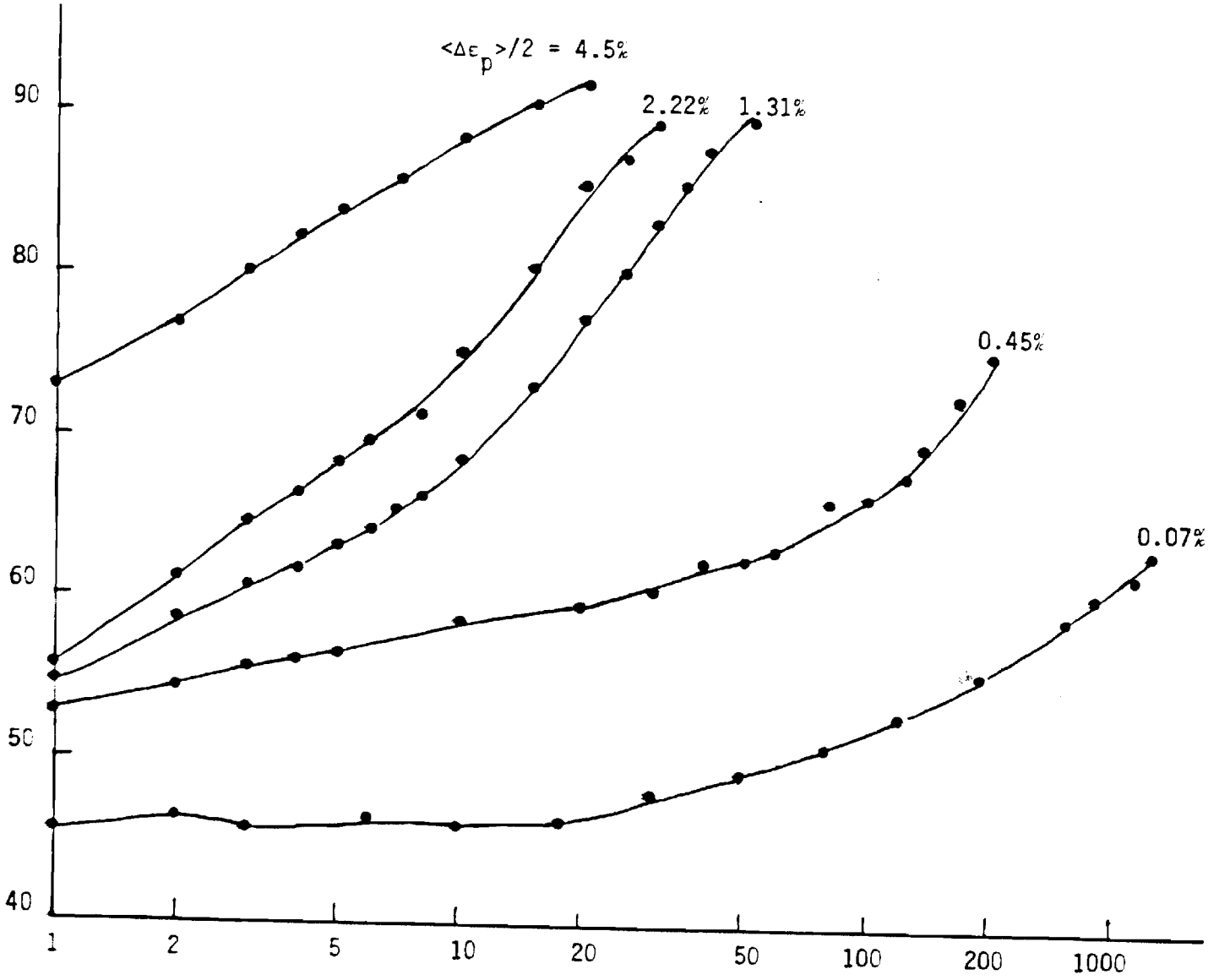

Figure 5. Stress amplitude versus number of cyclic curves for various plastic strain amplitudes for Ti-V alloys under as quenched conditions.

Figure 5b Ti-28%V

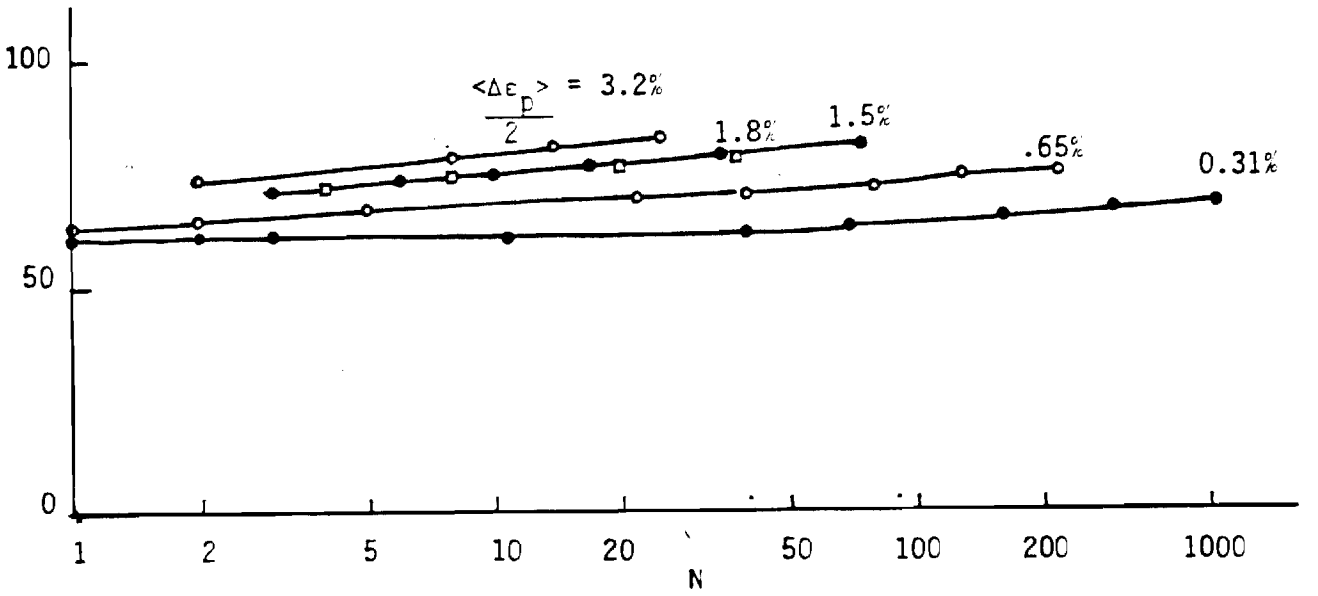

Figure 5c Ti-36%V

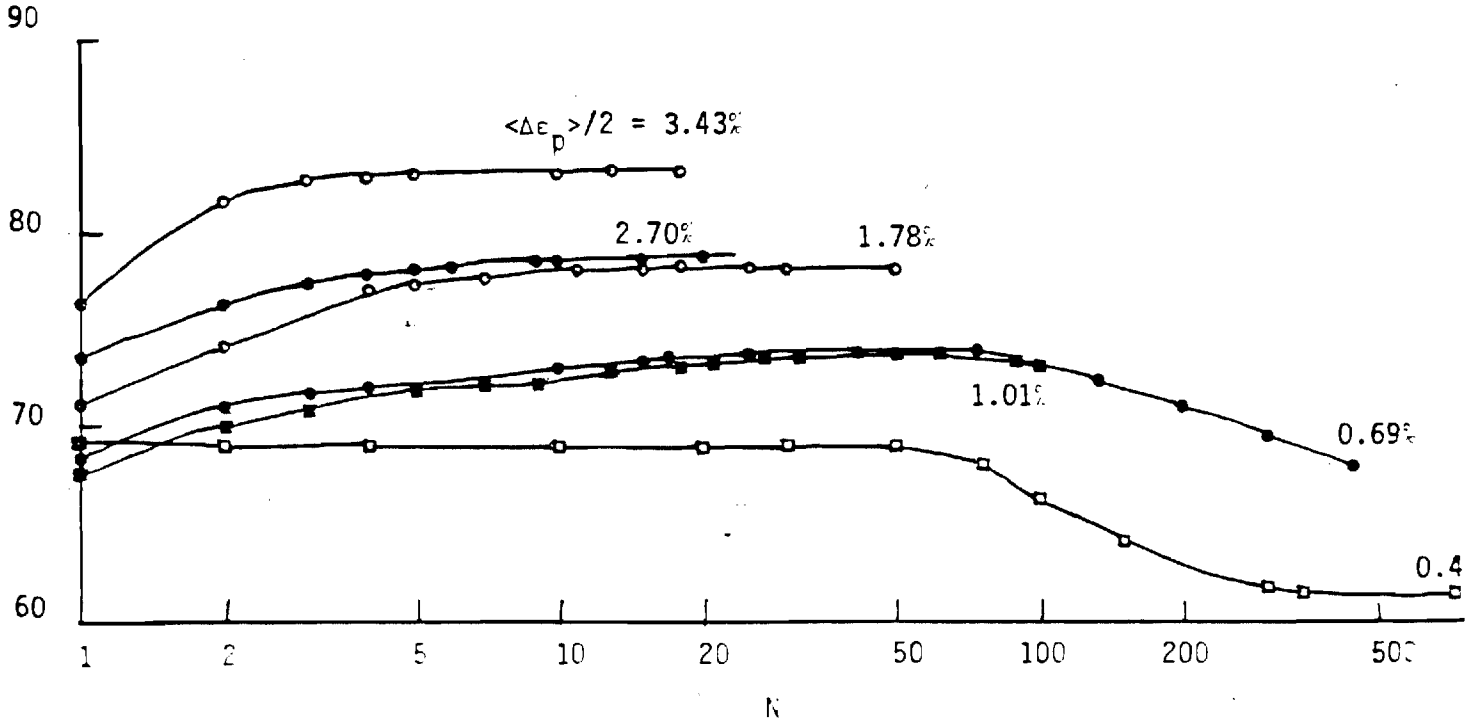

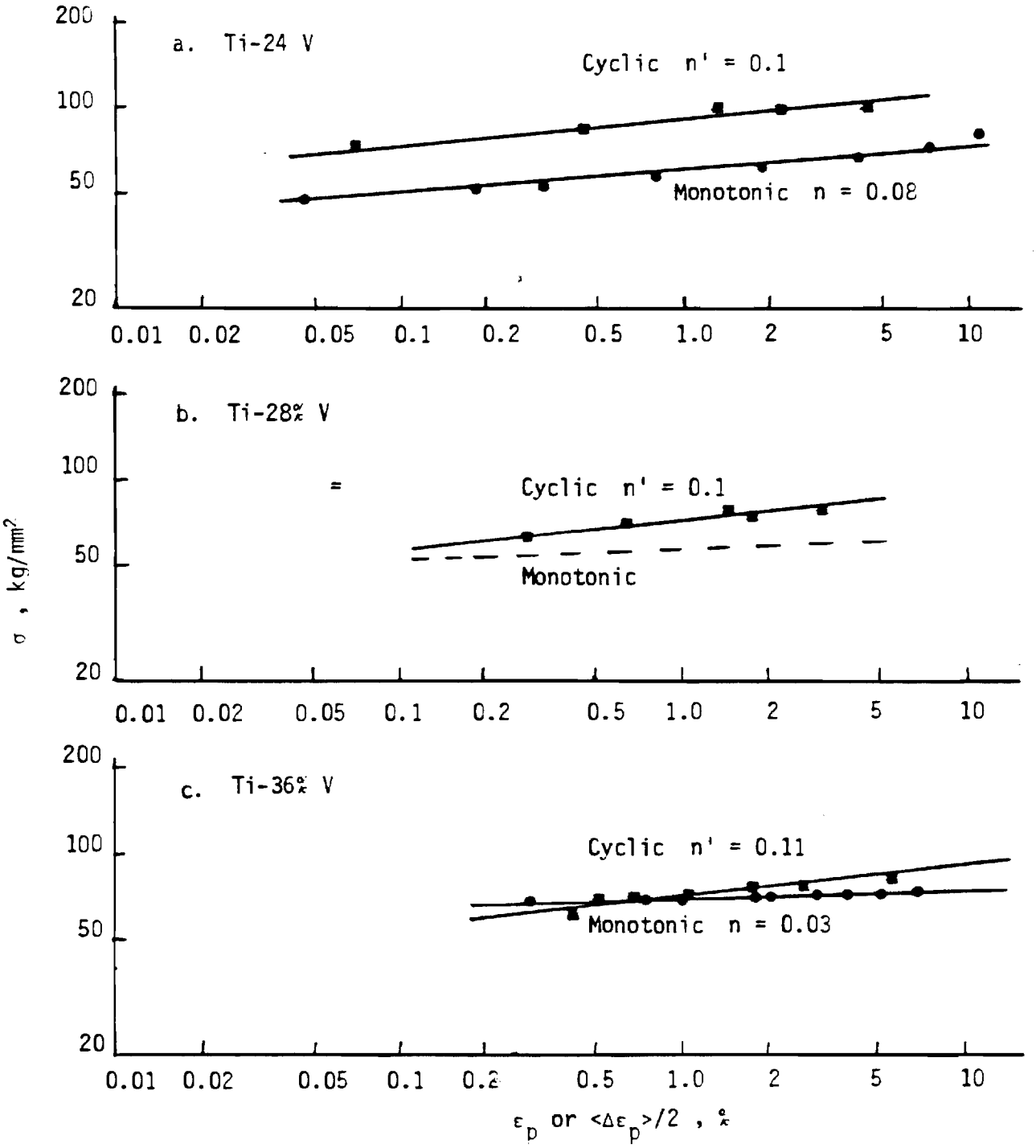

Figure 6. Monotonic and cyclic stress (σ) versus strain (ε_p or $\langle\Delta\varepsilon_p\rangle/2$) curves for alloys under as quenched condition.

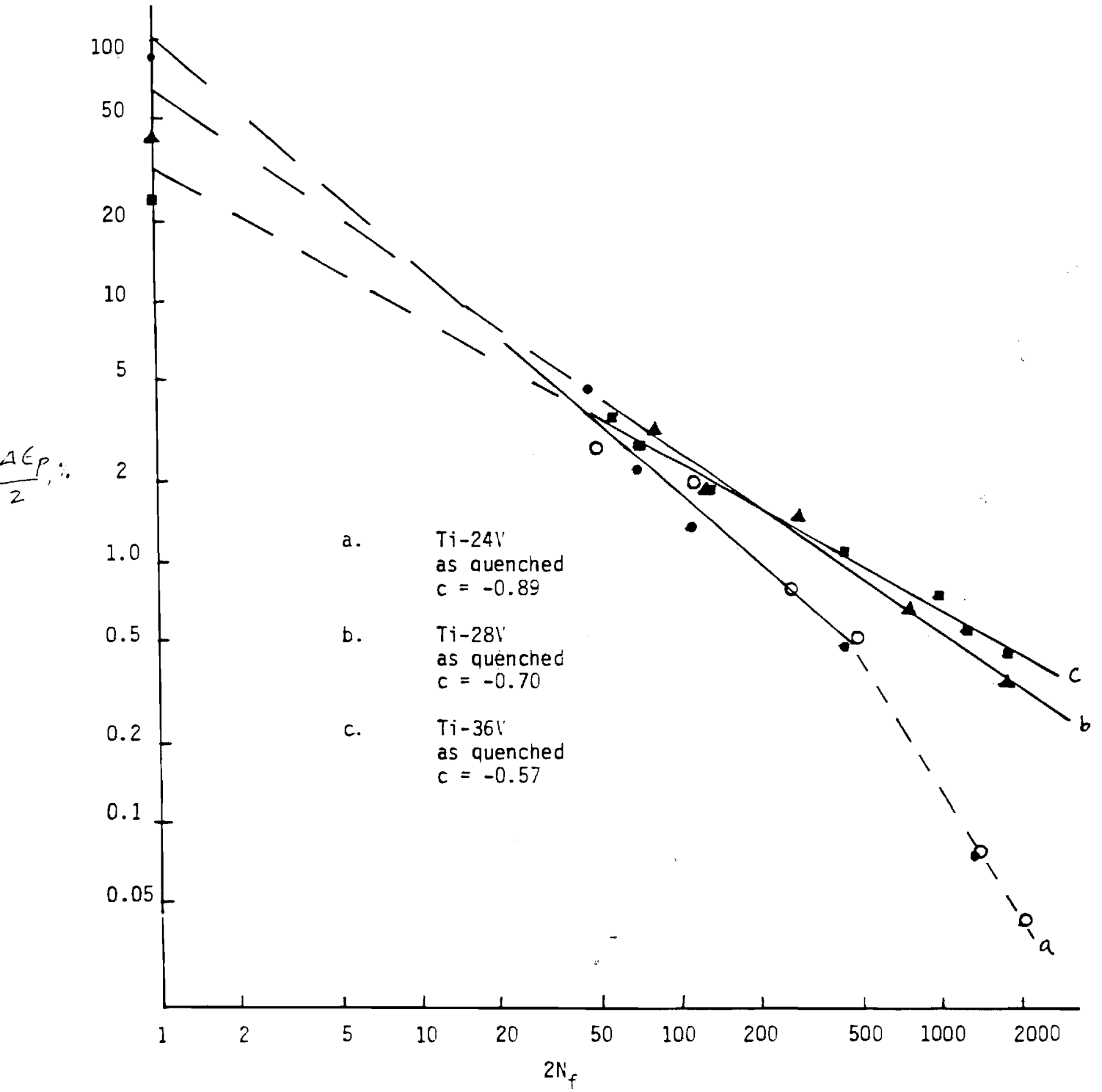

Figure 7. The strain amplitude ($<\Delta\varepsilon_p>/2$) plotted against the number of cycles to failure (N_f) for Ti-V, alloys under as quenched condition.

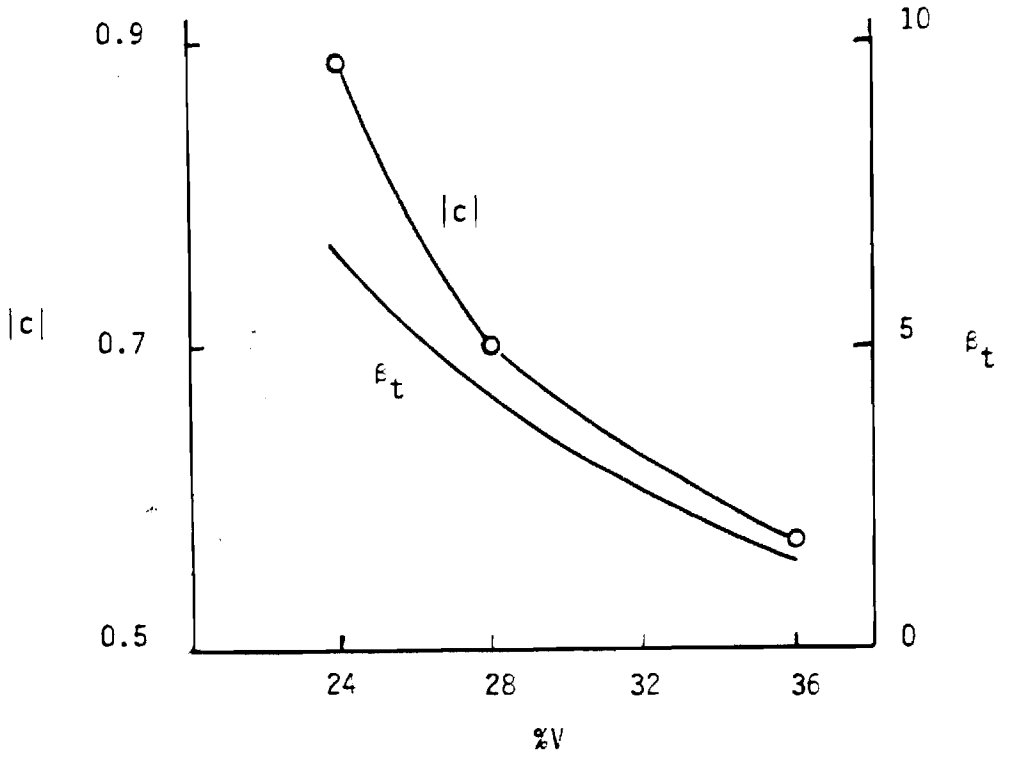

Figure 8. The negative slope of Coffin-Manson plot (|c|) and the twin fault probability (β_t) plotted against the vanadium content of the as quenched Ti-V alloys.

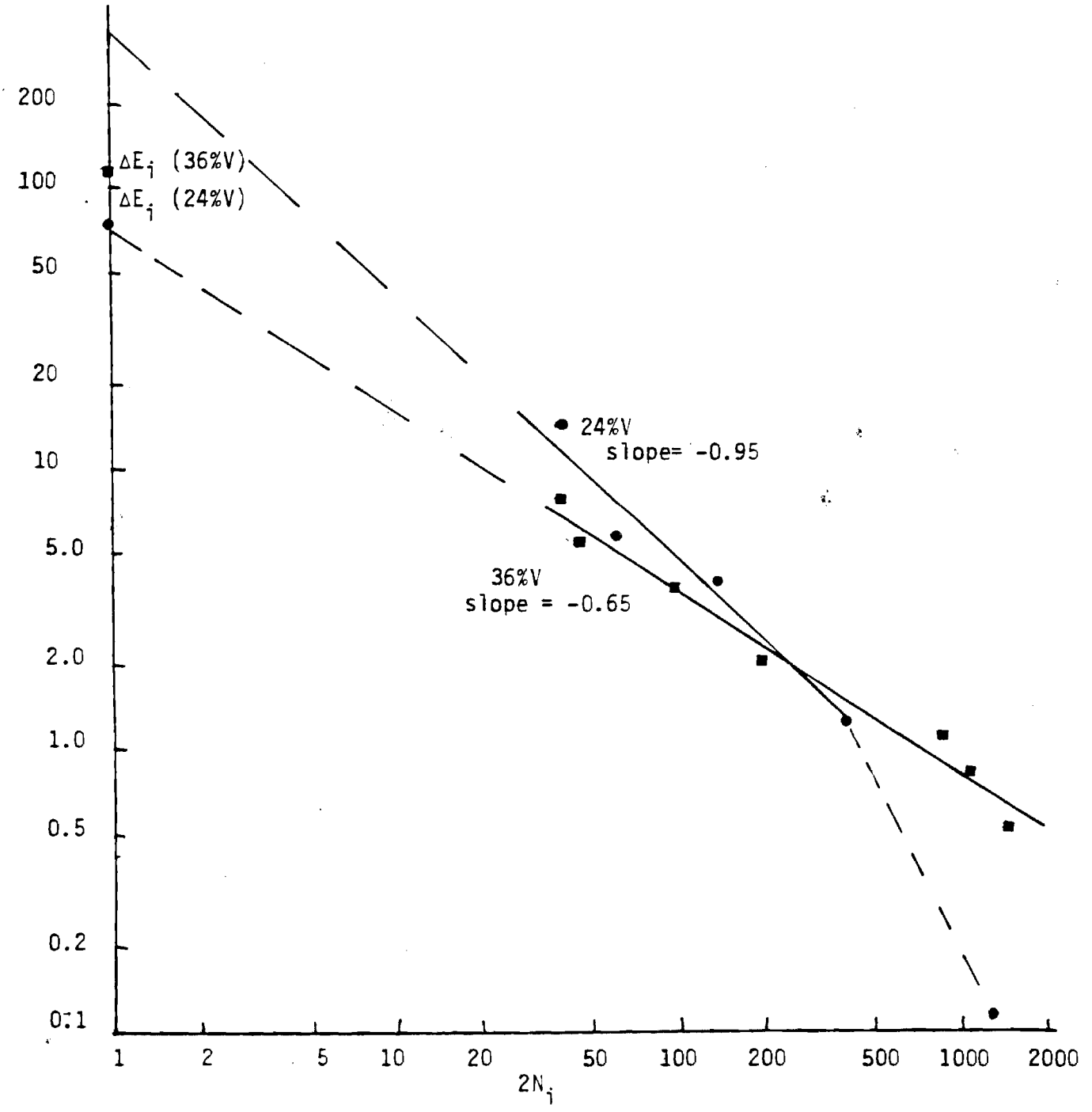

Figure 9. The average energy absorbed per cycle ($\Delta E_i/N_i$) plotted against the number of cycles for crack initiation (N_i) for Ti-24% V and Ti-36% V alloys in as quenched condition. Obtained from low cycle fatigue data.

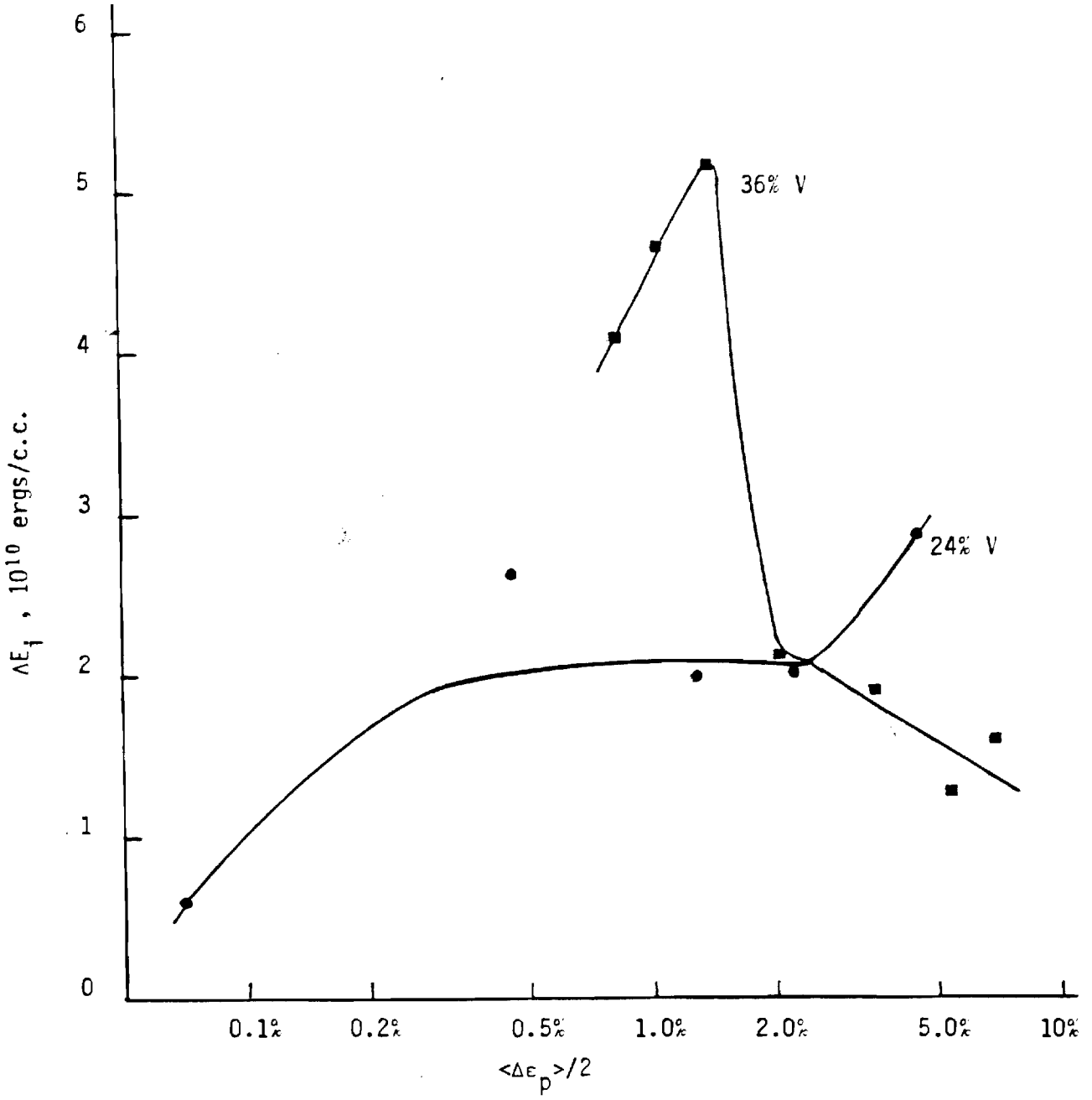

Figure 10. The total energy absorbed before crack initation (ΔE_i) plotted against average strain amplitude ($<\Delta\varepsilon_p>/2$) for the Ti-24%V and Ti-36% V alloys in as quenched condition. Obtained from low cycle fatigue data.

End of the Year Report

ONR Task Order No. N0014-75-C-0349
NO 031-751

December 7, 1977

A. Deformation Mechanisms in Beta Titanium Alloys

The general goal of this research is to obtain an understanding of the influence of microstructural features on the monotonic and cyclic deformation, and crack growth behavior of titanium alloys. Work on this contract has shown that the deformation mode (planar slip, multiple slip, coarse twinning, and fine twinning) and ductility of Ti-V alloys can be controlled to a large extent by controlling the solute content and volume fraction of omega. Consequently, the system is a unique one for studies directed at establishing the effect of microstructure and deformation mode on the fatigue performance of titanium alloys, and the experimental program has been designed to provide quantitative property-microstructure relationships.

The cyclic stress-strain response of four Ti-V alloys (24, 28, 32, and 36 wt% V), which have deformation modes ranging from coarse twinning to wavy and planar slip, has been measured and correlated with deformation mode and microstructure. Alloys which deform by coarse twinning exhibit an anomalous Bauschinger effect due to untwinning during reversed loading. Large cyclic hardening was due to twin interfaces acting as barriers to continued cyclic deformation and with lattice defects generated by the twinning mechanism. Crack initiation is associated with concentrated slip near twin bands. Alloys which deformed by wavy slip exhibited cyclic hardening and no saturation prior to crack initiation. The wavy slip character was due to multiple slip and not connected cross slip of screw dislocations. The lack of saturation and cell formation was associated with the intervention of deformation twinning which prevented dynamic recovery by cross slip. Alloys which deformed by planar slip showed cyclic softening at low strain amplitudes and cyclic hardening at high strain amplitudes. The softening behavior is associated with dislocation dynamics and the hardening behavior with deformation twinning. The hardening behavior of all the Ti-V alloys examined is due, at least in part, to deformation twinning inhibiting dynamic recovery. Although the large Coffin Manson slops, $|c|$, of the alloys that showed extensive twinning indicate

inferior fatigue performance in these strain controlled tests, their cyclic hardening behavior suggests that they may be superior in stress controlled applications.

Crack growth data has been collected on as-quenched samples of 24% V, 28% V, and 32% V alloys and on aged samples of 24% V. No major differences are observed for the different alloys in the as-quenched conditions although their deformation modes vary considerably, i.e., coarse twinning, wavy multiple slip, and planar slip. However, there are minor differences in the slopes of the da/dN vs. ΔK curves. The slope decreases with increasing vanadium content, and therefore with decreasing propensity for deformation twinning. This adverse effect of deformation twinning on crack growth rate may be related either to twin interfaces serving as an easy path for crack growth or to the fatigue hardening behavior of these alloys. At low strain amplitudes or ΔK, the samples which twin harden more extensively than those that don't, resulting in a smaller crack opening displacement. A detailed study of the crack path and crack propagation mechanism is now underway.

B. Implication of ONR Contract Research in Terms of Applied Significance

The research conducted thus far on this contract has shown that the deformation mechanisms of beta titanium alloys can be greatly influenced by variations in solute content and/or the presence of small amounts of a second phase. Variations in deformation mechanisms result in variations in texture development during processing, ductility, and cyclic behavior. The current research is directed at understanding fatigue mechanisms and determining the critical microstructural features which control both crack initiation and subcritical crack growth. Once these microstructural features have been established, alloys may be designed for fatigue resistance analogously to those developed for improved strength, fracture toughness, stress corrosion resistance.

C. Publications, Reports and Talks

i. Publications resulting from ONR Contract Research

1. S. B. Chakrabortty, T. K. Mukhopadhyay and E. A. Starke, Jr.," "The Cyclic Stress-Strain Response of Titanium-Vanadium Alloys," Acta Met. (in press).

2. H. G. Paris, "The Deformation Twinning Behavior of Omega Bearing Ti-V Alloys," Met. Trans. (in press).

3. H. G. Paris, B. G. LeFevre, and E. A. Starek, Jr., "Deformation Behavior in Quenched and Aged Beta Titanium Alloys," Met. Trans., 7A, 273-278 (1976).

4. Fu-Wen Ling. E. A. Starke, Jr., and B. G. LeFevre, "Deformation Behavior of Beta Ti-V Alloys," Met. Trans., 5, 179-188 (1974).

5. Fu-Wen Ling, H. J. Rack and E. A. Starke, Jr., "Deformation of Metastable Beta Ti-V Alloys," Met Trans., 4, 1671-1676 (1973).

6. Fu-Wen Ling and E. A. Starke, Jr., "Thermal Etching of β Ti-V Alloys," Metallography 5, 399-407 (1972).

ii. Reports and Talks on ONR Research During 1977

1. S. B. Chakrabortty, T. K. Mukhopadhyay, and E. A. Starke, Jr. "The Cyclic Stress-Strain Response of Titanium-Vanadium Alloys, Office of Naval Research, Contract N00014-75-C-0349. Technical Report 77-1, August 30, 1977.

2. S. B. Chakrabortty and E. A. Starke, Jr., "The Fatigue Behavior of Ti-24% V," Talk presented at the 106th AIME Annual Meeting, Atlanta, Georgia, March 9, 1977.

3. T. K. Mukhopadhyay and E. A. Starke, Jr., "The Cyclic Stress Strain Response of Ti-32% V and Ti-36% V Alloys," Talk presented at the 106th AIME Annual Meeting, Atlanta, Georgia, March 9, 1977.

D. Other Contracts

The Effect of Microstructural Features on the Response of Aluminum Alloys to Cyclic Deformation," Air Force Office of Scientific Research, $50,000.

Respectfully submitted

Edgar A. Starke, Jr.
Professor
Principal Investigator

E-19-632

End of the Year Report

ONR Task Order No. N0014-75-C-0349
NO 031-751

November 19, 1980

A. Deformation Mechanisms in Beta Titanium Alloys

The general goal of this research is to obtain an understanding of the influence of microstructural features on the monotonic and cyclic deformation, and fatigue and fracture behavior of titanium alloys. Work on this contract has shown that the deformation mode (planar slip, multiple slip, coarse twinning, and fine twinning), ductility and cyclic stress-strain response (CSSR) of Ti-V alloys can be controlled to a large extent by controlling the solute content and volume fraction of omega. Consequently, the system is a unique one for studies directed at establishing the effect of microstructure and deformation mode on the fatigue performance of titanium alloys, and the experimental program has been designed to provide quantitative property-microstructure relationships.

Research effort in the calendar year 1980 was focused primarily on some aspects of fatigue behavior of two as-quenched alloys (24%V and 32%V) with substantial differences in deformation modes. Ti-24%V alloy deforms by coarse twinning and multiple slip whereas Ti-32%V alloy deforms by coarse single slip. The results of these studies are summarized below.

(1) The Effect of Overload on Fatigue Crack Propagation: The purpose of this research is to study the influence of deformation behavior on the fatigue crack retardation effect in beta titanium alloys. It has been observed that at low stress intensity ranges, the degree of crack retardation due to overload is greater for the 32%V alloy compared to that for the 24%V alloy, while the opposite is true for the high stress intensity ranges. The retardation effect is greater at lower load ratios. The retardation effect increases with number of overload cycles and the increase is more pronounced for the 24%V alloy. For a given load ratio the retardation behavior appears to be dependent mainly on the peak stress intensity and almost independent of the stress intensity range of the overload cycles. These results indicate that the retardation effects are primarily due to the residual stresses arising from the application of overload. The magnitude of the residual stresses and their interaction with the subsequent fatigue stresses give rise to the retardation behavior and these

factors may be influenced by the material's properties like cyclic and montonic stress-stress response and fatigue crack growth behavior.

(2) The Effect of Strain Rate on Cyclic Stress-Strain Response: This study has been undertaken to observe the effect of strain rate on the cyclic deformation behavior of the two Ti-V alloys. The preliminary results of our strain controlled fatigue studies indicate that the reversibility of deformation as measured in terms of the degree of Bauschinger effect increases with increasing strain rate. This is substanially more pronounced for the Ti-24%V alloy, which has a greater tendency for multiple slip and twinning. Consequently, the degree of fatigue hardening is increased at lower strain rates and the fatigue life reduced. Once again the effect was larger for the 24%V alloy. It appears that the propensity of 'wavy' slip increases with decreasing strain rate for the 24%V alloy. This increases the dislocation-dislocation interaction and the irreversibility of cyclic deformation, leading to a greater extent of strain hardening and a greater propensity of intergranular cracking.

(3) Quantitative Fractography: We are developing techniques for quantitative evaluation of fatigue fractographs to have a better understanding of mechanisms of fatigue. The fracture behavior in air of the 32%V and 24%V alloys at low and intermediate stress intensity ranges and two frequencies of loading (1 and 50 Hz) are now being studied by these techniques. Preliminary results indicate that transition from multifaceted to faceted growth (from low to intermediate stress ranges) changes from one alloy to another and with the frequency of loading. Most abrupt transition is observed for the 32%V alloy at 1 Hz. We also find that multifacet fracture surface has a lower degree of orientation, higher roughness parameter, greater true fracture surface area, smaller facet size and more subsurface cracking compared to facet fracture surface. These results seem to support our proposed mechanisms of fatigue crack growth, that faceted growth is due to a coarse slip mechanism and multifaceted growth is due to a decohesion mechanism.

B. Implication of ONR Contract Research in Terms of Applied Significance

The studies conducted under this project have shown that the deformation mode of beta titanium alloys may be greatly influenced by variations in solute content and/or heat treatment. Our studies have also shown how the deformation mode influences the fatigue crack initiation and propagation processes. These

studies have considerable applied significance because development of structural titanium alloys requires understanding of the deformation mechanisms and their influence on monotonic and cyclic strength and ductility. Our research on the effect of overload, frequency of loading and environment on fatigue behavior should have a significant contribution toward understanding the response of modern structural materials under service conditions. Techniques that are being developed for quantitative evaluation of fracture surfaces should prove to be valuable for future investigations of fatigue fracture behavior of most materials.

C. Publications, Reports and Talks

i. Publications resulting from ONR Contract research

1. E. E. Underwood and S. B. Chakrabortty, "Quantitative Fractography of a Fatigued Ti-28 w/o V Alloy," ASTM Special Technical Publication, (in press).

2. S. B. Chakrabortty, E. A. Starke, Jr., L. Konopasek and E. W. Lee, "The Effect of Environment and Frequency of Loading on the Fatigue Crack Propagation of Titanium-Vanadium Alloys," Proceedings-ICM3, Vol. 2, pp. 365-370, Cambridge, U.K. (1979).

3. S. B. Chakrabortty, "A Model Relating Low Cycle Fatigue Properties and Microstructure to Fatigue Crack Propagation Rates," Fatigue of Engineering Materials and Structures, 2, 331-344 (1979).

4. S. B. Chakrabortty and E. A. Starke, Jr., "Fatigue Crack Propagation in Metastable Beta Titanium-Vanadium Alloys," Met. Trans. A, 10A, 1901-1911 (1979).

5. E. E. Underwood and E. A. Starke, Jr., "Quantitative Stereological Methods for Analyzing Important Microstructural Features in Fatigue of Metals and Alloys," in Fatigue Mechanisms, ASTM STP 675, ed., J. T. Fong, pp. 663-682 (1979).

6. S. B. Chakrabortty, T. K. Mukhopadhyay and E. A. Starke, Jr., "The Cyclic Stress-Strain Response of Titanium-Vanadium Alloys," Acta Met. 26, 909-920 (1978).

7. H. G. Paris, B. G. LeFevre and E. A. Starke, Jr., "Deformation Behavior in Quenched and Aged Beta Titanium Alloys," Met. Trans., 7A, 273-378 (1976).

8. Fu-Wen Ling, E. A. Starke, Jr., and B. G. LeFevre, "Deformation Behavior of Beta Ti-V Alloys," Met Trans., 5, 179-188 (1974).

9. Fu-Wen Ling, H. J. Rack and E. A. Starke, Jr., "Deformation of Metastable Beta Ti-V Alloys," Met. Trans., 4, 1671-1676 (1973).

10. Fu-Wen Ling and E. A. Starke, Jr., "Thermal Etching of β Ti-V Alloys," Metallography, 5, 399-407 (1972).

ii. Publications, Reports and Talks during 1980.

1. E. E. Underwood and S. B. Chakrabortty, "Quantitative Fractography of a Fatigued Ti-28 w/o V Alloy," ASTM Special Technical Publication (in press).

2. E. A. Starke, Jr., L. Konopasek, S. B. Chakrabortty and E. W. Lee, "Effect of Frequency of Loading and Environment on the Fatigue Crack Growth Behavior of Metastable Beta Titanium-Vanadium Alloys," paper presented in TMS-AIME Annual Meeting, Las Vegas, February 1980.

3. S. B. Chakrabortty and E. W. Lee, "Effect of Overload on Fatigue Crack Growth in Metastable Beta Titanium-Vanadium Alloys," paper presented in TMS-AIME Annual Meeting, Las Vegas, February 1980.

4. E. W. Lee and S. B. Chakrabortty, "The Effect of Strain Rate on Low Cycle Fatigue Behavior of Some Metastable Beta Titanium-Vanadium Alloys," paper presented in TMS-AIME Fall Meeting, Pittsburg, October 1980.

5. E. W. Lee and S. B. Chakrabortty, "The Effect of Overload on Fatigue Crack Propagation in Metastable Titanium-Vanadium Alloys," Technical Report 80-1, Office of Naval Research Contract N00014-75-C-0349, November 28, 1980.

D. Other Contracts

1. "The Effect of Powder Metallurgical Processing and Intermediate Thermal Mechanical Treatment on the Fatigue Properties of CT91 High Strength Aluminum Alloys," USARO Contract No. N00019-80-C-0491, $119,391 for a two year period.

Respectfully submitted,

Saghana B. Chakrabortty
Senior Research Scientist

E-19-632

End of the Year Report

ONR Task Order No. N00014-75-C-0349
NO 031-751

September 30, 1981

A. Deformation Mechanisms in Beta Titanium Alloys

The general goal of this research is to obtain an understanding of the influence of microstructural features on the monotonic and cyclic deformation, and fatigue and fracture behavior of titanium alloys. Work on this contract has shown that the deformation mode (planar slip, multiple slip, coarse twinning, and fine twinning), ductility and cyclic stress-strain response (CSSR) of Ti-V alloys can be controlled to a large extent by controlling the solute content and volume fraction of omega. Consequently, the system is a unique one for studies directed at establishing the effect of microstructure and deformation mode on the fatigue performance of titanium alloys, and the experimental program has been designed to provide quantitative property-microstructure relationships.

The research effort in the 1981 fiscal year focused on the effect of strain rate on the low cycle fatigue, and the effect of frequency and environment on fatigue crack propagation of Ti-24%V, Ti-28%V and Ti-32%V alloys in the metastable bcc state. Strain rates of 10^{-4}/sec and 10^{-2}/sec were used for the low cycle fatigue tests, and frequencies of 1 Hz and 10 Hz in laboratory air and vacuum environments were used for fatigue crack propagation tests. Chakrabortty's equation, developed on this research program, was used to correlate the low cycle fatigue parameters with the crack growth rate.

The Effect of Strain Rate on Cyclic Stress-Strain Response: This study was undertaken to observe the effect of strain rate on the cyclic deformation behavior of the three Ti-V alloys. The results of our strain controlled fatigue studies indicate that the reversibility of deformation as measured in terms of the Bauschinger strain increases with increasing strain rate. This is substantially more pronounced for the Ti-24%V alloy, which has a greater tendency for multiple slip and twinning. Consequently, the degree of fatigue hardening is increased at lower strain rates and the fatigue life is reduced. It appears that the propensity for "wavy" slip increases with decreasing strain rate for the 24%V alloy. This increases the dislocation-dislocation interaction and the irreversibility of cyclic deformation, which increases both strain hardening and intergranular cracking.

The major effect of the different strain rates on the 32%V was associated with the cyclic hardening and softening behavior. At low strain rates, cyclic hardening occurs in the strain amplitude region where cyclic softening occurs at high strain rates. Surface features of low cycle fatigue specimens suggest that the distribution of slip is more dense at lower strain rates and cracking occurs primarily along slip bands regardless of strain rate. This indicates that the intense slip bands, associated with the lack of slip reversibility at the low strain rate, result in a higher cyclic stress and consequently a shorter fatigue life. It is interesting to note that the fatigue life is closely related to the saturation stress level for the 32%V alloy. The smallest differences in both the fatigue life and in the saturation stress for the two strain rates occur at approximately the same plastic strain range ($\Delta\varepsilon_p/2$ = 0.7 to 0.8%). The fatigue life difference is approximately proportional to the saturation stress difference.

The Effect of Frequency and Environment on Fatigue Crack Propagation Rate: Tests were performed to evaluate the effect of frequency and environment on the fatigue crack propagation behavior. The data were collected at frequencies of 1 Hz and 10 Hz in vacuum and in laboratory air at room temperature (23 $\sim$ 25°C). Laboratory air ranged from 27 $\sim$ 30% relative humidity and the vacuum level was maintained at approximately 4×10^{-6} torr.

For the 24%V alloy, the highest crack growth occurs at 1 Hz in the air environment and the lowest crack growth rate occurs at 10 Hz in the vacuum environment. Even though an increase in frequency decreases the crack growth rate, the rate is higher at 10 Hz in air than at 1 Hz in vacuum. The same trend in crack growth behavior was observed for the 32%V alloy. However, the environmental effect is relatively constant from the low to the high ΔK regions, while the frequency effect decreases with increasing ΔK.

A comparison of the crack growth rates in air shows almost the same trends for the three alloys. However, in the intermediate ΔK range, an accelerated crack growth rate was observed for the 28%V and 32%V alloys but not for the 24%V alloy. A relatively large difference in crack growth rate of the three alloys, proportional to the difference in vanadium content, was observed in vacuum. The crack growth rate increases with decreasing solute content suggesting increasing environmental susceptibility with increasing vanadium content. The accelerated crack growth rate in the intermediate ΔK range was absent in vacuum, indicating that the accelerated crack growth rate in air is associated with environmental sensitivity. The environmental sensitivity is enhanced by coarse slip. Multi-

facet fracture features were observed for both the 1 Hz and 10 Hz tests. Featureless fracture characteristics were more predominant in air than in vacuum. In the facet region, the difference in fracture surface appearance between air and vacuum could be associated with more dense slip and a greater tendency to multiple slip in vacuum than in the air environment.

B. Implication of ONR Contract Research in Terms of Applied Significance

The studies conducted under this project have shown that the deformation mode of beta titanium alloys may be greatly influenced by variations in solute content and/or heat treatment. Our studies have also shown how the deformation mode influences the fatigue crack initiation and propagation processes. These studies have considerable applied significance because development of structural titanium alloys requires understanding of the deformation mechanisms and their influence on monotonic and cyclic strength and ductility. Our research on the effect of overload, frequency of loading and environment on fatigue behavior should have a significant contribution toward understanding the response of modern structural materials under service conditions. Techniques that are being developed for quantitative evaluation of fracture surfaces should prove to be valuable for future investigations of fatigue fracture behavior of most materials.

C. Publications, Reports and Talks

Publications Resulting from ONR Contract Research

1. E. E. Underwood and S. B. Chakrabortty, "Quantitative Fractography of a Fatigue Ti-28 w/o vanadium Alloy," ASTM Special Technical Publication, (In Press).

2. S. B. Chakrabortty, E. A. Starke, Jr., L. Konopasek and E. W. Lee, "The Effect of Environment and Frequency of Loading on the Fatigue Crack Propagation of Titanium-Vanadium Alloys," Proceedings ICM3, Vol. 2, 365-370, Cambridge, U.K. (1979).

3. S. B. Chakrabortty, "A Model Relating Low Cycle Fatigue Properties and Microstructure to Fatigue Crack Propagation Rates," Fatigue of Engineering Materials and Structures, 2, 331-344 (1979).

4. S. B. Chakrabortty and E. A. Starke, Jr., "Fatigue Crack Propagation in Metastable Beta Titanium-Vanadium Alloys," Met. Trans. A, 10A, 1901-1911 (1979).

5. E. E. Underwood and E. A. Starke, Jr., "Quantitative Stereological Methods for Analyzing Important Microstructural Features in Fatigue of Metals and Alloys," In Fatigue Mechanisms, ASTM STP 675, ed., J. T. Fong, 663-682 (1979).

6. 6. S. B. Chakrabortty, T. K. Mukhopadhyay and E. A. Starke, Jr., "The Cyclic Stress-Strain Response of Titanium-Vanadium Alloys," Acta Met. 26, 909-920 (1978).

7. H. G. Paris, B. G. LeFevre and E. A. Starke, Jr., "Deformation Behavior in Quenched and Aged Beta Titanium Alloys," Met. Trans., 7A, 273-278 (1976).

8. Fu-Wen Ling, E. A. Starke, Jr., and B. G. beFevre, "Deformation Behavior of Beta Ti-V Alloys," Met. Trans., 5, 179-188 (1974).

9. Fu-Wen Ling, H. J. Rack and E. A. Starke, Jr., "Deformation of Metastable Veta Ti-V Alloys," Met. Trans., 4, 1671-1676 (1973).

10. Fu-Wen Ling and E. A. Starke, Jr., "Thermal Etching of Beta Ti-V Alloys," Metallography, 5, 388-407 (1972).

Publications, Reports and Talks During 1980-1981:

1. E. W. Lee and S. B. Chakrabortty, "The Effect of Strain Rate on Low Cycle Fatigue Behavior of Some Metastable Beta Ti-V Alloys," paper presented in TMS-AIME Fall Meeting, Pittsburgh, October 1980.

2. E. W. Lee and S. B. Chakrabortty, "The Effect of Overload on Fatigue Crack Propagation in Metastable Titanium-Vanadium Alloys," Technical Report 80-1, Office of Naval Research Contract N00014-75-C-0349, November 28, 1980.

D. Other Contracts

1. The Effect of Powder Metallurgical Processing and Intermediate Thermal Mechanical Treatment on the Fatigue Properties of CT91 High Strength Aluminum Alloys," USARO Contract No. DAAG 29-80-C-0100, $119,391 for a three year period.

Respectfully submitted,

Edgar A. Starke, Jr.
Director, FFRL
for Saghana Chakrabortty
Principal Investigator

EIT-692

OFFICE OF NAVAL RESEARCH

Contract N00014-75-C-0349, NR 031-750

TECHNICAL REPORT 75-1

DEFORMATION BEHAVIOR IN QUENCHED AND AGED BETA TITANIUM ALLOYS

by

H.G. Paris, B.G. LeFevre and E. A. Starke, Jr.

April 28, 1975

Metallurgy Program, School of Chemical Engineering
Georgia Institute of Technology
Atlanta, Georgia 30332

OFFICE OF NAVAL RESEARCH

Contract N00014-75-C-0349, NR 031-750

TECHNICAL REPORT 75-1

DEFORMATION BEHAVIOR IN QUENCHED AND AGED BETA TITANIUM ALLOYS

by

H. G. Paris, B. G. LeFevre and E. A. Starke, Jr.
Metallurgy Program, School of Chemical Engineering
Georgia Institute of Technology
Atlanta, Georgia 30332

April 28, 1975

DEFORMATION BEHAVIOR IN QUENCHED AND AGED BETA TITANIUM ALLOYS

by

H. G. Paris, B. G. LeFevre and E. A. Starke, Jr.
Metallurgy Program, School of Chemical Engineering
Georgia Institute of Technology, Atlanta, Georgia

Abstract

The deformation characteristics of quenched and aged Ti-V alloys in the composition range 20 to 40% V have been examined by optical metallography and transmission electron microscopy. A coarse lenticular deformation product similar in appearance to previously reported strain induced "martensites" was found to be associated with the occurrence of the omega phase. These features proved to be $\{112\}$ $\langle 111 \rangle$ twins. Continued aging of the omega containing alloys resulted in a transition of the deformation mode from twinning to slip at a point which corresponded to the onset of embrittlement or α precipitation at the ω-β interfaces. The formation of deformation twins in a two-phase β-ω structure is discussed in terms of possible mechanisms.

INTRODUCTION

The research described in this paper is part of a study of the influence of solute content on the deformation modes of metastable beta titanium alloys. In previous papers[1,2] the crystallographic aspects of slip, twinning, and texture development of binary Ti-V quenched from above the β transus was found to vary significantly in the range 20 to 40% V. A point of particular interest was the occurrence of coarse deformation twins in samples containing athermal ω. This point, along with other mechanical property changes, was examined further in samples aged within the ω region. Certain aspects of twin formation and ω embrittlement are discussed.

EXPERIMENTAL

Alloys containing 20, 24, 28, 32, 36 and 40% vanadium were prepared by argon arc melting iodide titanium and 99.95 per cent purity vanadium. The ingots were vacuum encapsulated in quartz and homogenized for 100 hours at 950°C. The material was then cold rolled to a thickness of either 3 mm or 6.5 mm, recrystallized at 850°C (above the β transus) and quenched into ice water. Isothermal annealing sequences were carried out at 300°C, 400°C and 450°C (within the $\alpha + \beta$ region) for times out to 10,000 minutes. Knoop hardness curves were obtained on all compositions at these three temperatures while the corresponding microstructures were examined by means of thin foil transmission electron microscopy (at 125KV) and x-ray diffraction. Strip and rectangular tensile specimens were machined and aged for selected times at 400°C. These specimens were deformed in tension or by rolling approximately 3 to 5%. The deformation modes were revealed by three different techniques: optical metallography on transverse sections;

optical metallography on pre-polished surfaces parallel to the tensile axis; transmission electron microscopy (TEM) on longitudinal or transverse sections.

The procedure for preparation of TEM foils and x-ray diffractometer specimens is given in reference 1. For metallography examination the specimens were polished by standard metallographic techniques and etched in a solution of nitric acid, hydrofluoric acid and water.

RESULTS AND DISCUSSION

A. Aging Sequences

The aging sequences at 300°C, 400°C and 450°C were monitored initially by microhardness measurements. A double hardening effect was seen at the 400°C anneal in all compositions from 20 to 40% V but was most pronounced in the 20 to 24% alloys (Fig. 1). The initial hardening occurred very rapidly and peaked within 100 minutes. The secondary hardening was much more gradual and continued to show an increase out to the longest aging time of 583 hours. At 300°C and 450°C hardening was monotonic with very large increases occurring over a long time at the lower temperature and only slight increases at the higher temperature. In general the following trends were observed over the range of temperatures and compositions studied: The hardness increase varied inversely with vanadium content and temperature (i.e. greatest for 20%V at 300°C) and the changes occurred more rapidly with increasing temperature.

To ascertain the types and distribution of phases produced during aging the 400°C samples were examined by thin foil TEM. The initial hardening stage was accompanied by the formation and growth of the metastable ω phase which eventually appeared as cuboidal shape particles (Fig. 2a). The drop in the initial hardness and the subsequent secondary hardening

were found to be associated with the formation and growth of α phase particles at prior ω-β interfaces. As noted by previous investigators[3,4] further aging resulted in the linking of the α particles into plates or needles (Fig. 2b). Selected area diffraction patterns generally showed partial ring patterns at α positions indicating that the precipitate was generally of a non-Burgers orientation with the matrix.

It has been suggested by Williams and Blackburn[3] that α formation at the ω-β interface occurs when the interface becomes incoherent. The ω particles in this study were too small and occurred in too high a density to reveal possible interfacial dislocations. A loss of coherency is however consistent with the drop from the initial peak hardness.

The occurrence of the $\beta \rightarrow \omega \rightarrow \alpha$ sequence at the 400°C anneal was confirmed by x-ray diffraction measurements on the aged bulk samples. X-ray measurements on the 300°C samples indicated that the monotonic hardening observed out to the longest aging time was due entirely to ω formation, i.e., no α peaks were observed to accompany the slight hardening at that temperature indicating that the α phase formed directly. These results are in agreement with those of Blackburn and Williams[5] and of Hichman.[6]

B. Deformation Modes of Aged Samples

Considerable interest has been shown in the mechanical behavior of metastable beta alloys in two areas: (a) the embrittlement of those alloys containing high volume fractions of ω[7-9]; (b) stress induced transformations in alloys which tend to form athermal ω on quenching.[10-14] In an earlier portion of the present study[1,2] the deformation characteristics of Ti-V samples quenched from above the beta transus were investigated. It was

found at that time that coarse deformation twins formed readily when ω was produced during the quench. That study was extended to cover the effects of aging.

The aged samples of Ti-V exhibited a strong tendency to form coarse deformation twins when the ω phase was present. This is illustrated in the optical micrographs of aged and deformed 24 and 28%V (Figures 3a and b). Coarse lenticular products of the type shown here have been referred to as deformation "martensites" also known to occur some β alloys.[10,13,14] In this particular case, however, these features proved to be primary and secondary {112} <111> twins. This was established by means of trace analysis and selected area diffraction in the TEM. Additionally, x-ray scans on bulk polycrystalline samples showed no extraneous peaks that could be attributed to the orthohombic structure of deformation martensites in Ti alloys.[14]

Deformation structures of the above type are characteristic of β alloys which exhibit relatively high ductility.[10] Continued aging of ω containing alloys at the proper conditions to produce large volume fractions of ω (0.6 or better) results in partial or complete embrittlement. It has been shown that although such alloys are macroscopically brittle, the failure occurs by microvoid coalescence[7,8] suggesting extensive deformation by slip. Our results indicate that the onset of ω embrittlement is accompanied by a transition from coarse twinning to predominant slip. This point is best illustrated by the behavior of the 20%V material (Fig. 4). The kinetics of ω formation at this composition are so rapid that ω is present in the quenched condition for the section sizes used. This condition is ductile and exhibits coarse twinning (Fig. 4a). After 6 minutes the material exhibited no coarse twins (Fig. 4b) and was partially

brittle. At 10 minutes the alloy was so brittle it failed in the grips before yielding. Similar results were obtained in 24%V aged at 300°C and deformed by rolling. At each of these temperatures and compositions embrittlement occurred at aging times which, according to the data of Hickman,[6] yields volume fractions of ω in excess of 0.6.

Our results also indicate that the onset of α precipitation in the ω containing alloys induces a transition from coarse twinning to a mixture of fine twins and slip. All alloys between 20 and 40%V exhibited deformation microstructures similar to that shown in Figure 5 when aged 100 minutes at 400°C and deformed 3 to 5% in tension. Complete tensile curves were not determined; however these results indicate at least a partial restoration of ductility in previously embrittled materials and continued ductility in those for which the amount of ω was insufficient to produce embrittlement.

The tendency for deformation twinning in ω containing alloys has been noted previously but has not been studied in complete detail. In Beta III alloys at least three different types of twins have been identified, {332}, {112} and {2, 4.8, 4.8} [11,12,13] whereas in Ti-V only the {112} mode has been found. Blackburn and Feeney[13] rationalized the occurrence of {332} twins in Beta III on the grounds that the attendant shears are compatible with the ω structure. This argument fails to explain the occurrence of {2, 4.8, 4.8} twins in Beta III or {112} twins in Ti-V.

The geometric problem of passing a/6 <111> twinning shears from the β matrix through the ω structure is shown schematically in Figure 6*.

*For a given ω variant only the one η_1 variant need be considered. The other three <111> directions are parallel to irrational directions in the ω structure (J. M. Silcock, Acta Met., 1958, vol. 6, p. 481).

When ω is sheared by successive a/6 <111> partials its structure is not preserved. This suggests that either the ω particles are sheared and destroyed by formation of the twins or they are looped by the twinning partials. It is difficult to see how the latter mechanism could operate without causing unusually high strength levels and very low ductilities considering the volume fractions and particle sizes involved. Concentration of slip in the β matrix is in fact the type of argument used by Koul and Breedis[8] to explain ω embrittlement.

It has been established experimentally that under certain conditions deformation by slip results in shearing and destruction of ω particles.[9,15] We suggest that there are two possibilities regarding twin propagation in the β-ω structure: (a) similar shearing and destruction of ω by twinning partials or (b) reversion of ω by dilation in advance of the twin interface.[16] The latter suggestion is based on the fact that athermal ω formation has been established as a diffusionless displacement controlled reaction which is reversible and is influenced by lattice strain.[17-20]

Bilby and Crocker define a deformation twin as "a region of crystalline body which has undergone a homogeneous shape change in such a way that the product structure is identical with that of the parent, but oriented differently".[21] A macroscopic deformation process in Ti-V alloys containing ω can be envisioned as occurring by the sequence: (1) Initiation of a cubic twinning shear in the matrix, (2) reversion of the ω precipitates immediately ahead of the twinning shear, (3) passage of the twinning shear, (4) a restoration of the omega structure by an athermal process within the resulting deformation twin. The athermally created ω could transform the entire cubic twin volume or occur by the normal precipitation

of finely dispersed small particles of athermal ω. Phenomenologically, this process satisfies Bilby and Crocker's formulation of the definition of a deformation twin. The existence of such a process seems to be supported by recent work of Kuan, Ahrens and Sass.[22] In an examination of Ti-V alloys of slightly lower solute content than those of the present investigation, a deformation "martensite" product was observed with habit plane {554} and a structure entirely ω. Although such martensite plates were not observed in this study, nor reported in studies of similar alloys by Paton and Williams,[23] this work indicates that a deformation product may occur which results in a net increase in ω. In light of the above this seems to support the mechanism of reversion and reformation.

The transition from twinning and ductile behavior to slip and macroscopic brittle behavior appears to depend only upon the volume fraction of ω. An examination of previous work on the ω transformation by Hickman[6] indicates that over the aging time interval up to 11 hours at 300°C in Ti-24a/o V and up to 10 minutes at 400°C in Ti-20 a/o V (produces a transition from twinning to slip in both cases) the volume fraction consistently has increased to about 0.6 or 0.7, while misfit and particle size appear to be almost unchanged. It is suggested that the amount of cubic material present for effecting a macroscopic twinning process controls deformation behavior. As long as there exists sufficient volume of the matrix, twinning (with preservation of the ω structure) is favored over a slip. The initiation of concentrated slip at high ω volume fractions produces destruction of ω within the bands[9] or confinement of slip within the β matrix[8] and macroscopic embrittlement.

In those alloys for which the ω volume fraction remains low, a transition from twinning to slip may occur at the onset of α precipitation.

SUMMARY

The occurrence of deformation twins in ω bearing Ti-V alloys can be understood in terms of athermal reversion and reformation of ω. The transition from twinning to predominant slip depends primarily on the volume fraction of β matrix available for twinning. At high volume fractions of ω, slip predominates the results in either ω destruction or concentration of deformation within the matrix. In either case embrittlement results. The onset of α precipitation is also accompanied by deformation by predominant slip, however, ductility is retained.

ACKNOWLEDGEMENTS

The authors wish to acknowledge the assistance of Dr. J. C. Williams for helpful discussion, and the support of the office of Naval Research, Contract #N0014-75-C-0349, in preparation of this work.

REFERENCES

1. Fu-Wen Ling, H. J. Rack and E. A. Starke, Jr., Met. Trans., 1973, Vol. 4, p. 1671.

2. Fu-Wen Ling, E. A. Starke, Jr. and B. G. LeFevre, Met. Trans., 1974, Vol. 5, p. 179.

3. J. C. Williams and M. J. Blackburn, Trans. Met. Soc. AIME, 1969, Vol. 245, p. 2352.

4. C. G. Rodes, Metallography, 1969, Vol. 2, No. 2, p. 257.

5. M. J. Blackburn and J. C. Williams, Trans. Met. Soc. AIME, 1968, Vol. 242, p. 2461.

6. B. S. Hickman, J. Inst. of Met., 1968, Vol. 96, p. 2487.

7. J. C. Williams, B. S. Hickman and H. C. Marcus, Met. Trans., 1971, Vol. 2, p. 1913.

8. M. K. Koul and J. F. Breedis, Met. Trans., 1970, Vol. 1, p. 1451.

9. E. Levine, S. Hayden and H. Margolin, Acta Met., 1974, Vol. 22, p.1443.

10. D. N. Williams, R. A. Wood and E. S. Bartlett, Met. Trans., 1972, Vol. 3, p. 1529.

11. J. A. Roberson, S. Fryishiro, V. S. Arunachalam and C. M. Sargent, Met. Trans., 1974, Vol. 5, p. 2317.

12. H. J. Rack, D. Kalish and K. D. Fike, Mat. Sci. & Eng., 1970, Vol. 6, p. 181.

13. M. J. Blackburn and J. A. Feeney, J. Inst. Met., 1971, Vol. 99, p. 132.

14. J. C. Williams, Proc. Sec. Int. Conf. on Ti, MIT, Ti Sci. and Tech., Jaffee and Burt, ed., Plenum Press, N. Y., 1973, p. 1433.

15. A. Gysler, W. Bunk and V. Gerold, Zeit, Metal., 1974, Vol. 65, p. 411.

16. J. C. Williams, Private Communication.

17. J. C. Williams, D. deFontaine and N. E. Paton, Met. Trans., 1973, Vol. 4, p. 2701.

18. D. deFontaine, N. E. Paton and J. C. Williams, Acta. Met., 1971, Vol. 19. p. 1153.

19. J. M. Silcock, Acta. Met., 1958, Vol. 6, p. 481.

20. B. S. Hickman, J. Mat. Sci., 1969, Vol. 4, p. 554.

21. B. A. Bilby and A. G. Crocker, Proc. Roy. Soc. [A], 1965, Vol. 288, p. 240.

22. T. S. Kuan, R. R. Ahrens, and S. L. Sass, The Stress Induced Omega Transformation in Ti-V Alloys, Report 2335, The Materials Research Center, Cornell University, Ithaca, New York.

23. N. E. Paton and J. C. Williams, Second Int. Conf. Strength of Metals and Alloys, ASM, Metals Park, 1970, p. 108.

Figure Captions

Figure 1. Microhardness changes in quenched and aged samples at 400°C as a function of composition.

Figure 2. Typical microstructures in β Ti-V alloys aged at 400°C (b) cuboidal ω in 20%V aged 10 minutes (DF) (b) α particles in 28% V aged 1000 minutes (DF).

Figure 3. Coarse deformation twins in Ti-V alloys aged at 400°C (a) 24% V aged 20 minutes (b) 28% V aged 60 minutes (150X).

Figure 4. Showing twin to slip transition in 20% V alloy deformed $\simeq$ 3 to 5% in tension: (a) as-quenched contains ω, (b) aged 6 minutes at 400°C, failed in gage section. Micrographs on the left are of prepolished surfaces parallel to tensile axis, micrographs on right are polished sections of tensile specimens perpendicular to gage length. (150X)

Figure 5. Deformation microstructures of Ti-V samples aged 100 minutes at 400°C and pulled $\simeq$ 3% in tension (a) 28% V (b) 32% V.

Figure 6. Schematic representation of a/6 <111> twinning shears in the ω structure. Note that the original ω structure is not preserved. Open symbols denote untwinned atom positions and filled symbols represent twinned atom positions. Squares represent atoms in plane above paper.

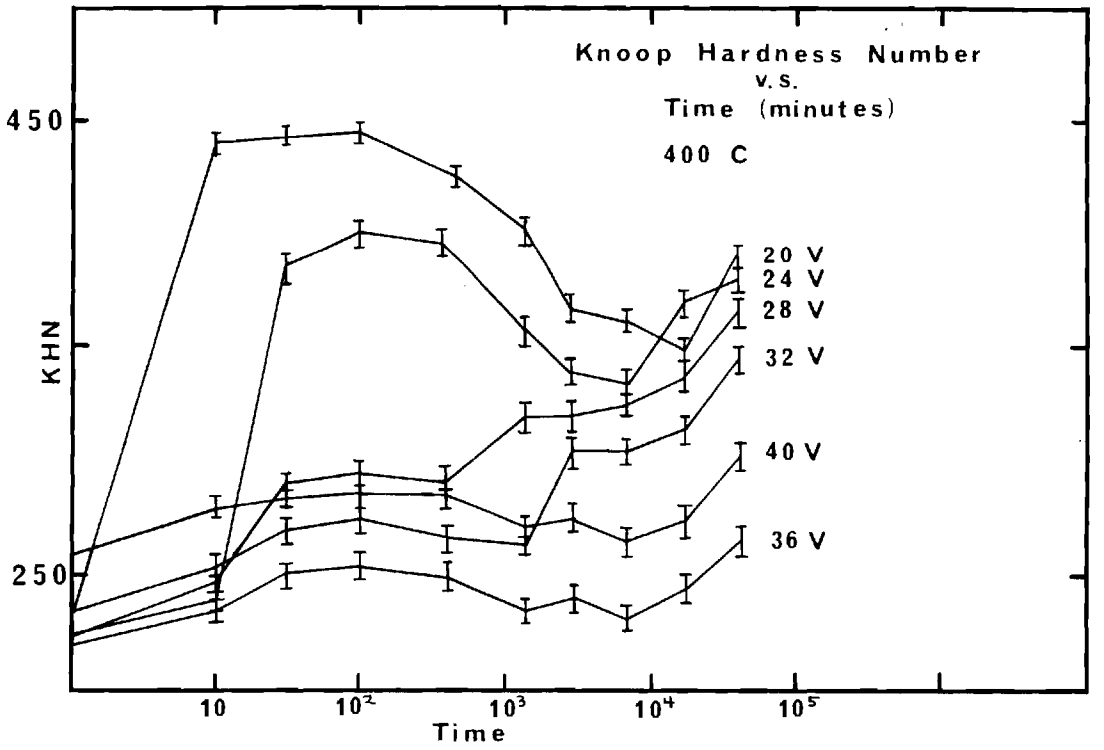

Figure 1. Microhardness changes in quenched and aged samples at 400°C as a function of composition.

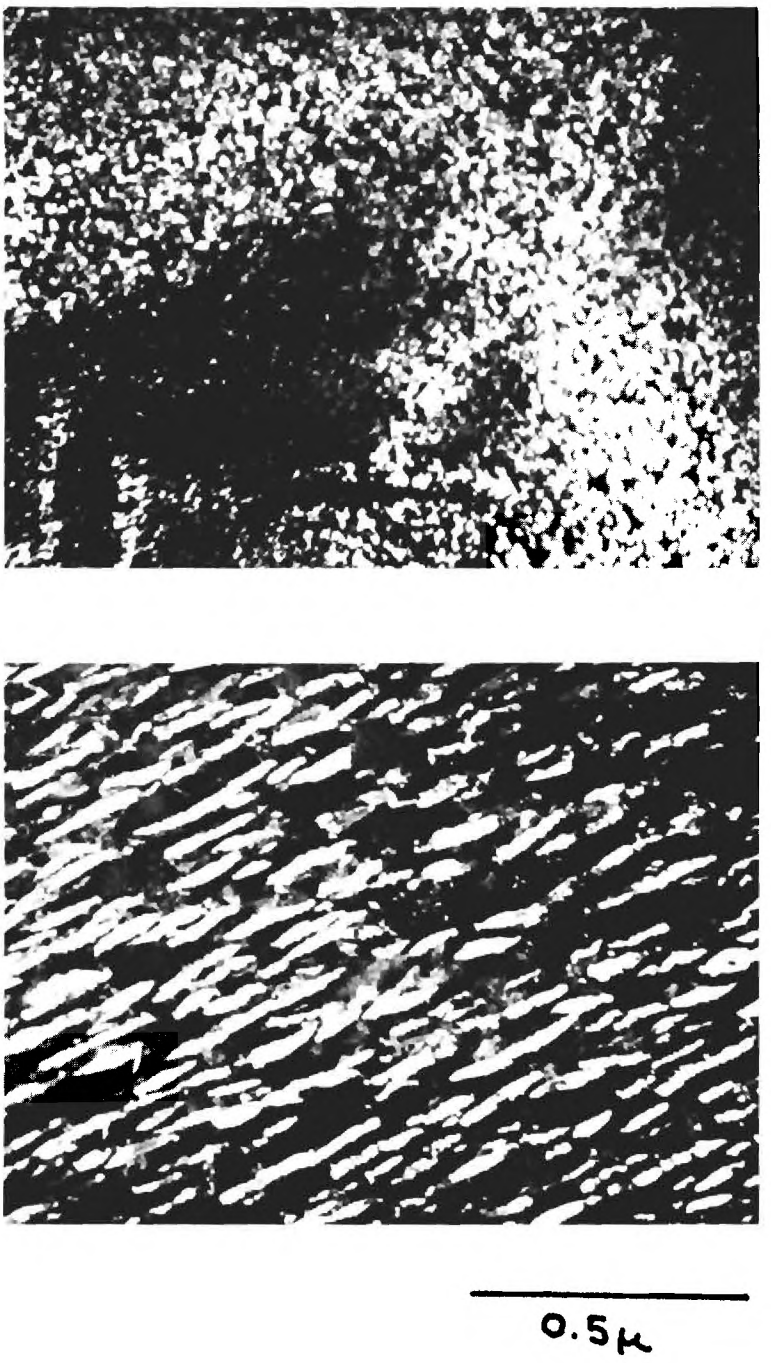

Figure 2. Typical microstructures in β Ti-V alloys aged at 400°C (a) cuboidal ω in 24% V aged 20 minutes (DF) (b) α particles in 28% V aged 1000 minutes. (DF)

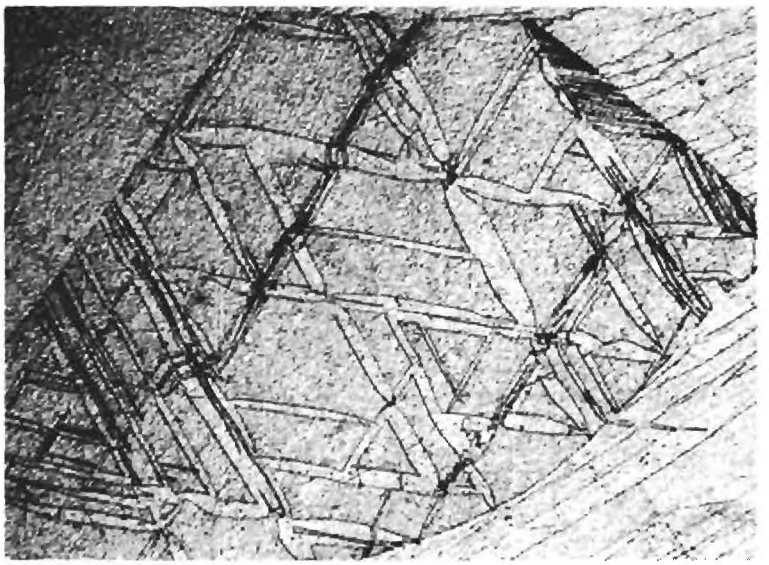

(a)

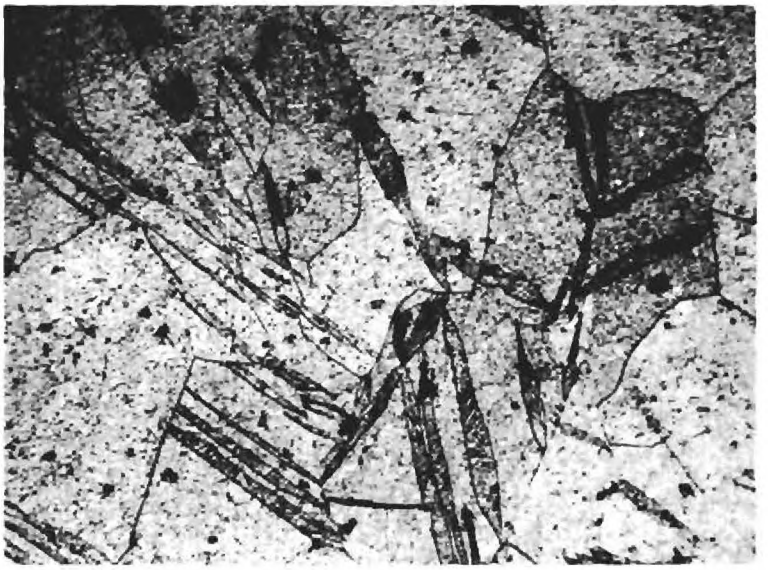

(b)

Figure 3. Coarse deformation twins in Ti-V alloys aged at 400°C (a) 24% V aged 20 minutes, (b) 28% aged 60 minutes. (150X)

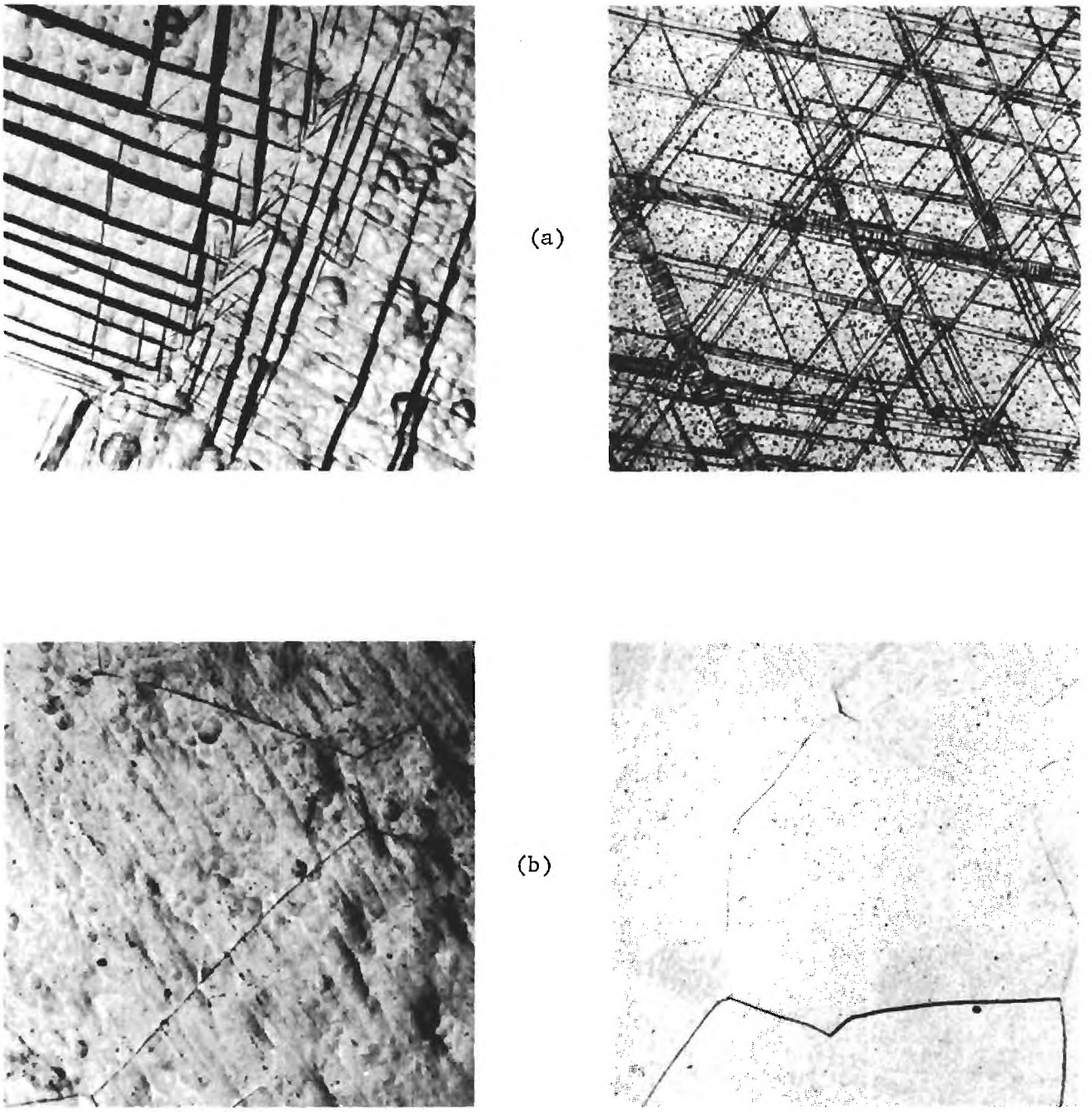

Figure 4. Showing twin to slip transition in 20% V alloy deformed $\simeq$ 3 to 5% in tension: (a) as-quenched contains ω, (b) aged 6 minutes at 400°C, failed in gage section. Micrographs on the left are of prepolished surfaces parallel to tensile axis, micrographs on right are polished sections of tensile specimens perpendicular to gage length. (150X)

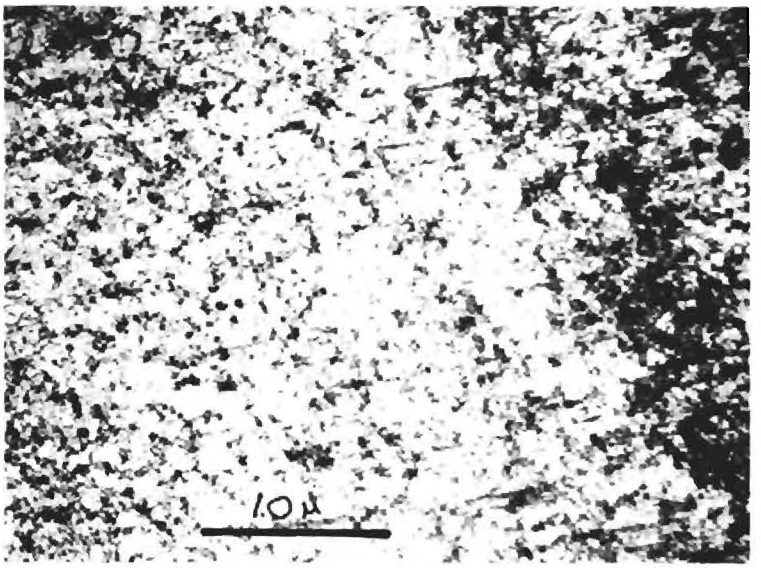

(a)

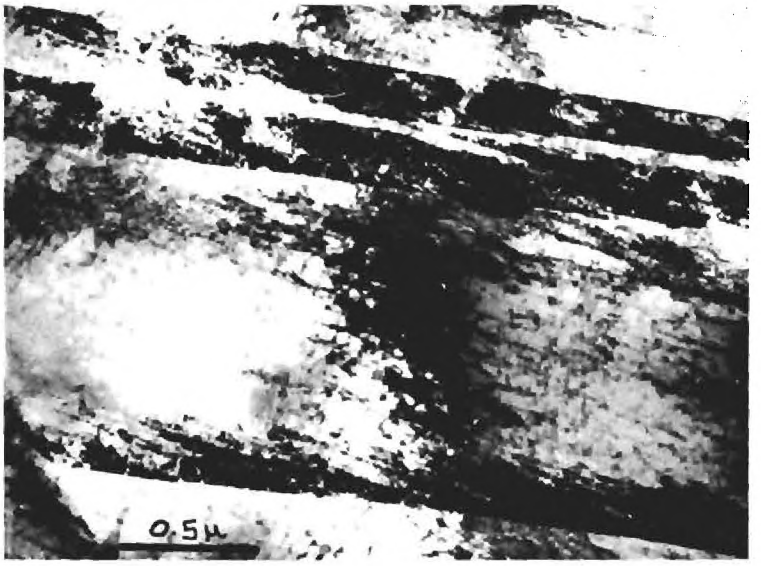

(b)

Figure 5. Deformation microstructures of Ti-V samples aged 100 minutes at 400°C and pulled $\simeq$ 3% in tension (a) 28% V (b) 32% V.

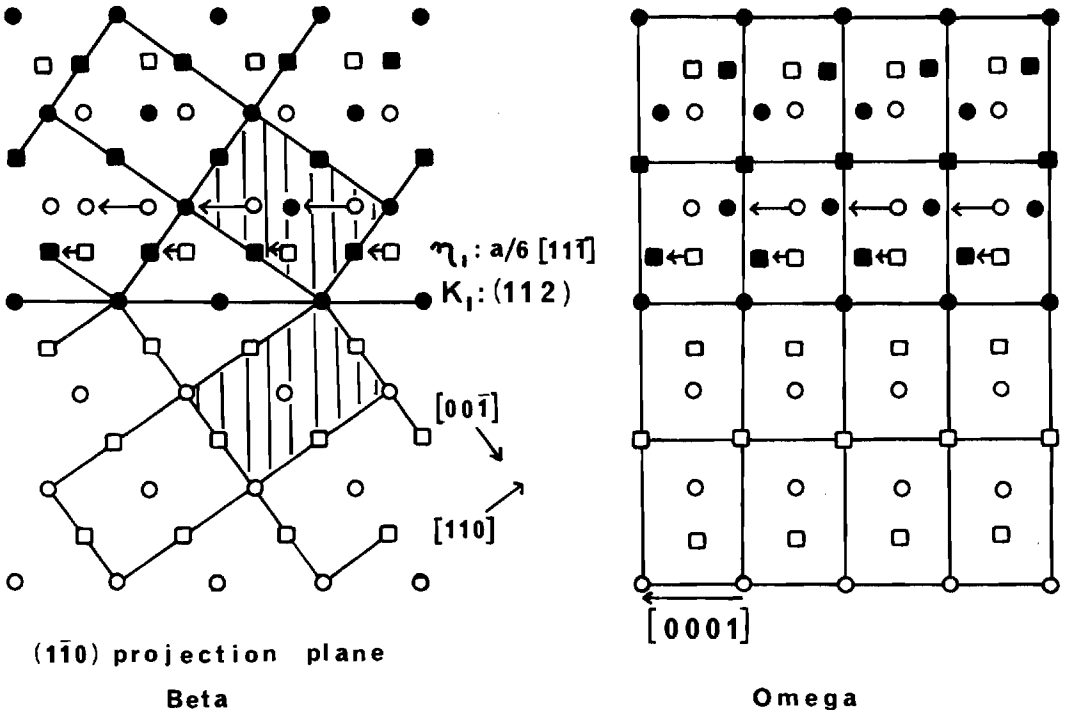

Figure 6. Schematic representation of a/6 <111> twinning shears in the ω structure. Note that the original ω structure is not preserved. Open symbols denote untwinned atom positions and filled symbols represent twinned atom positions. Squares represent atoms in plane above paper.

unclassified

SECURITY CLASSIFICATION OF THIS PAGE *(When Data Entered)*

REPORT DOCUMENTATION PAGE

READ INSTRUCTIONS BEFORE COMPLETING FORM

1. REPORT NUMBER: 75-1	2. GOVT ACCESSION NO.
3. RECIPIENT'S CATALOG NUMBER	
4. TITLE *(and Subtitle)*: Deformation Behavior in Quenched and Aged Beta Titanium Alloys	5. TYPE OF REPORT & PERIOD COVERED: Technical Report
	6. PERFORMING ORG. REPORT NUMBER
7. AUTHOR(s): H. G. Paris, B. G. LeFevre and E. A. Starke, Jr.	8. CONTRACT OR GRANT NUMBER(s): N00014-75-C-0349 NR 031-750
9. PERFORMING ORGANIZATION NAME AND ADDRESS: Metallurgy Program, School of Chemical Engr. Georgia Institute of Technology Atlanta, Georgia 30332	10. PROGRAM ELEMENT, PROJECT, TASK AREA & WORK UNIT NUMBERS
11. CONTROLLING OFFICE NAME AND ADDRESS: Metallurgy Program Office of Naval Research, 800 North Quincy St. Arlington, Virginia 22217	12. REPORT DATE: April 1974
	13. NUMBER OF PAGES
14. MONITORING AGENCY NAME & ADDRESS *(if different from Controlling Office)*	15. SECURITY CLASS. *(of this report)*: unclassified
	15a. DECLASSIFICATION/DOWNGRADING SCHEDULE

16. DISTRIBUTION STATEMENT *(of this Report)*

unlimited

17. DISTRIBUTION STATEMENT *(of the abstract entered in Block 20, if different from Report)*

18. SUPPLEMENTARY NOTES

Preprint of article submitted to Metallurgical Transactions

19. KEY WORDS *(Continue on reverse side if necessary and identify by block number)*

titanium alloys
deformation
microstructure

20. ABSTRACT *(Continue on reverse side if necessary and identify by block number)*

The deformation characteristics of quenched and aged Ti-V alloys in the composition range 20 to 40% V have been examined by optical metallography and transmission electron microscopy. A coarse lenticular deformation product similar in appearance to previously reported strain induced "martensites" was found to be associated with the occurrence of the omega phase. These features proved to be {112} <111> twins. Continued aging of the omega containing alloys resulted in a transition of the deformation mode from twinning to slip at a point which corresponded to the onset of embrittlement or

DD FORM 1 JAN 73 1473 EDITION OF 1 NOV 65 IS OBSOLETE
S/N 0102-014-6601

unclassified

SECURITY CLASSIFICATION OF THIS PAGE *(When Data Entered)*

E-19-632

OFFICE OF NAVAL RESEARCH

Contract N00014-75-C-0349, NR 031-750

TECHNICAL REPORT 77-1

THE CYCLIC STRESS–STRAIN RESPONSE OF TITANIUM–VANADIUM ALLOYS

By
S. B. Chakraborty, T. K. Mukhopadhyay,
and E. A. Starke, Jr.

August 30, 1977

Metallurgy Program, School of Chemical Engineering
Georgia Institute of Technology
Atlanta, Georgia 30332

OFFICE OF NAVAL RESEARCH

Contract N00014-75-C-0349, NR 031-750

TECHNICAL REPORT 77-1

THE CYCLIC STRESS-STRAIN RESPONSE OF TITANIUM-VANADIUM ALLOYS

by

S. B. Chakrabortty, T. K. Mukhopadhyay and E. A. Starke, Jr.
School of Chemical Engineering and Metallurgy
Georgia Institute of Technology
Atlanta, Georgia 30332

August 30, 1977

THE CYCLIC STRESS-STRAIN RESPONSE OF TITANIUM-VANADIUM ALLOYS

S. B. Chakrabortty, T. K. Mukhopadhyay
and E. A. Starke, Jr.

School of Chemical Engineering and Metallurgy
Georgia Institute of Technology
Atlanta, Georgia 30332

ABSTRACT

The cyclic stress-strain response of four Ti-V alloys (24, 28, 32 and 36wt.% V), which have deformation modes ranging from coarse twinning to wavy and planar slip, has been measured and correlated with deformation mode and microstructure. When coarse twinning is the primary deformation mode an anomalous Bauschinger effect, associated with untwinning during load reversal, is observed. A saturation flow stress is not obtained for the wavy slip alloy due to the intervention of microtwinning which inhibits cross slip and cell formation. Cyclic hardening of all alloys appears to be related, in some degree, to deformation twinning. Cyclic softening occurs for the planar slip alloys in the absence of microtwinning due to increasing mobile dislocation density.

INTRODUCTION

Laird[1,2] has recently reviewed the cyclic deformation of metals and alloys and has described the rapid hardening or softening which occurs in the early stages of fatigue life. It is clear from his reviews that the majority of work has been on fcc materials having either planar or wavy slip character, and very few studies have been concerned with the effect of alloying and deformation mode on the cyclic stress strain response of bcc metals. In addition, to the author's knowledge, there has been no previous study of ductile bcc alloys whose primary deformation mode is twinning. This paper is concerned with the cyclic stress strain response of a series of Ti-V alloys having deformation modes which vary from coarse twinning to wavy and planar slip.

Our previous studies[3-6] have shown that the deformation mode and ductility of titanium alloys containing from 20 to 40 weight percent vanadium can be controlled to a large extent by solute content and volume fraction of omega. Slip has been observed to change in character from fine wavy slip to coarse planar slip as the solute content is increased from 28% V to 40% V[3]. Both {110} and {112} slip occurs in the 28% V alloy, although {110} slip dominates, whereas planar {112} slip dominates in the 40% V alloy. In addition, {112} <111> twinning has been identified as an important deformation mode in the Ti-V system and can be controlled by proper solute content and thermal treatment. A change in deformation mode from slip to coarse twinning, with no loss in ductility, occurs in the low solute (20, 24, 28% V) alloys when the volume fraction of omega exceeds $\sim$ 0.1. Volume fractions larger than 0.6 result in partial or complete

embrittlement with an accompanied change in deformation mode from coarse twinning to slip. The onset of α precipitation in alloys containing less than 0.6 omega also induces a transition from coarse twinning to a mixture of fine twins and slip but without excessive loss in ductility. {112} <111> twins have been observed in electron micrographs of the 40% V alloy, but are too fine to be detected optically. X-ray line broadening measurements[3] have shown that a minimum in the twin fault probability exists for this system at 36% V.

The coarse twinning behavior in the low solute alloy is unusual since it is associated with the presence of omega, whose structure is incompatible with the a/6 <111> twinning shears of the bcc matrix. Dark-field and electron diffraction analysis showed that the $\{\bar{1}\bar{1}2\}$ <111> coarse twins contain omega precipitates suggesting a stress assisted $\omega \rightleftarrows \beta$ transformation during deformation twinning.[6] If the twinning mechanism is associated with a reversible omega transformation, and there is extensive evidence supporting this view[6,7], untwinning may occur under reversed or cyclic loading similar to that of Fe-Be[8] or the shape-memory alloy Au-Cd[9]. Such pseudoelastic effects can greatly effect the cyclic stress strain response and fatigue life of alloys[10-12].

The Ti-V system offered the possibility of studying the CSSR of bcc alloys having wavy and planar slip character, with the added bonus that the effects of both coarse and fine deformation twinning could be examined.

EXPERIMENTAL

Four Ti-V alloys, containing 24, 28, 32, and 36 weight percent vanadium were prepared by argon arc melting 99.95 percent purity

starting materials. The 50 gram ingots were vacuum encapsulated in quartz and homogenized for 100 hours at 950°C. They were then cold rolled in a random fashion to obtain a uniform thickness of 5 mm, recrystallized under vacuum for two hours at 850°C (above the β transus) and quenched in water. The recrystallized samples had a uniform grain size of ∿ 0.2 mm and a random texture. In addition, a 24% V alloy was prepared by Titanium Metals Corporation, Henderson, Nevada, where 14 cm diameter ingots were hot-forged and cross-rolled to produce plates 15 cm x 15 cm x 0.8 cm, having a random texture and an equiaxed grain size of ∿ 0.10 mm. The chemical analysis of this alloy is given in Table 1. Samples from the as-received plates were solutionized at 850°C and quenched in water. Property differences between laboratory and commercially prepared materials were within experimental error and measurements from the different lots are not distinguished in this paper.

As described in the Introduction, significant differences in deformation character exists for the selected alloys in the as-solutionized and quenched conditions. The microstructure and deformation behavior were characterized by x-ray diffraction, optical, scanning, and electron microscopy using procedures described previously[3-5]. Monotonic and cyclic property measurements were made on all alloys in the as-quenched condition, and after various heat treatments which were chosen to slightly alter the microstructure and deformation characteristics. The heat treatment, resulting microstructure, deformation characteristics, and tensile properties are listed in Table 2. Tensile samples were machined according to ASTM E-8-66 for sub-size specimens, and

tests were made at a strain rate of 10^{-3}/sec on an Instron testing machine equipped with a 1-in clip-on extensometer.

Low cycle fatigue samples were smooth and cylindrical, with a gage section approximately 6 mm long by 3.5 mm diameter, and were polished through a 1μ alumina and chromium oxide solution to remove all circumferential scratches. Most cyclic-stress-strain measurements were made on an electrohydraulic, closed-loop MTS testing machine under constant total strain control, with saw-tooth wave form, and at a strain rate of 10^{-3}/sec. However, the erratic response of the closed-loop system under strain control during deformation twinning of the 24% V alloy necessitated the use of stroke control for its CSS measurements. Strain was monitored by a 4 mm clip-on extensometer and the stroke was changed throughout the test so that the plastic strain range remained essentially constant.

RESULTS AND DISCUSSION

Coarse Twinning Conditions

The combination of vanadium content and quenching speed was not sufficient to suppress the omega formation in the 24% V alloy, and the primary deformation mode of the as-quenched condition was coarse twinning. The aged samples contained some alpha and showed a greater propensity for slip and an accompanying reduction in ductility, Table 2. The cyclic-stress-strain loops showed anomalies at the low strain amplitudes similar to those observed by Bolling and Richmond[8] for spontaneous untwinning in single crystals of Fe-25 at. % Be, although the magnitude of the effect was somewhat less in our polycrystalline samples. The Bauschinger effect, Figure 1, which is indicative of

the type III kinematic hardening described by Asaro[13,14], was measured by the method of Stoltz and Pelloux,[15] Figure 2. The Bauschinger back stress, $\Delta\sigma_b$, is indicative of the ease of recovery of the forward strain and the reversed Bauschinger strain, β, shows the extent of the recovery. Since a change in $\Delta\sigma_b$ indicates a similar change in β and since less error is involved in the measurement of $\Delta\sigma_b$, most conclusions in this paper are drawn from the values of $\Delta\sigma_b$. The Bauschinger back stress for the first cycle, $\Delta\sigma_b{}^1$, decreased with increasing strain amplitude, Figure 3a. The Bauschinger back stress also decreased with cycling at constant strain amplitude, Figure 3b. A greater strain dependency was observed for the aged samples which deformed by both twinning and slip. The reversed Bauschinger strain, β^{+1}, was almost completely recoverable for forward strain amplitudes up to 2% for both conditions tested, Figure 3c. The shape of the hysteresis loop was not symmetric, the compression side being narrower than the tension side, i.e., $B_- < B_+$. This is associated with a higher strength of the alloy in compression and was observed for both stroke and total strain control. The effect was larger for smaller strain amplitudes and diminished during the later part of life, Figure 4.

The anomalous Bauschinger effect described above is very similar to the pseudoelasticity associated with reversible stress-induced martensitic transformations in shape-memory alloys (for review, see Delaey et al.[16]). This is not surprising when one considers the similarity between deformation twinning and martensite reactions[17,18], and the fact that twinning in these low-solute alloys is associated with a stress-induced reversion of omega[7]. How and why this occurs is

not clear; however, it is evident that some type of energy absorption is associated with twinning (in addition to elastic accommodation energy). For small forward strains, small undamaged twins are formed and the twin energy is not dissipated. Consequently the twins should untwin to matrix when the applied stress is removed, Figure 1. For large strain amplitudes, the twins are damaged by interactions from other twins and dislocations, and some of the elastic accommodation energy is dissipated. Therefore, only part of the total energy associated with a twin is recoverable upon unloading and the Bauschinger back stress, which is a measure of the ease of stored energy recovery, decreases with increasing strain amplitude. The effect is magnified as the propensity for slip increases, as observed for the aged alloy.

It is known that deformation twin growth generates lattice defects in the vicinity of the twin interface, and as a consequence untwinning does not occur uniformly along the interface resulting in fragmented and damaged twins. This is quite evident when comparing the optical micrograph of twins formed under monotonic deformation, Figure 5a, with the optical micrograph of damaged twins formed under cyclic deformation, Figure 5b. A transmission electron micrograph of the damaged twins is shown in Figure 5c. In addition, untwinning leaves dislocation damage and accommodation kinking.[19] Consequently, the absorbed energy due to twinning is never completely recoverable during reversed loading, even for low strain amplitudes, and as cycling continues the Bauschinger back stress decreases as the accumulated plastic strain increases, Figure 3b.

The results of the low cycle fatigue tests are presented for the as-quenched, and aged 24% V alloy in Figures 6 and 7 respectively, as: (a) average cyclic stress amplitude versus accumulated plastic strain, (b) log of the plastic strain amplitude versus log of the number of reversals for crack initiation and (c) logarithmic monotonic and cyclic stress strain curves. The termination points of the curves in Figures 6a and 7a correspond to the first visual observation of cracks. The fatigue ductility coefficients, ε_f', the Coffin-Manson slopes, -c, and the monotonic and cyclic work hardening exponents n and n', are given on the Figures. The differences in these data for the two conditions was minimal, as would be expected since only small differences in deformation behavior were observed. The fatigue hardening observed for this alloy was the largest for any of the alloys tested, and saturation was never reached for any strain amplitude. Cyclic hardening began on the first cycle for the larger strain amplitudes; however, for the smaller strain amplitudes, the stress amplitude remained essentially constant for as many as 30 cycles before hardening commenced. The large degree of cyclic hardening is associated with twin interfaces acting as barriers to continued deformation and with lattice defects generated by the twinning mechanism. The lack of initial hardening observed during the low strain amplitude tests is associated with the reversibility of the deformation process, i.e., untwinning. However, as described previously, this reversibility disappears with cycling, at which time hardening begins. The twins formed at low strain amplitudes were smaller than those formed at high strain amplitudes, creating more interfaces and resulting in a relatively larger total hardening

effect for low strain amplitude cycling than for high strain amplitude cycling. This is reflected in the small cyclic hardening exponent, n', compared with the monotonic hardening exponent, n.

In order to study the effect of the large twins produced at high strain amplitudes on the cyclic hardening behavior at low strain amplitudes, a few samples were cycled as follows: one complete cycle at a strain amplitude of $\Delta\varepsilon_p/2 = 2.7\%$, followed by three cycles at $\Delta\varepsilon_p/2 = 1.3\%$, and then cycled to failure at $\Delta\varepsilon_p/2 = 0.1\%$. Figure 8 shows the results of this test, curve 2, along with a sample cycled to failure at a constant strain amplitude of $\Delta\varepsilon_p/2 = 0.1\%$, curve 1. Curve 2 always falls below curve 1 for the same $\Delta\varepsilon_p/2$. The high strain amplitude deformation results in large damaged twins within the grains. The presence of these twins reduces the propensity for further deformation twinning, and thus inhibits the formation of the numerous small (and relatively undamaged) twin interfaces responsible for the rapid hardening observed in the constant low strain amplitude test; AB in Figure 8. Consequently, the hardening is far less rapid for the variable strain amplitude test; FG in Figure 8. The rapid hardening observed along EF is due to the reduction in reversibility of the small twins caused by the presence of large damaged twin interfaces. A comparison of the twins produced in the constant amplitude test with those produced in the variable amplitude test is shown in Figure 9 (a and b). The most striking effect of the variable loading was its influence on crack propagation. The difference between N_f and N_i was approximately 1100 cycles for the variable loaded samples and approximately 15 cycles for the constant amplitude samples. Further crack propagation studies are now underway.

The Coffin-Manson-type plots for the two conditions tested for the 24% V alloy have unusually large slopes |c| and had a distinct break at low strain amplitudes similar to those observed for aluminum alloys.[20,21] It has been noted previously[21] that the deviation from the semi-empirical prediction of the Coffin-Manson relationship is related to the fatigue deformation processes prior to crack initiation; as must be the case here since the cycles to initiation, and not failure, are used for the abscissa. The resistance to fatigue crack initiation depends upon the homogeneity and reversibility of deformation. When deformation is reversible the damage is not accumulated to a great extent with cycling, and when it is homogeneous the accumulation is not localized. Since the deformation mode, i.e., twinning, is not reversible for large accumulated strains, and is accompanied by slip dislocations and formation of other lattice defects, a stable microstructure is never formed, resulting in early crack initiation and therefore a large |c|. The worst situation occurs at low strain amplitudes, because here the deformation is not only irreversible but also inhomogeneous.

There have been numerous observations[19,22] that plastic deformation is enhanced parallel to a twin boundary and that this localized slip leads to cracking at the twin matrix interface. The fact that the slip and twinning planes are the same in the Ti-V system suggests that this mechanism may be responsible for early crack initiation. Concentrated slip was observed near twin bands prior to crack initiation, Figure 10a, and cracks were later observed along the twin bands, Figure 10b.

Wavy Slip Condition

The as-quenched 28% V alloy was all beta phase (no omega detected by x-ray diffraction) and optical examination of deformed tensile samples revealed fine wavy slip and no deformation twins. The anomalous Bauschinger effect, observed for the 24% V alloy, was absent during cyclic deformation and measurements of the normal type I[13,14] Bauschinger strain were not made. The results of the low cycle fatigue test are presented in Figure 11. Unlike most materials that deform by wavy slip,[1,2,23,24] a saturation flow stress was never reached and cyclic hardening persisted until crack-initiation, Figure 11a. The magnitude of the hardening and the Coffin-Manson slope, $|c|$, were somewhat smaller than those observed for the 24% V alloy.

Optical examination of surface slip bands and polished cross sections of samples cycled to failure, Figure 12, confirmed that the primary deformation mode was wavy slip; at least on a macroscopic scale. No coarse deformation twins were observed. Although most similar studies have been on fcc metals and alloys, low cycle fatigue studies of iron[24,25] have shown that a saturation flow stress is obtained during cyclic deformation of that wavy-slip bcc metal. The related microstructure had well defined cells[25], analogous to those found in fcc metals.[26] Transmission electron microscopy studies of LCF samples of our as-quenched 28% V alloy revealed mostly wide deformation bands, Figure 13a, although microtwins were frequently observed, Figure 13b. Consequently, one must conclude that the wavy slip character observed optically is not due to the cross slip of screw dislocation which is normally associated with the

spreading of glide from two to three dimensions, but is most likely associated with the multiple slip systems previously observed for this alloy.[4] The lack of saturation and cell formation may be due to the intervention of a different deformation process, i.e., twinning, which inhibits dynamic recovery by cross slip and leads to early crack initiation in these strain controlled tests. In addition, connected cross-slip may be hindered by stress-induced omega precipitation similar to that detected in our early work on cold-rolled Ti-28%V single crystals.[3] The absence of a saturation stress, extensive hardening and lack of cell formation, similar to that observed here, was found in an Fe-1.5% Cu alloy containing noncoherent precipitate particles.[27] The authors concluded that the small precipitates were the cause of the continuous cyclic hardening and lack of cell formation.

In order to study the effect of a very small volume fraction of omega on the cyclic stress strain response of the Ti-28% V alloy, samples were aged for 360 minutes at 300°C. Previous hardness studies[5] had indicated that a small amount (less than can be routinely detected by x-ray diffraction) of isothermal omega is formed for this time, temperature, and vanadium concentration. The results of the low-cycle fatigue tests are shown in Figure 14, and should be compared with the as-quenched data of Figure 11. The cyclic hardening behavior and Coffin-Manson slopes, $|c|$, are very similar for the two conditions, as are the optically observed slip markings, Figure 15a. Transmission electron micrographs, Figure 15b, showed deformation structures similar to those of the fatigued as-quenched samples. However, omega precipitates were far more numerous than observed in deformed as-quenched samples.

The larger volume fraction of precipitates can certainly account for the higher strength of the aged alloy; however, the similarity in hardening behavior appears to be more related to the deformation mode and microtwin formation. This conclusion is drawn from the fact that although the amount of omega precipitates in the aged samples was considerably higher than in the deformed as-quenched samples, the magnitude of the cyclic hardening was essentially the same.

Planar Slip Conditions

The as-quenched 32% V and 36% V alloys contained all beta phase and optical examination of deformed tensile samples revealed coarse planar slip and no deformation twins. Previous studies[4,28,29] have shown that planar {112} slip dominates in these bcc Ti-V alloys. No anomalous Bauschinger effect was observed and Bauschinger strain measurements were not made. The results of the low cycle fatigue tests are presented in Figures 16 and 17. The Coffin-Manson slopes, $|c|$, were smaller than found for the other two alloys, and approximately equal to that found for most materials, i.e., ~ 0.5. The cyclic hardening/softening behavior was somewhat anomalous, in that cyclic softening was observed for low strain amplitude tests while cyclic hardening was found for high strain amplitude tests, Figures 16a, c and 17a, c.

Optical examination of polished cross sections of fatigued samples showed planar slip for all conditions, Figure 18, although there were some minor differences in homogeneity of slip band distribution. Transmission electron microscopy studies did, however, reveal differences which could at least qualitatively account for the hardening/

softening observed for the high/low strain amplitude tests. Foils taken from samples of both alloys, which were fatigued to failure at low strain amplitudes where softening occurred, revealed inhomogeneous deformation as ill defined dislocation bands separated by dislocation debris, Figure 19a. No microtwins were observed in any of these failures. In contrast, relatively homogeneous deformation, represented by evenly distributed dislocation debris and microtwins, Figure 19b, was observed in foils from as-quenched samples showing moderate cyclic hardening.

Cyclic softening, similar to that observed here, was found by Koss et al.[29,30] for a Ti-40 at.% V alloy cycled at a plastic strain amplitude of 0.5%. They concluded that the softening was not due to a metallurgical instability, but a result of dislocation dynamics wherein the mobile dislocation density increases in the presence of a high drag stress and low work hardening rate. We agree with their interpretation of the softening behavior. Koss did not observe cyclic hardening; however, he did not conduct tests at strain amplitudes as large as those that produced hardening in this study. Our earlier suggestion that the hardening behavior is associated with deformation twinning in this alloy system is supported by the microstructural study of the 32% V and 36% V alloys. The as-quenched alloys contained no precipitates, and in all cases where hardening occurred, microtwins were found; whereas microtwins were never observed for the conditions where softening occurred. Koss[31] has also never observed twinning in cyclic softened samples.

In order to collect more information on this hypothesis, low cycle fatigue tests were conducted on Ti-32% V and Ti-35% V samples aged to produce precipitates which enhance twinning, i.e., omega, and

homogenize slip, i.e., alpha. The results of these tests are presented in Figures 20, 21, and 22. No major differences in LCF behavior was observed in these aged alloys when compared with the results of their as-quenched counterparts. The Coffin-Manson slopes were essentially the same, cyclic softening was observed at low strain amplitudes and cyclic hardening at high strain amplitudes. Microtwins were infrequently observed in the aged cyclic-softened samples, and were certainly far fewer than observed in as-quenched cyclic hardened samples.

CONCLUSIONS

1. Alloys which deform by coarse twinning exhibit an anomalous Bauschinger effect due to untwinning during reversed loading. Large cyclic hardening was due to twin interfaces acting as barriers to continued cyclic deformation and with lattice defects generated by the twinning mechanism. Crack initiation is associated with concentrated slip near twin bands.

2. Alloys which deformed by wavy slip exhibited cyclic hardening and no saturation prior to crack initiation. The wavy slip character was due to multiple slip and not connected cross slip of screw dislocations. The lack of saturation and cell formation was associated with the intervention of deformation twinning which prevented dynamic recovery by cross slip.
3. Alloys which deformed by planar slip showed cyclic softening at low strain amplitudes and cyclic hardening at high strain amplitudes. The softening behavior is associated with dislocation dynamics and the hardening behavior with deformation twinning.

4. The hardening behavior of all the Ti-V alloys examined is due, at least in part, to deformation twinning inhibiting dynamic recovery.
5. Although the large Coffin-Manson slopes, $|c|$, of the alloys that showed extensive twinning indicate inferior fatigue performance in these strain controlled tests, their cyclic hardening behavior suggests that they may be superior in stress controlled applications.

REFERENCES

1. Campbell Laird in Plastic Deformation of Materials, R. J. Arsenoult, ed., pp. 101-102, Academic Press, San Francisco, 1975.

2. Campbell Laird in Work Hardening in Tension and Fatigue, Anthony W. Thompson, ed., pp. 150-176, AIME, New York, 1977.

3. Fu-Wen Ling, H. J. Rack, and E. A. Starke, Jr., Met. Trans., 4, (1973) 1671.

4. Fu-Wen Ling, E. A. Starke, Jr., and B. G. LeFevre, Met. Trans., 5, (1974) 179.

5. H. G. Paris, B. G. LeFevre, and E. A. Starke, Jr., Met. Trans. 7A, (1976) 273.

6. H. G. Paris, B. G. LeFevre, and E. A. Starke, Jr., "The Deformation Twinning Behavior of $\beta + \omega$ Microstructure in Ti-V Alloys," Technical Report 76-1 Office of Naval Research Contract N00014-75-C-0349, NR 031-750, June 15, 1976.

7. H. G. Paris, Ph.D. Thesis, Georgia Institute of Technology, Atlanta, Georgia, August, 1975.

8. G. F. Bolling and R. H. Richman, Acta Met., 13, (1965) 709, 723, 745.

9. D. S. Lieberman, M. A. Schmerling and R. W. Kary, in Shape Memory Effects in Alloys, J. Perkins, ed., pp 203-244, Plenum Press, New York, 1975.

10. W. A. Rochinger, Brit. J. Appl. Phys., 9, (1958) 250; J. Aust. Inst. Metals, 5, (1960) 114.

11. W. J. Buehler and F. W. Wang, Ocean Eng., 1, (1968) 105.

12. N.Y.C. Yang, C. Laird and D. P. Pope, Met. Trans. A, 8A, (1977) 955.

13. R. J. Asaro, Acta Met., 23, (1975) 1255.

14. R. J. Asaro, in Work Hardening in Tension and Fatigue, Anthony W. Thompson, ed., pp 206-223, AIME, New York, 1977.

15. R. E. Stoltz and R. M. Pelloux, Met. Trans A., 7A, (1976) 1295.

16. L. Delsey, R. V. Krishnan, H. Tas, and H. Warlimont, J. Mat. Sci., 9, (1974), p 1521, 1536, and 1545.

17. Robert E. Reed-Hill, Physical Metallurgy Principles, D. Van Nostrand Co., Inc., New Jersey, 1964, p 399.

18. D. V. Wield and E. Gillam, Acta Met., 25, (1977) p 725.

19. P. G. Partridge, Phil. Mag., 12, (1965) p 1043.

20. T. H. Sanders, Jr. and E. A. Starke, Jr., Met. Trans. A, 7A, (1976) p 1407.

21. R. E. Sanders, Jr. and E. A. Starke, Jr., Mat. Sci. & Eng., 28, (1977) p 53.

22. I. A. Gendin and Ya. D. Starodubov, Soviet Physics - Solid State, 2, (1960) p 968.

23. C. E. Feltner and C. Laird, Acta Met., 15, (1967) p 1621.

24. C. E. Feltner and C. Laird, Trans. TMS-AIME, 245, (1969) p 1372.

25. H. Abdel-Raouf and A. Plumtree, Met. Trans., 2, (1971) p 1251.

26. D. Kuhlmann-Wilsdorf and C. Laird, Mat. Sci. & Eng., 27 (1977) p 137.

27. J. T. McGrath and W. J. Bratina, Phil. Mag., 21, (1970) p 1087.

28. N. E. Paton and J. C. Williams in Second Inter. Conf. on the Strength of Metals and Alloys, Asilomar, Pacific Grove, California, (1970) Vol. 1, Paper 1.8 p 108.

29. Donald A. Koss and Craig C. Wocik, Met. Trans A, 7A, (1976) p 1243.

30. G. Theodorski and D. A. Koss, to be published in Third Int. Conf. on Ti (Moscow, May, 1976).

31. Donald A. Koss, Michigan Technological University, Houghton, Michigan, private communication, 1977.

TABLE 1

Compositions of the Titanium-Vanadium Alloy

Alloy	V	Fe	O	N	Ti
Ti-24	24.1	0.04	0.06	0.007	Balance

TABLE 2

	Alloy	Heat Treatment	Microstructure	Deformation Mode	Yield Strength $\sigma_{0.2}$ (MPa)	$\epsilon_f (\ln \frac{a_o}{a_f})$
1a	Ti-24V	As-Quenched	β + athermal ω	Primarily Coarse Twins	520	0.82
1b	Ti-24V	90 min @ 515°C	$\beta + \alpha$ + athermal ω	Coarse Twins + Slip	565	0.51
2a	Ti-28V	As-Quenched	β	Fine Wavy Slip + Microtwins	618	0.63
2b	Ti-28V	360 min @ 300°C	$\beta + \omega$	Primarily Wavy Slip + Twins	720	0.50
3a	Ti-32V	As-Quenched	β	Planar Slip	782	0.47
3b	Ti-32V	4700 min @ 350°C	$\beta + \omega$	Fine Slip	956	0.46
4a	Ti-36V	As-Quenched	β	Coarse Planar Slip	664	0.86
4b	Ti-36V	100 min @ 400°C	$\beta + \omega + \alpha$	Fine Slip	772	0.72
4c	Ti-36V	10,000 min @ 400°C	$\beta + \alpha$	Fine Slip	880	0.11

FIGURE CAPTIONS

1. Cyclic stress strain response during the first cycle for Ti-24%V at various strain amplitudes showing an anamalous Bauschinger effect.

2. Graphical construction for measuring the Bauschinger effect. After Stoltz and Pelloux.[15]

3. Bauschinger Stress and strain data for Ti-24%V alloy.

4. Graphical representation of assymmetry of hysteresis loop with fatigue life for Ti-24%V alloy.

5. Deformation structure of as-quenched Ti-24%V alloy. (a) Optical micrograph after monotonic deformation. (b) Optical micrograph after cyclic deformation (c) TEM after cyclic deformation.

6. Low cycle fatigue behavior of Ti-24%V, as-quenched. (a) stress amplitude vs. accumulative plastic strain, (b) Coffin-Manson plot, (c) cyclic and monotonic stress-strain curves

7. Low cycle fatigue behavior of Ti-24%V, aged 90 minutes at 515°C.

8. Cyclic hardening curves for Ti-24%V alloy using a constant strain amplitude,curve 1; and a variable strain amplitude, curve 2.

9. Deformation twins produced under cyclic straining of Ti-24%V. (a) constant strain amplitude, (b) variable strain amplitude.

10. Scanning electron micrograph of the surface of Ti-24%V fatigue samples. (a) concentrated slip near twin bands, (b) crack along twin bands.

11. Low cycle fatigue behavior of Ti-28%V, as quenched.

12. Optical micrograph of polished and etched cross section of Ti-28%V fatigue sample.

13. Transmission electron micrographs of Ti-28%V fatigue sample. (a) deformation bands, (b) microtwins.

14. Low cycle fatigue behavior of Ti-28%V aged 360 minutes at 300°C.

15. Deformation structure of fatigue samples of aged 360 minutes at 300°C. (a) Optical micrograph (b) transmission electron micrograph.

16. Low cycle fatigue behavior of Ti-32%V, as quenched.

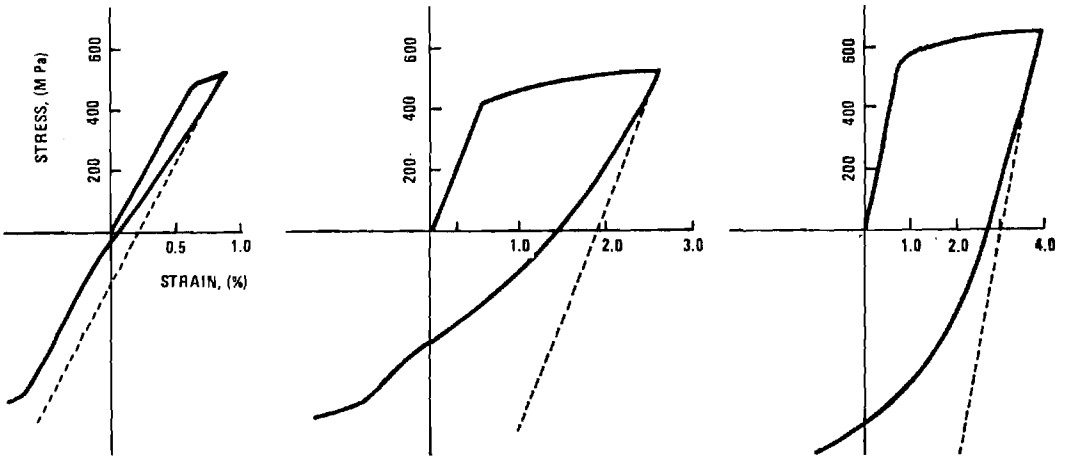

Figure 1. Cyclic stress strain response during the first cycle for Ti-24%V at various strain amplitudes showing an anamalous Bauschinger effect.

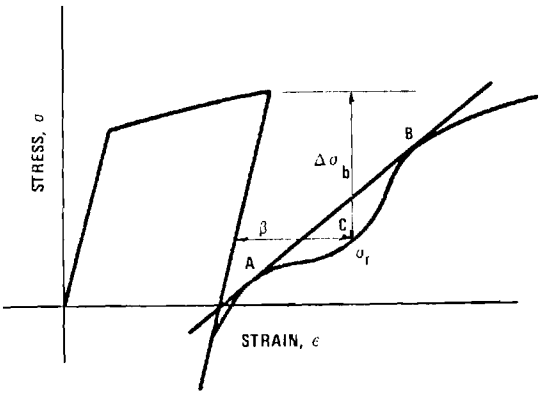

Figure 2. Graphical construction for measuring the Bauschinger effect. After Stoltz and Pelloux.[15].

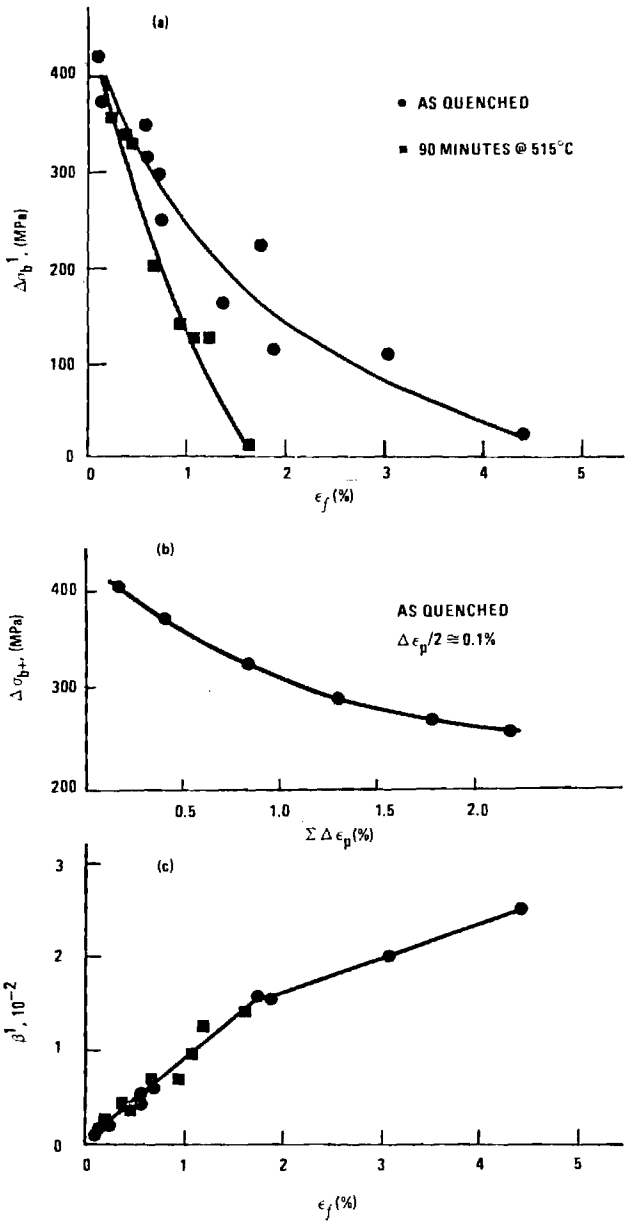

Figure 3. Bauschinger stress and strain data for Ti-24%V alloy.

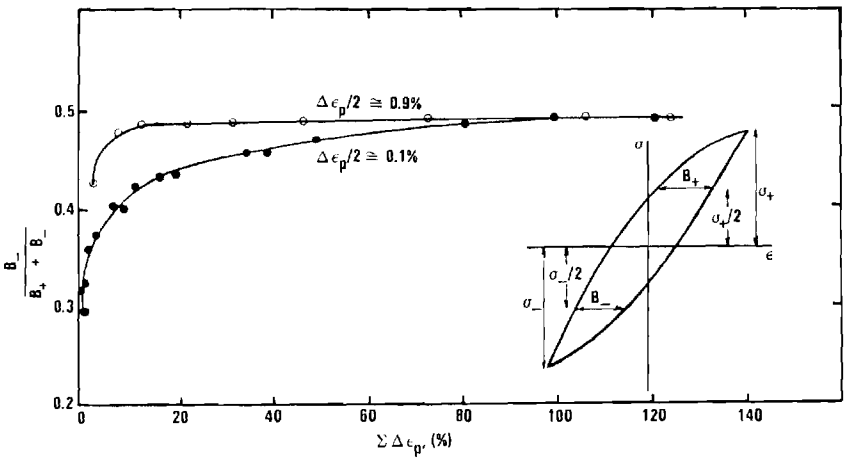

Figure 4. Graphical representation of assymmetry of hysteresis loop with fatigue life for Ti-24%V alloy.

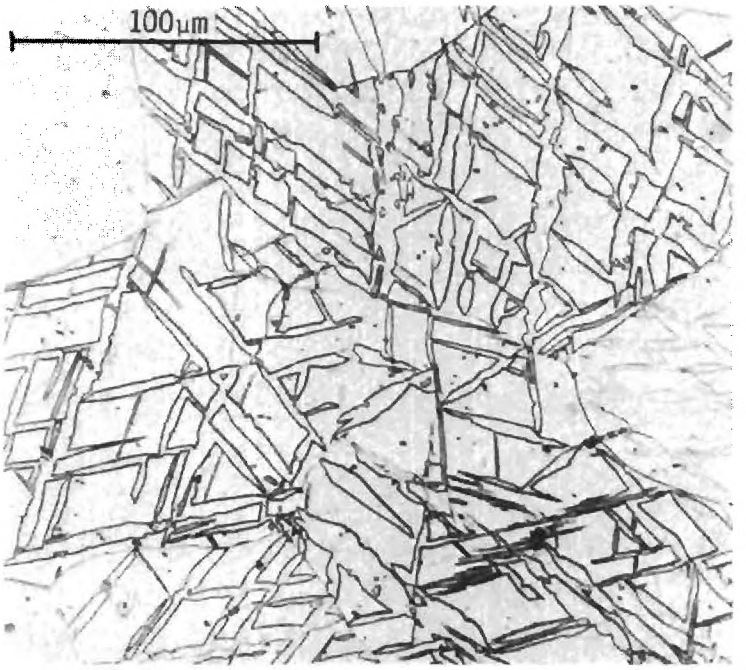

5a

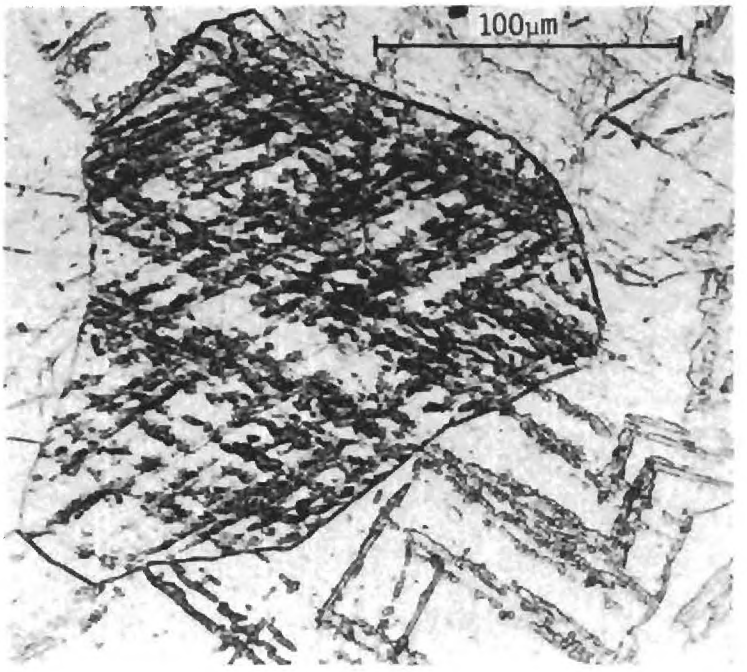

5b

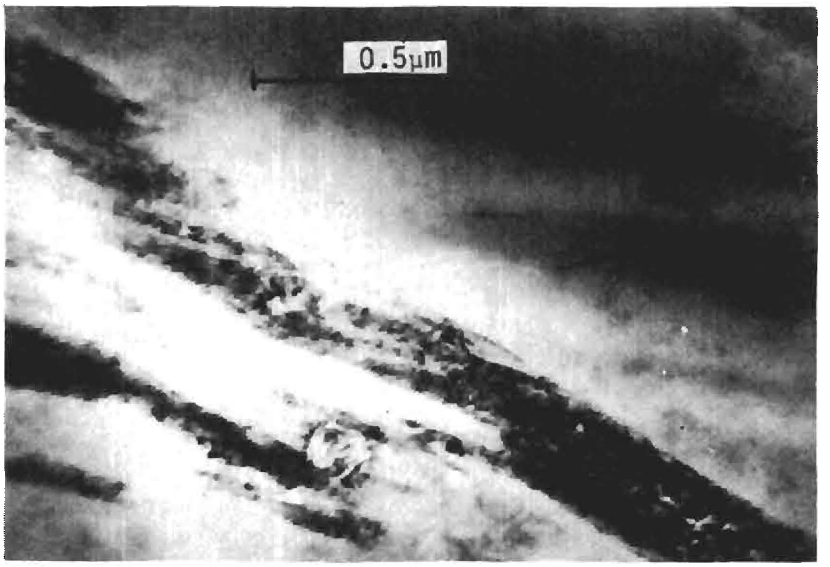

5c

Figure 5. Deformation structure of as-quenched Ti-24%V alloy. (a) Optical micrograph after monotonic deformation. (b) Optical micrograph after cyclic deformation (c) TEM after cyclic deformation.

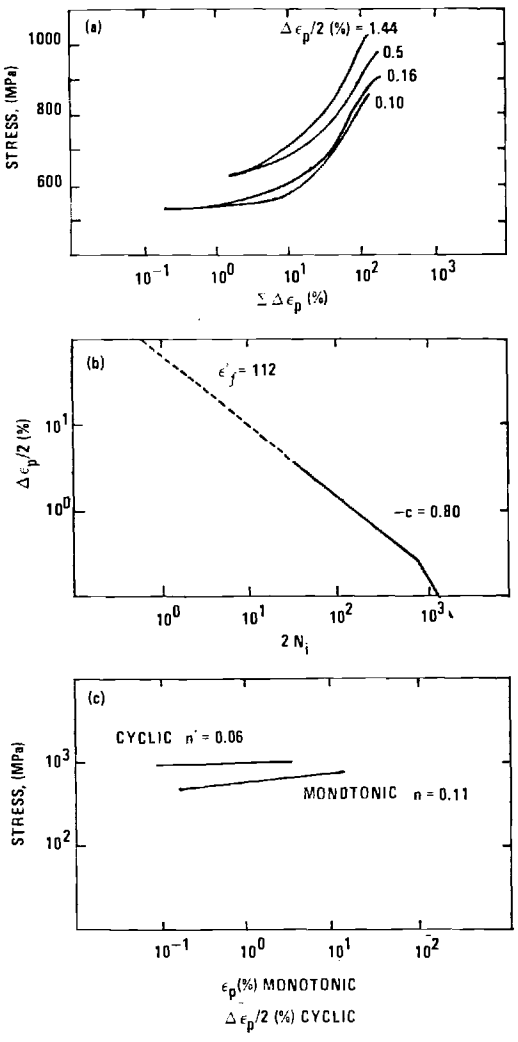

Figure 6. Low cycle fatigue behavior of Ti-24%V, as-quenched.

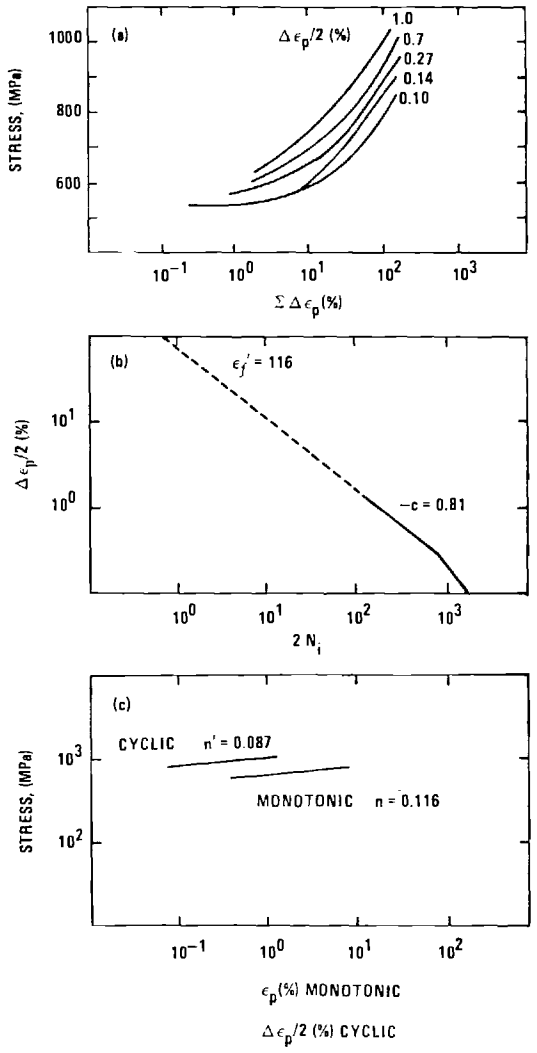

Figure 7. Low cycle fatigue behavior of Ti-24%V, aged 90 minutes at 515°C.

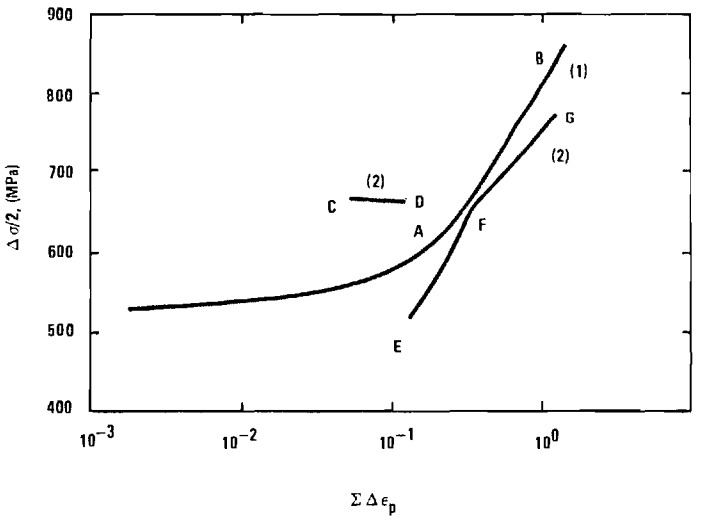

Figure 8. Cyclic hardening curves for Ti-24%V alloy using a constant strain amplitude curve 1; and a variable strain amplitude, curve 2.

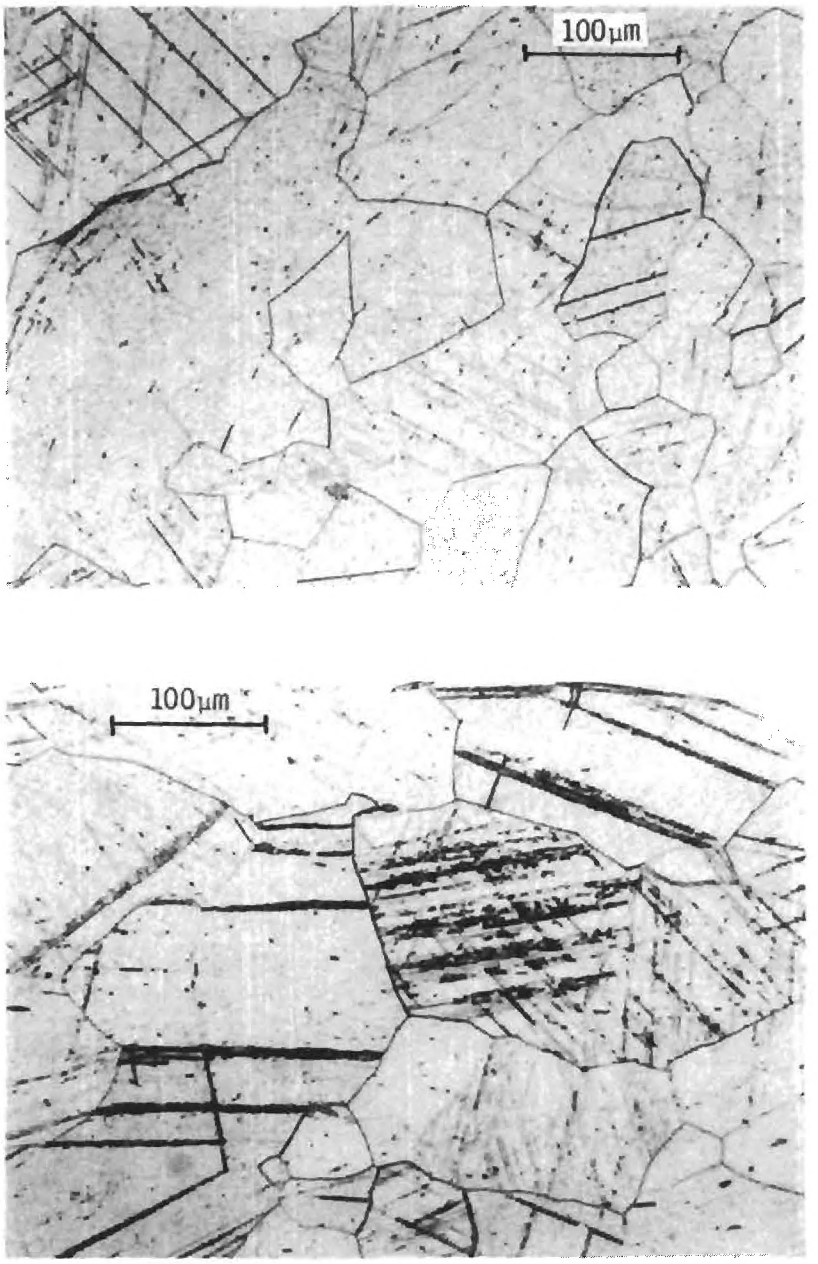

Figure 9. Deformation twins produced under cyclic straining of Ti-24%V. (a) constant strain amplitude, (b) variable strain amplitude.

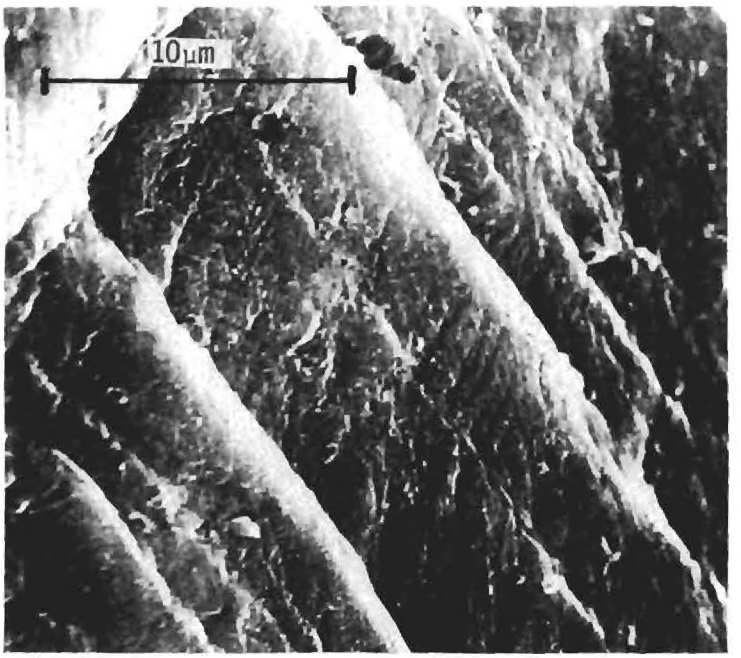

a

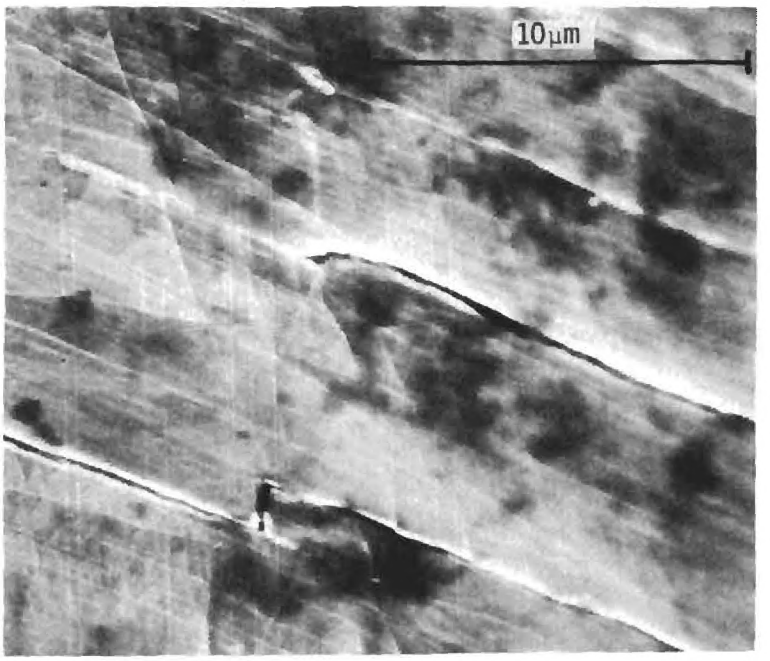

b

Figure 10. Scanning electron micrograph of the surface of Ti-24%V fatigue samples. (a) concentrated slip near twin bands, (b) crack along twin bands.

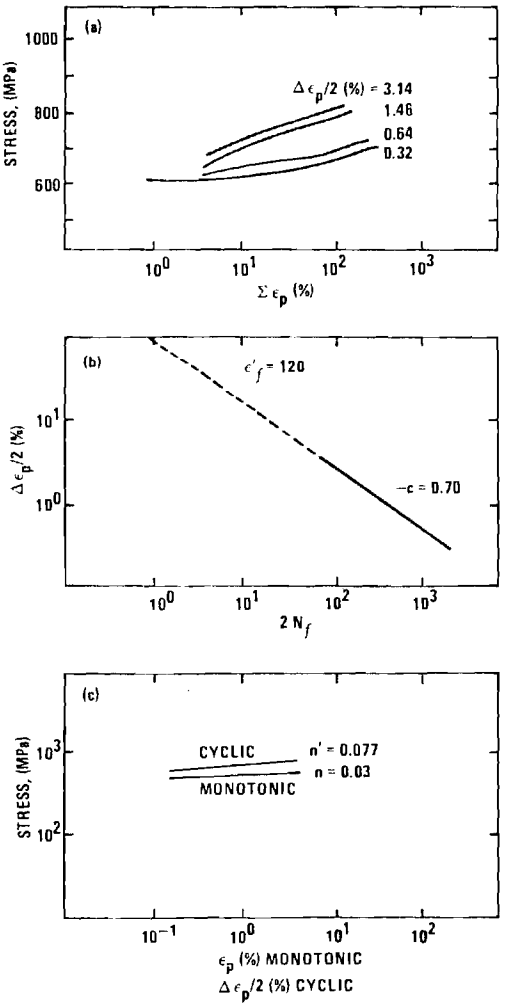

Figure 11. Low cycle fatigue behavior of Ti-28%V, as quenched.

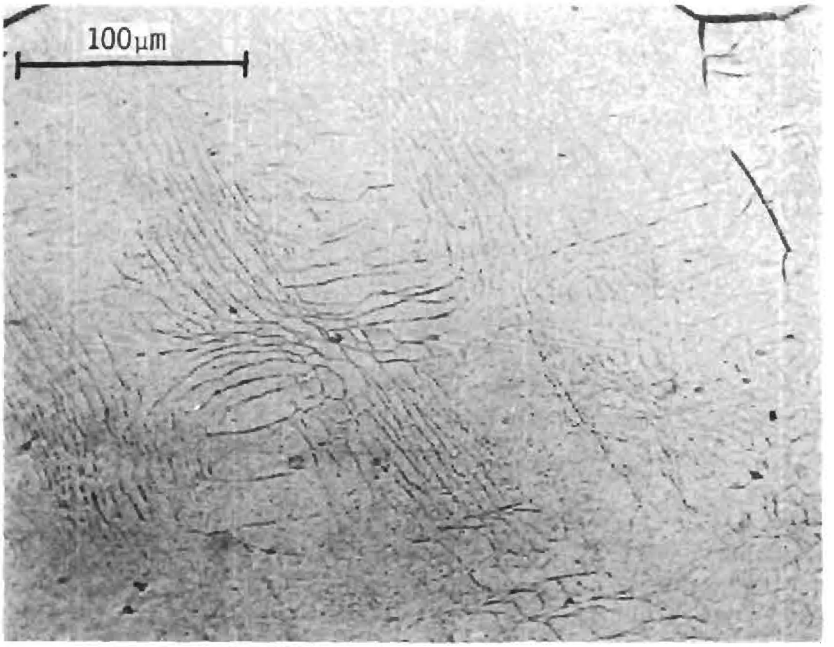

Figure 12. Optical micrograph of polished and etched cross section of Ti-28%V fatigue sample.

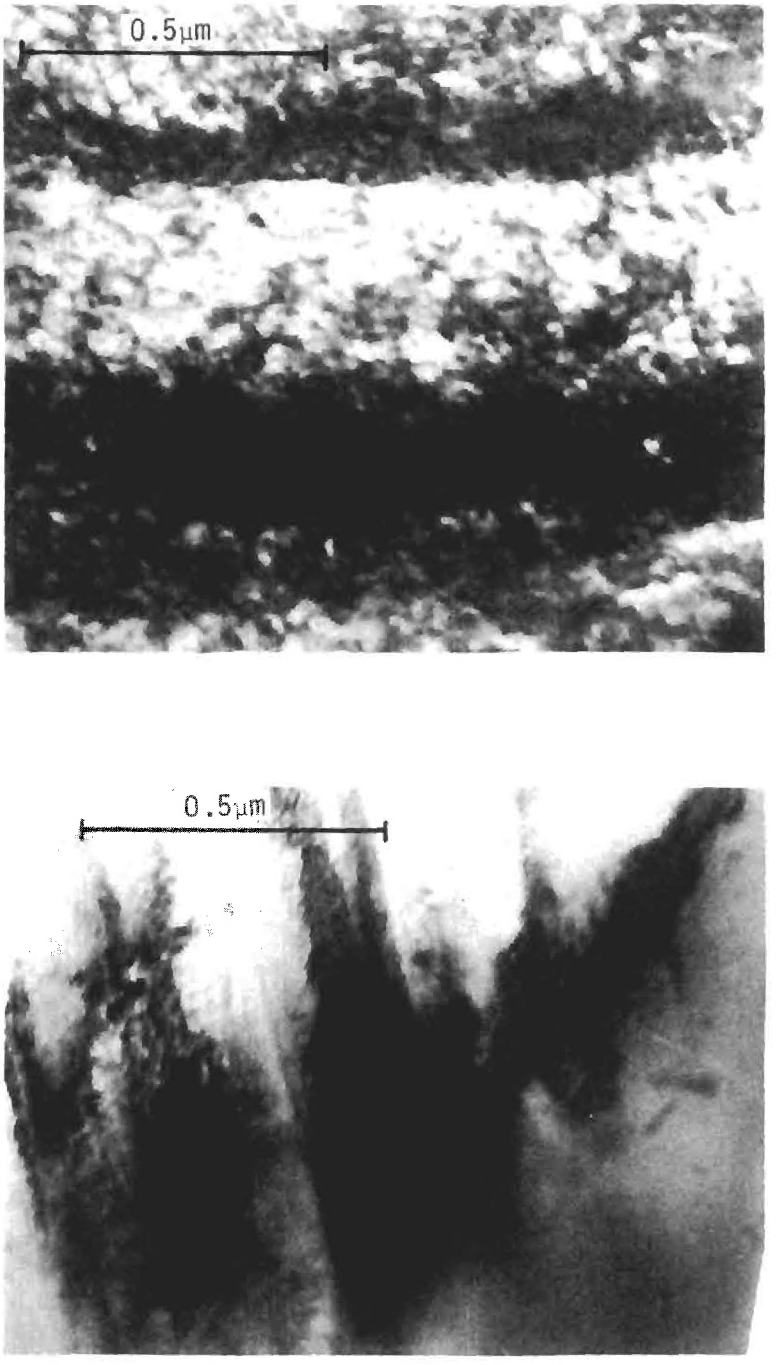

Figure 13. Transmission electron micrographs of Ti-28%V fatigue sample. (a) deformation bands, (b) microtwins.

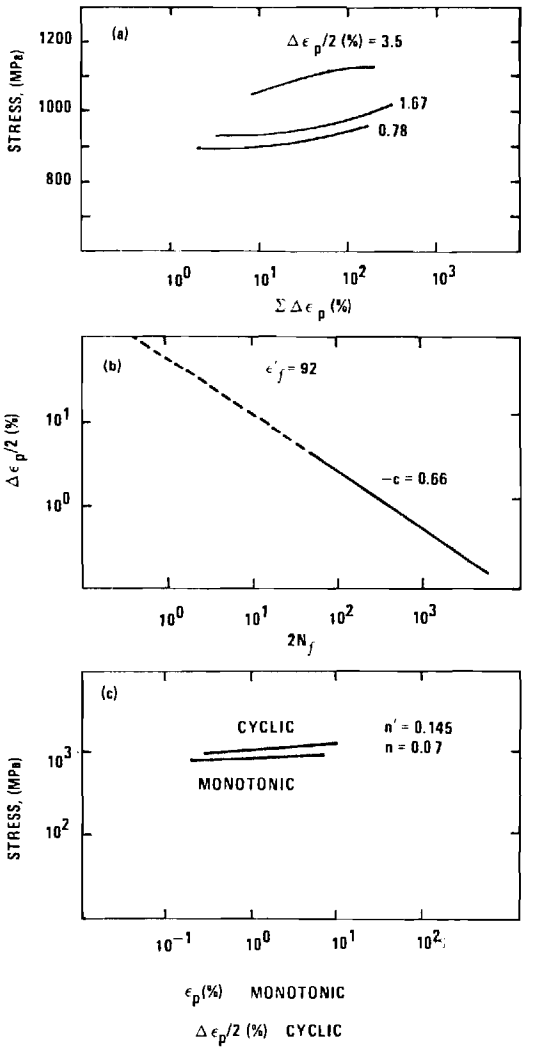

Figure 14. Low cycle fatigue behavior of Ti-28%V aged 360 minutes at 300°C.

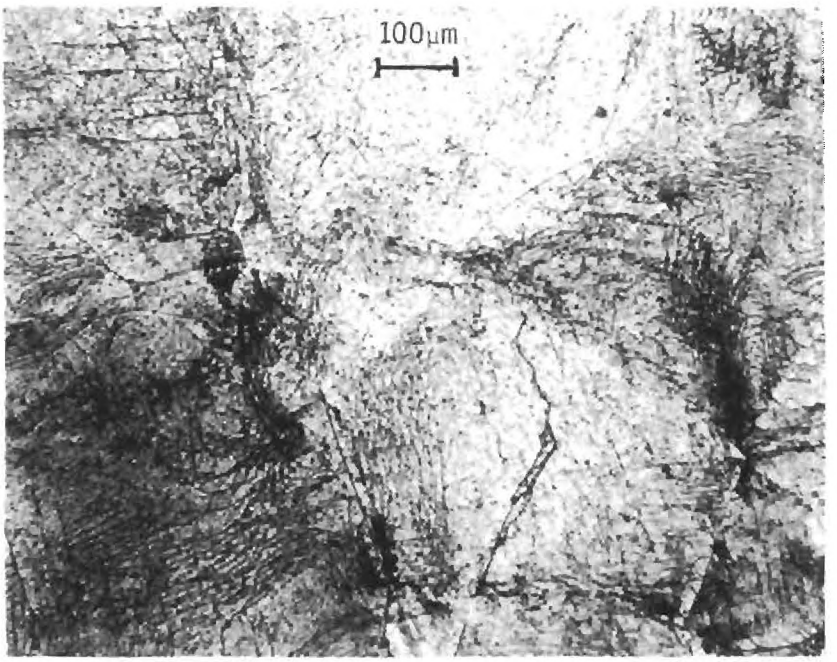

a

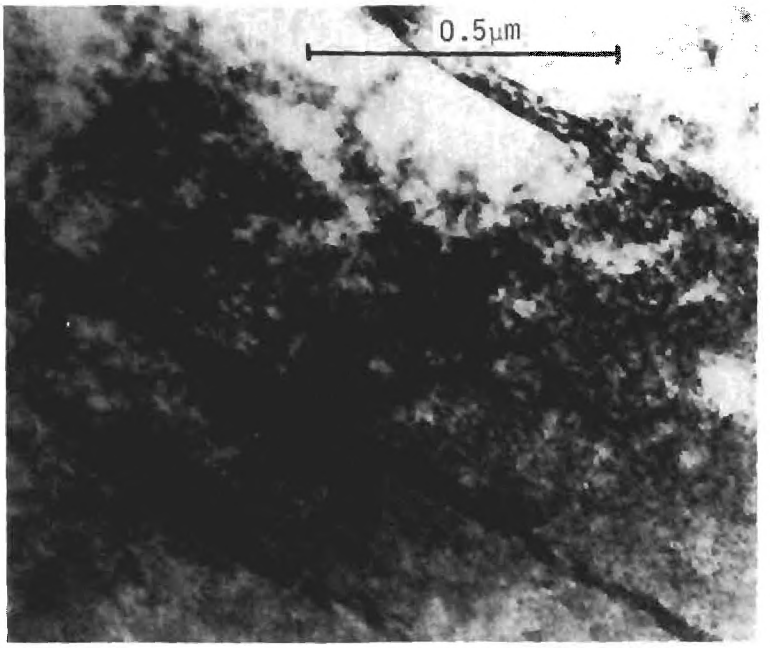

b

Figure 15. Deformation structure of fatigue samples of aged 360 minutes at 300°C. (a) Optical micrograph (b) transmission electron micrograph.

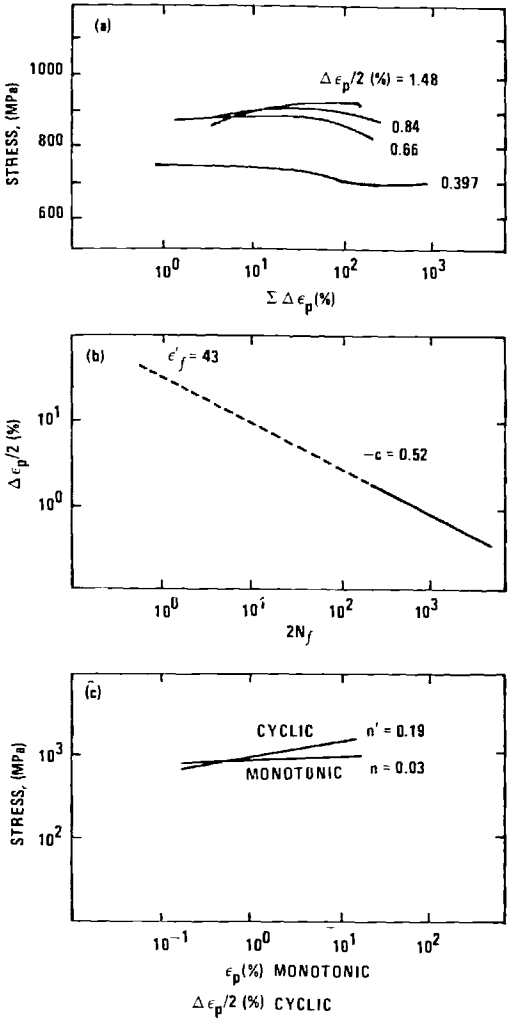

Figure 16. Low cycle fatigue behavior of Ti-32%V, as quenched.

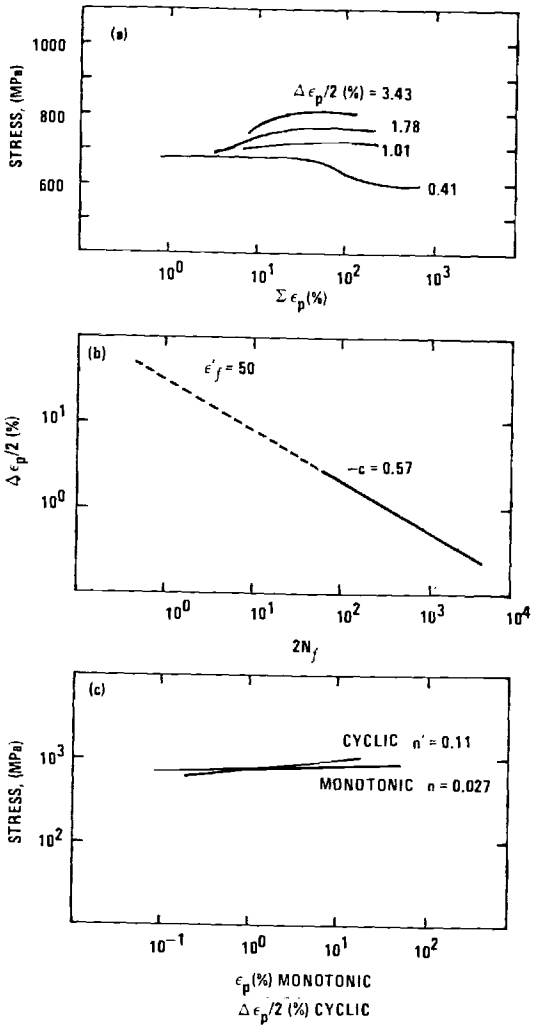

Figure 17. Low cycle fatigue behavior of Ti-36%, as quenched.

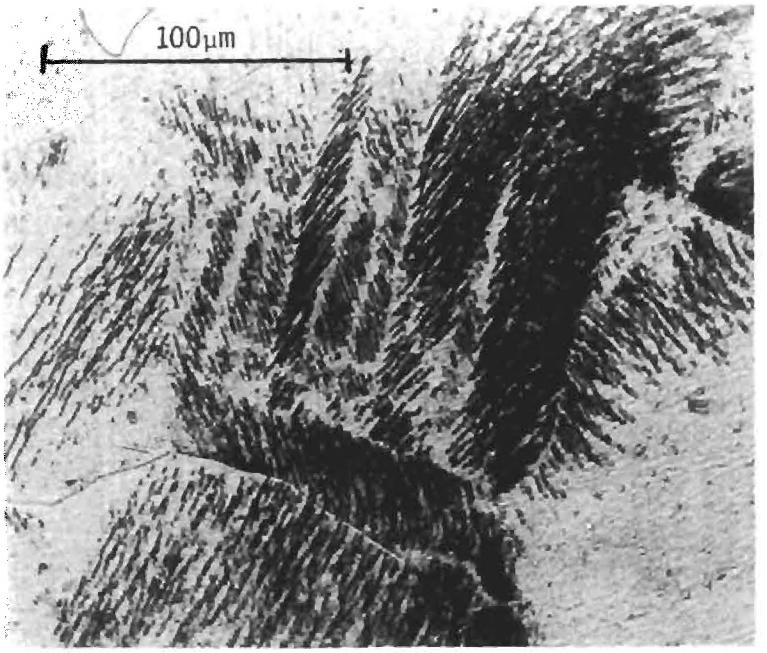

Figure 18. Optical micrograph showing typical slip markings observed in polished and etched cross sections of as quenched fatigue samples of both 32% and 36% alloys.

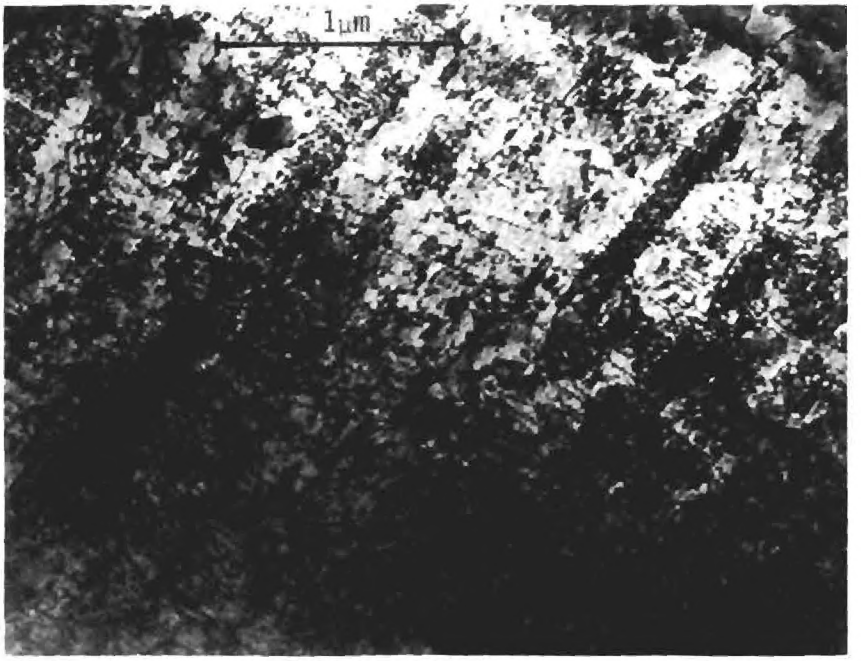

a

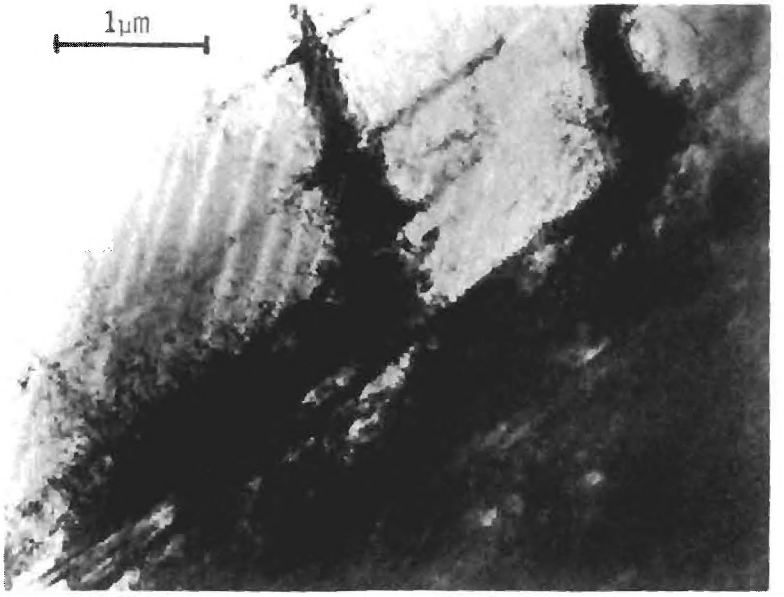

b

Figure 19. Typical deformation structure of as quenched fatigued 32% and 36%V alloys. (a) low strain amplitude where cyclic softening occurred. (b) high strain amplitude where moderate hardening occurred.

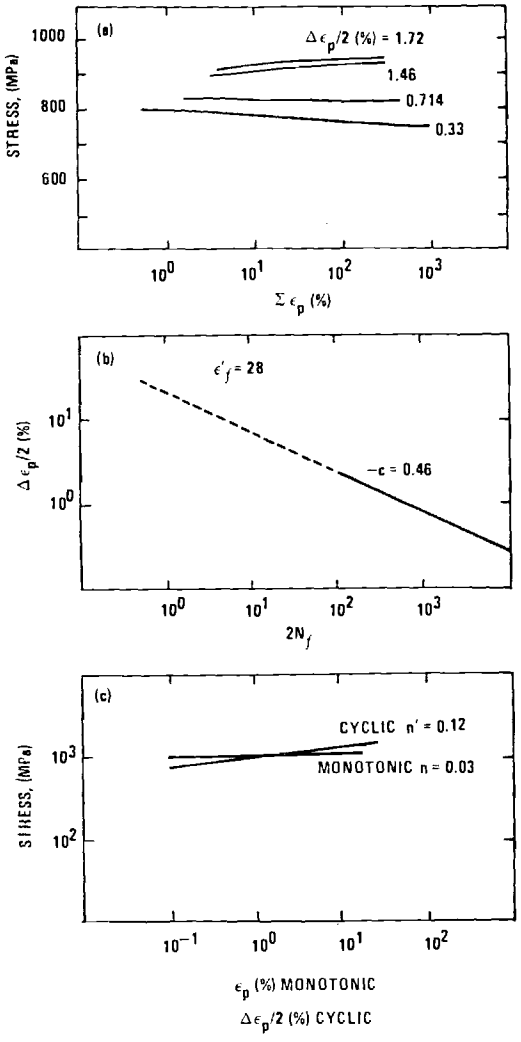

Figure 20. Low cycle fatigue behavior of Ti-32%V aged 4,700 minutes at 350°C.

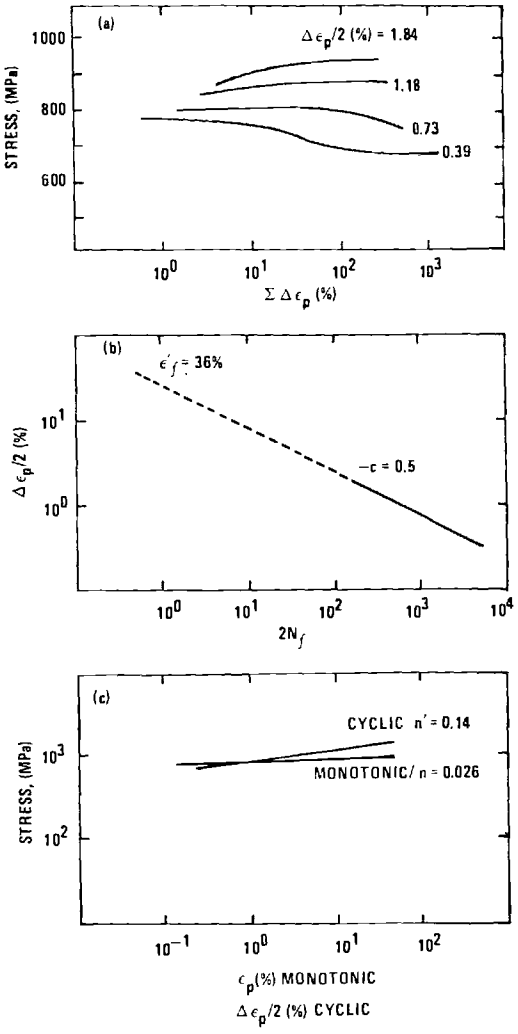

Figure 21. Low cycle fatigue behavior of Ti-36%V aged 100 minutes at 400°C.

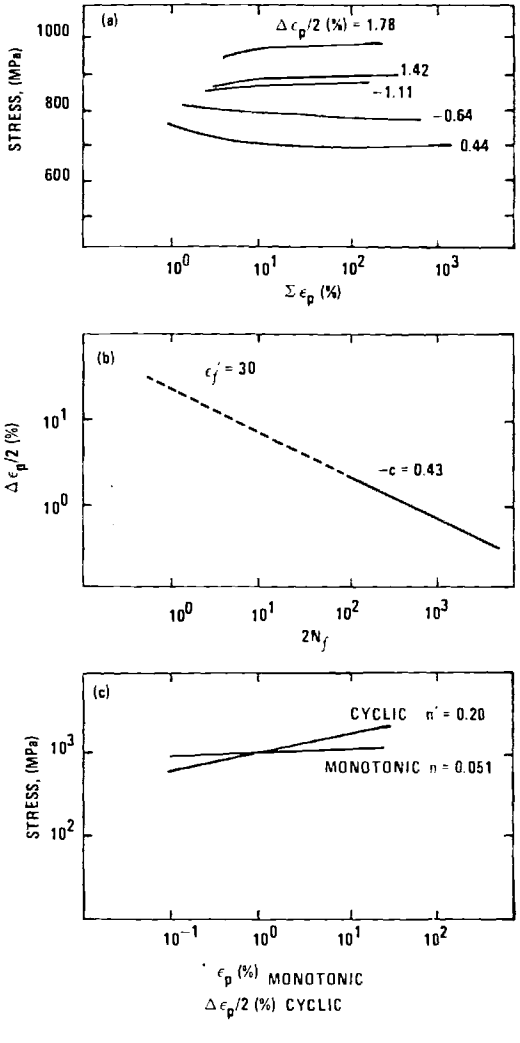

Figure 22. Low cycle fatigue behavior of Ti-36%V aged 10,000 minutes at 400°C.

SECURITY CLASSIFICATION OF THIS PAGE *(When Data Entered)*

REPORT DOCUMENTATION PAGE

READ INSTRUCTIONS BEFORE COMPLETING FORM

1. REPORT NUMBER: 77-1	2. GOVT ACCESSION NO.
3. RECIPIENT'S CATALOG NUMBER	
4. TITLE *(and Subtitle)*: The Cyclic Stress-Strain Response of Titanium-Vanadium Alloys	5. TYPE OF REPORT & PERIOD COVERED: Technical Report
	6. PERFORMING ORG. REPORT NUMBER
7. AUTHOR*(s)*: S. B. Chakrabortty, T. K. Mukhopadhyay and E. A. Starke, Jr.	8. CONTRACT OR GRANT NUMBER*(s)*: N00014-75-C-0349 NR 031-750
9. PERFORMING ORGANIZATION NAME AND ADDRESS: Metallurgy Program, School of Chemical Engr. Georgia Institute of Technology, Atlanta, GA 30032	10. PROGRAM ELEMENT, PROJECT, TASK AREA & WORK UNIT NUMBERS
11. CONTROLLING OFFICE NAME AND ADDRESS: Metallurgy Program, Office of Naval Research 800 North Quincy Street Arlington, Virginia 22217	12. REPORT DATE: August 30, 1977
	13. NUMBER OF PAGES
14. MONITORING AGENCY NAME & ADDRESS*(if different from Controlling Office)*	15. SECURITY CLASS. *(of this report)*: unclassified
	15a. DECLASSIFICATION/DOWNGRADING SCHEDULE

16. DISTRIBUTION STATEMENT *(of this Report)*

unlimited

17. DISTRIBUTION STATEMENT *(of the abstract entered in Block 20, if different from Report)*

18. SUPPLEMENTARY NOTES

19. KEY WORDS *(Continue on reverse side if necessary and identify by block number)*

titanium alloys
deformation
microstructure
fatigue

20. ABSTRACT *(Continue on reverse side if necessary and identify by block number)*

The cyclic stress-strain response of four Ti-V alloys (24, 28, 32 and 36 wt % V) which have deformation modes ranging from coarse twinning to wavy and planar slip, has been measured and correlated with deformation mode and microstructure. When coarse twinning is the primary deformation mode an anamolous Bauschinger effect, associated with untwinning during load reversal, is observed. A saturation flow stress is not obtained for the wavy slip alloy due to the intervention of microtwinning which inhibits cross slip and cell formation.

DD FORM 1 JAN 73 1473 EDITION OF 1 NOV 65 IS OBSOLETE

SECURITY CLASSIFICATION OF THIS PAGE *(When Data Entered)*

Cyclic hardening of all alloys appears to be related, in some degree, to deformation twinning. Cyclic softening occurs for the planar slip alloys in the absence of microtwinning due to increasing mobile dislocation density.

E-19-632

OFFICE OF NAVAL RESEARCH

Contract N00014-75-C-0349, NR 031-75

TECHNICAL REPORT 78-3

FATIGUE CRACK PROPAGATION OF METASTABLE BETA TITANIUM-VANADIUM ALLOYS

By
Saghana B. Chakrabortty and Edgar A. Starke, Jr.

December 7, 1978

FRACTURE AND FATIGUE RESEARCH LABORATORY
GEORGIA INSTITUTE OF TECHNOLOGY
ATLANTA, GEORGIA 30332

FATIGUE CRACK PROPAGATION OF METASTABLE BETA TITANIUM-VANADIUM ALLOYS

S. B. Chakrabortty and E. A. Starke, Jr.
Fracture and Fatigue Research Laboratory
Georgia Institute of Technology
Atlanta, Georgia 30332

ABSTRACT

The fatigue crack propagation behavior of three titanium-vanadium alloys (24, 28 and 32 wt. % V) which have (tensile) deformation modes ranging from coarse twinning to wavy and planar slip has been measured in laboratory air and correlated with their low cycle fatigue properties and microstructure. The fatigue crack growth rate of alloys with similar microstructures but different deformation modes, and of alloys with similar deformation modes but different microstructures have been compared. Increasing the deformation barrier mean free path and improving low cycle fatigue properties has been observed to reduce the fatigue crack growth rate at low and intermediate ΔK levels. The fatigue crack growth data have been compared with that calculated from equations which use microstructure and low cycle fatigue parameters. The predictive capability of these equations which contain only measurable parameters has been found to be quite adequate.

GLOSSARY

a = total crack length

b = fatigue strength exponent

c = Coffin-Manson exponent

COD = crack opening displacement at maximum load

da = change in crack length

dN = change in number of cycles

E = modulus of elasticity

H = half height of specimen

k' = cyclic strain hardening coefficient $\{\Delta\sigma = k' (\Delta\varepsilon_p)^{n'}\}$

K = stress intensity level

n = monotonic strain hardening exponent

n' = cyclic strain hardening exponent

N = total number of cycles

W = width of sample

$\Delta\varepsilon_p$ = plastic strain amplitude

ΔK = stress intensity range

$\Delta\sigma$ = applied stress amplitude

ε_f = monotonic fracture strain

ε_f' = fatigue ductility coefficient

ε_y' = cyclic yield strain

λ = mean free path between major deformation barriers

ρ^* = microstructural parameter from the Majumdar and Morrow equation

ρ_i' = microstructural deformation zone size of the i^{th} order

σ_f' = monotonic strength coefficient

σ_{ys} = montonic yield strength

σ'_{ys} = cyclic yield strength

INTRODUCTION

Various theories have been proposed to explain the fatigue crack propagation (FCP) behavior of metals and alloys[1-15]. Most theories describe FCP with equations having adjustable constants which can be obtained only after the FCP study is completed. Therefore, they do not suggest those metallurgical variables that can be changed to improve FCP resistance. Two equations have recently been developed which predict FCP behavior using material properties and no adjustable constants.

Liu and Iino[7] assume that cummulative damage by strain cycling causes cracks to propagate. The material of a finite element in the reverse plastic zone (RPZ) ahead of the crack-tip experiences cyclic strain of increasing magnitude as the crack propagates toward it. Each cycle produces damage to the material and if one used Miner's[16] cumulative damage law and Coffin-Manson's[17-18] cyclic life-strain response law an expression for fatigue crack growth rate (FCGR) per cycle may be derived. Majumdar and Morrow[6] and recently Chakrabortty[15] have proposed some modifications of the Liu and Iino approach to incorporate a microstructural parameter along with low cycle fatigue (LCF) parameters to predict the FCGR. The microstructural parameter is taken in terms of the mean free path (λ) between major deformation barriers and the LCF parameters are the cyclic ductility and the cyclic flow stress.

This work concerns the study of the effect of changes in the microstructure and LCF properties of metastable β Ti-V alloys on their FCGR in laboratory air. Starke and coworkers[19-22] have shown that the

deformation modes, microstructure and LCF properties of these alloys may be varied substantially by varying the vanadium content and aging time and temperature. Three alloys (24% V, 28% V and 32% V) were chosen for this study. In the as-quenched condition the deformation behavior changes from coarse twinning and fine wavy slip for the 24% V alloy to coarse planar slip for the 32% V alloy. When the 24% V alloy is aged to contain small amounts (up to $\sim$ 5%) of α precipitates the deformation mode and LCF behavior remains almost unchanged. However, with further aging the volume fraction of α increases, and the deformation behavior changes to planar slip. During LCF the as-quenched and low-α 24% V alloys deform initially by twinning and subsequently by wavy multiple slip. The as-quenched 32% V usually deforms by planar slip. The behavior of the as-quenched 28% V alloy is somewhat intermediate between the 24% V and 32% V alloys. By using the Ti-V system, one may independently vary microstructure or deformation mode by suitably varying the heat treatment and/or composition. This allows an examination of the effect of each parameter on the FCP resistance.

EXPERIMENTAL

Three Ti-V alloys containing 24, 28, and 32 wt.% vanadium were prepared by Titanium Metals Corporation (Henderson, Nevada), where 14 cm diameter ingots were hot forged and cross rolled to produce 15X15X0.8 cm plates having a random texture. The chemical analysis and grain intercept lengths of these materials are shown in Table 1. Samples from the as-received plates were solutionized at 850°C in dry argon and quenched in iced brine. Some samples were aged to produce the desired microstructure and deformation mode (Table 1). Compact

tension[23] samples with H/W of 0.486 and W = 44.5 mm were used to measure the fatigue crack growth rate (FCGR). FCGR measurements were performed on a servohydraulic closed-loop MTS testing machine using tension-tension loading with a maximum/minimum load ratio (R) of 0.1 at a frequency of 10 Hz. The tests were carried out in laboratory air with a relative humidity of 27-30% and a temperature of 23-25°C. The crack length was measured on the polished surface of the specimen using a Gaertner travelling microscope within ± 0.01 mm. The microstructure, deformation and fracture behavior was characterized by x-ray diffraction, and optical and electron microscopy

RESULTS

General Crack Growth Behavior: The measured FCGR versus ΔK curves for all the materials tested in our studies were very similar in character. At low ΔK the FCGR increases slowly with ΔK (AB in Figure 1). At intermediate ΔK accelerated crack growth occurs and there is a sharp increase in da/dn with a small increase in ΔK (BC in Figure 1), after which the FCGR again increases slowly (CD in Figure 1). The fractographic features for all alloys corresponding to this FCGR behavior at various ΔK ranges may be described as follows:

(1) MULTIFACETED crack growth at low rates ($da/dn < 1X10^{-8}$m/cycle). The fracture surface appears to have small ill-defined cleavage facets which are considerably smaller than the grain size. The fracture surface is extremely rough in appearance and crack branching is prevalent. Even though the growth is crystallographic, no single path is preferred. This coincides with the range AB in Figure 1. The typical multifaceted fracture surface features are shown in Figure 2.

(2) FACETED crack growth at intermediate rates ($\sim 1X10^{-8}$ m/cycle < da/dn < $\sim 2.5X10^{-7}$ m/cycle). The fracture surface is composed of large facets each of which usually covers one whole grain. The appearance is similar to that observed on other metallic samples fatigued in air[24]. Facets are shiny and have many river pattern markings. Fracture planes of one system are preferred for each grain resulting in the familiar "stair case" morphology. Fatigue striations become visible on these surfaces above a FCGR of $\sim$ 0.02 μm/cycle. The striation spacing is approximately equal to the crack growth distance per cycle. The transition from multifaceted to faceted growth appears to be associated with an accelerated crack growth rate behavior (region BC of Figure 1). Faceting persists approximately up to point D after which a slow transition to noncrystallographic crack growth occurs. The typical faceted fracture surface features are shown in Figure 3. Transmission electron diffraction studies showed that the facet planes are close to either {100} or {112}.

(3) NONCRYSTALLOGRAPHIC crack growth at higher rates (da/dn > $\sim 2.5X10^{-7}$ m/cycle). The fracture surface is more or less flat, is perpendicular to the stress axis, and is composed of fatigue striations and microvoids (at higher FCGR). The crack path appears to be noncrystallographic. The typical noncrystallographic fracture surface features are shown in Figure 4.

Fracture features are seldom completely of one type. Mixed mode of fracture is present to a different extent in different cases. For the 24A alloy the fracture features indicate some multifaceted growth even

for growth rates as high as 1 μm/cycle. Fatigue striations are never observed on such features which appear to be cleavage. However, fatigue striations are observed on faceted areas, perhaps indicating a fracture involving plastic flow. The crack path appears transcrystalline in most cases. Some intergranular cracking is sometimes observed. Frequent crack branching is observed, especially at lower ΔK ranges (Figure 2).

Comparison of Crack Growth Behavior of Alloys: The materials tested in our studies may be divided into three groups as shown in Table 1. Fatigue crack growth behavior of each of these groups is discussed below:

GROUP 1. This group has three as-quenched alloys with changing vanadium content (i.e., 24A, 28A and 32A), with somewhat similar microstructures, and different deformation modes. 24A deforms primarily by coarse twinning and wavy slip, 28A deforms by wavy slip and 32A deforms by planar slip. At low ΔK ranges, 32A has the lowest FCGR and 24A has the highest (Figure 5). However, the opposite seems to be true at an intermediate range. The accelerated crack growth behavior at this range is maximum for 32A and minimum for 24A. Similar anomalous accelerated growth behavior has been found in Ti-6-4[25] and Al-7Mg[26] alloys. Our results show that the extent of accelerated growth and the associated faceting is increased by increasing the propensity of coarse slip by increasing the vanadium content (24A << 28A < 32A).

24A alloys deform by coarse twinning during tensile and low-cycle and high-cycle fatigue tests. However, no deformation twins were observed by optical microscopy during the FCP test when the ΔK was below $\sim$ 10 MPa$\sqrt{m}$. Perhaps, the deformation at the crack tip is restricted

to a narrow area at such low ΔK and the formation of coarse twins is not possible. Consequently, the material at the crack-tip deforms by wavy slip. At higher ΔK, deformation twins form. When the crack intersects a twin it sometimes follows the twin boundary for a short distance and again becomes transgranular. However, twin boundaries do not appear to play a major role in FCP.

GROUP 2. This group consists of three different heat-treated conditions of the Ti-24 V alloy. All conditions deform primarily by twinning and wavy slip. The propensity of twinning decreases with increasing amount of alpha precipitation. Figure 6 shows the da/dn versus ΔK curves for these materials. Increasing the volume fraction of α precipitates in the β matrix increases the FCGR. From the fractographic examination of areas around α precipitates, it appears that these particles do not embrittle the material. Ductile fatigue striations are observed in and around the precipitate/matrix interface and the spacing appears to be the same as that observed away from the precipitates (Figure 7). The fracture features for this alloy group were very similar for the same da/dN; however, they were quite different for the same ΔK, as seen by the comparison of 24A and 24C in Figure 8. More extensive deformation occurs for 24C than for 24A at similar ΔK values. It appears that the effect of increasing the amount of precipitate is to increase the extent of crack-tip plasticity for a given ΔK and therefore to increase the FCGR. At high ΔK when non-crystallographic growth occurs, the FCGR is more or less similar for all of the three structures.

GROUP 3. This group has two materials which deform by planar slip. 32A is an all-beta-phase alloy, and 24D has been heat treated to produce a large amount of alpha precipitates in the beta matrix. As for Group 2, the effect of the precipitates is to increase the FCGR (Figure 9) for the crystallographic growth region. Both 32A and 24D deform by coarse planar slip and consequently show an accelerated crack growth behavior for intermediate ΔK.

Comparison Between Calculated and Experimental FCGR: To our knowledge only two equations are available to calculate the FCGR from LCF data and microstructural parameters without the use of any adjustable constants. The equation proposed by Majumdar and Morrow[6] is

$$\frac{da}{dN} = \frac{-2(b+c)}{b+c+1}\left[\frac{\sigma'_y}{4(1+n')\sigma'_f\varepsilon'_f}\right]^{\frac{-1}{b+c}}\left\{\left[1+\frac{2\rho^*}{COD}\right]^{\frac{b+c+1}{b+c}}-\left[4(1+n')\varepsilon'_y\right]^{-\frac{b+c+1}{b+c}}\right\}\frac{\varepsilon'_y\Delta K^2}{\pi\,\sigma'^2_y} \quad (1)$$

Chakrabortty[15] related FCGR to ΔK and low cycle fatigue parameter with the following equation:

$$\frac{da}{dn} = 2\sum_{n=1}^{\infty}\rho'_n\left(\frac{\Delta\varepsilon_{pn}}{2\varepsilon_f'}\right)^{-\frac{1}{c}} \quad (2)$$

where, $\Delta\varepsilon_{p_n} = \int_{x=r_{n-1}}^{x=r_n}\Delta\bar{\varepsilon}_p\, x^{\frac{1}{2}}dx \Big/ \int_{x=r_{n-1}}^{x=r_n} x^{\frac{1}{2}}dx$

$$x = \frac{\Delta K^2}{(1+n')\pi E k'}\cdot\frac{1}{(\Delta\bar{\varepsilon}_p)^{n'+1+\frac{k'}{E}}(\Delta\bar{\varepsilon}_p)^{2n'}}$$

$$r_n = r_o + \sum_{i=1}^{n}\rho_i'$$

and $r_o = \frac{\Delta K^2}{\pi\sigma'_y E}$

The microstructure parameter ρ of equations (1) and (2) is proportional to λ. The results of calculations using equations (1) and (2) are presented in Figure 10. Calculations were made only for 24A, 24B, and 24C since these have the smallest environmental effect. The results obtained by equation (2) fall well within the expected scatter band of the experimental data. The Majumdar and Morrow equation appears to be good only at high ΔK, and at low ΔK values it considerably underestimates the FCGR.

DISCUSSION

Modes of Crack Growth: In order to explain our results we propose that the following three mechanisms of fatigue crack propagation are operative in the stress intensity ranges which correspond to the three fractographic features described.

1. At low ΔK, multifaceted crack growth occurs by decohesion along {110} and/or {112} slip bands or possibly by either {100}, {110}, or {123} cleavage in the cyclic plastic zone ahead of the crack-tip. Cracking may occur simultaneously in numerous areas of the same grain, and depending upon the material all cracks may not be on parallel crystallographic planes. The observed multifaceted appearance results from link-up of numerous cracks. Other authors have proposed a similar model to explain the FCP behavior of some alloys at low ΔK.[27-29]
2. Faceting behavior observed at intermediate ΔK is due to shearing along coarse slip band(s) at the crack-tip. The coarse slip bands form ahead of the crack-tip during cyclic deformation and the crack extends due to shearing off the coarse slip band(s) during tensile

loading. However, depending on the environment and number of active slip bands some "rewelding" of the crack may occur during compression. This mode of crack propagation should be enhanced for a material with coarse slip character and by any environment which would inhibit rewelding. The fracture plane will depend on the number and type of operative slip systems at the crack-tip, and within one grain will be determined by the stress-axis-grain orientation relationship. The resulting faceted appearance is composed of long planar surfaces with lengths equal to the grain size and parallel to the crack growth direction, having the stair case morphology of Figure 3. Other authors have proposed models explaining the detailed crystallographic aspects of this mode of growth.[30-32]

3. At high ΔK, the noncrystallographic growth is due to a crack-tip stretching mechanism. The crack tip moves by inward contraction of the material during tensile deformation until blunting occurs. The crack resharpens during compression. The extent of crack growth per cycle should depend mainly upon the cyclic flow stress of the material. The geometry of crack-tip stretching dictates that the fracture plane be perpendicular to the loading direction. Therefore, the observed noncrystallographic fractographic appearance with ductile fatigue striations is expected. A similar mechanism has been proposed previously for high-stress fatigue.[33-35]

The operating fracture mode depends upon the deformation behavior of the material, the environment and the stress intensity range. The require-

ments for faceting are the formation of coarse slip and lack of complete reweldability of the freshly formed "crack" during the compressive cycle. Therefore, there may be a critical value of stress intensity range (ΔK_f), below which faceting is not possible. Below ΔK_f coarse slip may not occur; or even if it does occur the crack extension in the tensile stroke may be sufficiently small for rewelding to be complete during compression. The value of ΔK_f should decrease as the environment becomes aggressive, although faceting may occur even without an aggressive environment. A suitable environment only reduces the energy necessary for such growth by reducing crack-tip reweldability and/or by increasing cyclic coarse slip. The probability of faceting fracture will also be increased when the material has greater propensity of coarse slip. Below ΔK_f faceting is reduced because the decohesion mechanism requires less energy. As ΔK increases the probability of multiple slip increases and coarse planar slip decreses. Consequently, there is also a ΔK above which faceting diminishes. Here the environment becomes inconsequential becasue the crack-tip blunts due to plasticity effects. Figure 11 is a schematic illustration of FCGR corresponding to each mode of growth for a Ti-V alloy.

The proposed modes of crack growth explain the observed fractographic features. The accelerated phenomenon associated with the onset of faceting is schematically illustrated in Figure 11. Our results show that accelerated growth and faceting increases when the propensity of coarse slip is increased either by increasing the vanadium content (24A << 28A < 32A) or by varying the heat treatment (24A $\leq$ 24B $\leq$ 24C < 24D). Furthermore, as expected from the proposed modes, our results

indicate that there is a ΔK_f for faceting, which appears to decrease with increasing propensity of coarse slip. Recent results[36] have shown that ΔK_f decreases and the probability of faceting increases in more aggressive environments than used in this study. The coarse slip-fracture model proposed by Neumann,[31] predicts {001} and {112} fracture planes for alloys having {110} <111> and {112} <111> operative slip systems. This prediction is consistent with our results.

Correlation Between Calculated and Measured FCGR: Equation (1) proposed by Majumdar and Morrow,[6] and Equation (2) by Chakrabortty[15] assume that the material ahead of the crack-tip undergoes cyclic plastic deformation, and crack extension occurs due to exhaustion of the fatigue ductility of the material. The Chakrabortty model[15] estimates the cyclic plastic strain by dividing the cyclic plastic zones into elements of size ρ_i and assuming that the cyclic deformation is more or less uniform within these elements. According to this model the element nearest to the crack-tip contributes most to the FCGR at low ΔK. Majumdar and Morrow's model[6], on the other hand, ignores the contribution of this element because continuun mechanics and bulk properties are not applicable with such a small zone. This explains why the calculated FCGR values from the Majumdar and Morrow equation falls orders of magnitude below the experimental data for the lower ΔK range. The Chakrabortty equation appears to predict the FCGR values more accurately over all ranges of ΔK (Figure 10). However at low ΔK, the experimental curves are somewhat below the predicted curves. This is expected due to crack branching since crack branching reduces the effective ΔK and the measured crack growth rate (if the projected crack-length is used).

The crack growth data and fractographic features support the Chakrabortty model.[15] According to the model the FCGR increases as one decreases the cyclic flow stress, the cyclic ductility and the mean free path (λ) between the major deformation barriers. This predicts that the group 1, 2 and 3 alloys should be ranked 24A, 28A, 32A; 24B, 24A; and 24D, 32A, respectively in order of reducing FCGR. The experimental data agree well with this prediction with one exception; for the faceted growth region for Group 1 alloys the order is reversed. This is possibly a result of a different environmental effect for the different alloys. 32A, which has the highest propensity of coarse slip, should have the largest environmental effect. The value of λ is decreased in Group 2 alloys by heat treatments which produce α particles within the β matrix. The cyclic flow stress and ductility remains more or less unchanged. According to the model, a reduction in λ causes an increase in cyclic plastic deformation in the element just ahead of the crack-tip and this should increase the FCGR as observed in our experiments, Figure 6. Furthermore, the fractographic features seem to indicate that for the same ΔK, the cyclic deformation is largest for 24C which has the lowest value for λ. On the other hand, the deformation appears very similar for the same da/dn, Figure 8. A similar behavior was observed for Group 3 alloys. The model also predicts that when ΔK is large, the crack growth rate becomes less dependent on λ and the FCP should become structure insensitive. The data again supports this prediction -- 24A, 24B and 24C which have same fatigue flow stress and ductility but different λ have similar crack growth rate values at high ΔK.

Both the Majumdar and Morrow and Chakrabortty equations predict that a decrease in λ will increase the FCGR unless the fatigue flow stress and/or fatigue ductility is improved drastically.[15] Therefore, these equations propose that a decrease in λ, which is usually benefical for the strength, ductility, LCF and HCF properties, may be detrimental for FCP resistance. Experimental results on various alloy systems support this prediction.[24]

SUMMARY

Three different modes of fatigue crack growth have been observed for the metastable beta titanium-vanadium alloys tested. They are: (1) The fracture surface is composed of small cleavage-like areas at low ΔK and is assumed to be a product of decohesion along slip planes or cleavage planes as a result of fatigue cycling. (2) At intermediate ΔK faceting is observed and is assumed to occur by a cyclic coarse slip mechanism where crack extension is due to irreversable shearing off in coarse slip bands. This mode of crack growth appears to be sensitive to environment. (3) At high ΔK the crack surface has a striated non-crystallographic appearance. Here, it is assumed that the crack grows by the inward contraction of the crack-tip due to stretching of the material at the tip. The faceting mechanism appears to be enhanced by coarse slip and aggressive environments. Transition from multifaceted to faceted growth is always associated with an accelerated crack growth rate behavior.

Comparison of some of the experimental data with those calculated from the equations of Chakrabortty[15] and Majumdar and Morrow[6] shows good correlation. Fractographic features also seem to support the model proposed by Chakrabortty.[15] It is observed that where cyclic flow

stress and ductility is kept nearly constant, the FCGR value increases when the mean free path between the major deformation barrier (λ) is decreased. Also when λ is kept nearly constant the FCGR is increased when the cyclic flow stress and/or ductility is decreased. When the environment has a large effect, the material with higher propensity of coarse slip shows a very high crack growth rate regardless of the values of cyclic ductility, flow stress, and λ.

ACKNOWLEDGEMENTS

The authors would like to acknowledge the help of Mr. Eui Whee Lee with the experimental measurements. This research was supported by the Office of Naval Research under Contract N00014-75-C-0349, Dr. Bruce A. McDonald, Contract Monitor. The United States Government is authorized to reproduce and distribute reprints for Government purposes notwithstanding any copyright notation hereon.

REFERENCES

1. J. Weertman, Int. J. Fract. 9, 125 (1973).

2. T. Mura and C. T. Lin, Int. J. Fract. 20, 284 (1974).

3. J. R. Rice, Fatigue Crack Propagation, ASTM STP No. 415, 247 (1967).

4. G. P. Cherepanov and H. Halmanov, Eng. Fract. Mech. 4, 219 (1972).

5. P. E. Irving and L. N. McCartney, Metal Sciences, 11, 351 (1977).

6. S. Majumdar and J. Morrow, Fracture Toughness and Slow-Stable Cracking, ASTM STP No. 559, 159 (1974).

7. H. W. Liu and N. Iino, Proc. 2nd Int. Conf. on Fract., Chapman and Hall, p. 812 (1969).

8. S. D. Antolovich, A. Saxena and G. R. Chanani, Eng. Frac. Mech. 7, 649 (1975).

9. F. A. McClintock, ASTM STP No. 415 (1967). Discussion to article by C. Laird, p. 170.

10. F. A. McClintock, Fracture of Solids, Interscience Publishers, NY, p. 65 (1963).

11. R. W. Larder, Phil. Mag., 17, 71 (1968).

12. H. W. Lin, Trans. ASME 85, 116 (1963).

13. N. E. Frost and J. R. Dixon, Int. J. Fract., 3, 301 (1967).

14. A. J. McEvily, Jr. and T. L. Johnston, Int. J. Fract. Mech., 3, 45 (1967).

15. S. B. Chakrabortty, "Cyclic Ductility, Cyclic Strength and Fatigue Crack Propagation of Metals and Alloys," Technical Report 78-2 Office of Naval Research Contract N00014-75-C-0349, NR 031-750, May 16, 1978.

16. M. A. Miner, J. Appl. Mech. 12A, 159 (1945).

17. L. F. Coffin, Jr., Trans. ASME, 76, 931 (1954).

18. S. S. Manson and H. M. Hirschberg, "Fatigue-An Interdisciplinary Approach" ed. by J. J. Burke, N. L. Reed, and V. Weiss, Syracuse University Press, p. 133 (1964).

19. Fu-Wen Ling, H. J. Rack and E. A. Starke, Jr., Met. Trans., 4, 1671 (1973).

20. Fu-Wen Ling, E. A. Starke, Jr., and B. G. LeFevre, Met. Trans., 5, 179 (1974).

21. H. G. Paris, B. G. LeFevre and E. A. Starke, Jr., Met. Trans., 7A, 273 (1976).

22. S. B. Chakrabortty, T. K. Mukhopadhyay and E. A. Starke, Jr., Acta Met., 26, 909 (1978).

23. ASTM Specification E-399.

24. C. J. Beevers, Fracture, Waterloo, Canada, 1, p. 239 (1977).

25. P. E. Irving and C. J. Beevers, Mat. Sci. and Eng., 14, 229 (1974).

26. F. P. Ford and T. P. Hoar, III Int. Conf. on the Strength of Metals and Alloys, 1, p. 467 (1973).

27. C. D. Beachem and D. A. Meyn, ASTM STP No. 436, 59 (1968).

28. D. J. Duquette and M. Gell, Met. Trans., 2, 1325 (1971).

29. R. W. Hertzberg and W. J. Mills, ASTM STP No. 600, 220 (1976).

30. P. Neumann, Acta Met., 17, 1219 (1969).

31. P. Neumann, Acta. Met., 22, 1155 (1974).

32. G. G. Garrett and J. F. Knott, Acta Met., 23, 841 (1975).

33. D. A. Meyn, Trans. ASM, 61, 42 (1968).

34. C. Laird, ASTM STP No. 415, 131 (1967).

35. C. Laird and G. C. Smith, Phil. Mag., 7, 847 (1962).

36. S. B. Chakrabortty and E. A. Starke, Jr., unpublished work.

TABLE 1: Composition, Heat Treatment, Microstructure and Deformation Modes of Alloys Used for Fatigue Crack Propagation Studies

GROUP	DESIGNATION	COMPOSITION (wt%)	TREATMENT	MICROSTRUCTURE λ*	TENSILE DEFORMATION MODE
1	24A	24V, 0.20_2	AS QUENCHED	$(\beta+\omega)$ $\lambda = 64\mu$	Coarse Twinning + (Wavy Slip)
	28A	28V, 0.20_2		β $\lambda = 97\mu$	Wavy Slip
	32A	32V 0.20_2		β $\lambda = 108\mu$	Coarse Single Slip
2	24A	24V, 0.20_2	AS QUENCHED	$(\beta+\omega)$ $\lambda = 64\mu$	Coarse Twinning + (Wavy Slip)
	24B	24V, 0.20_2	QUENCHED AND AGED	$(\beta+\omega)+\alpha$ $\lambda = 30\ \mu$	
	24C	24V, 0.20_2	QUENCHED AND AGED	$(\beta+\omega)+\alpha$ $\lambda = 12\mu$	
3	24D	24V, 0.20_2	QUENCHED AND AGED	$\beta+\alpha$ $\lambda = 6\mu$	Coarse Single Slip
	32A	32V, 0.20_2	AS QUENCHED	β $\lambda = 108\mu$	

* λ is the mean free path between α particles for alloys with α precipitates, or the grain intercept length for all other alloys.

LIST OF FIGURES

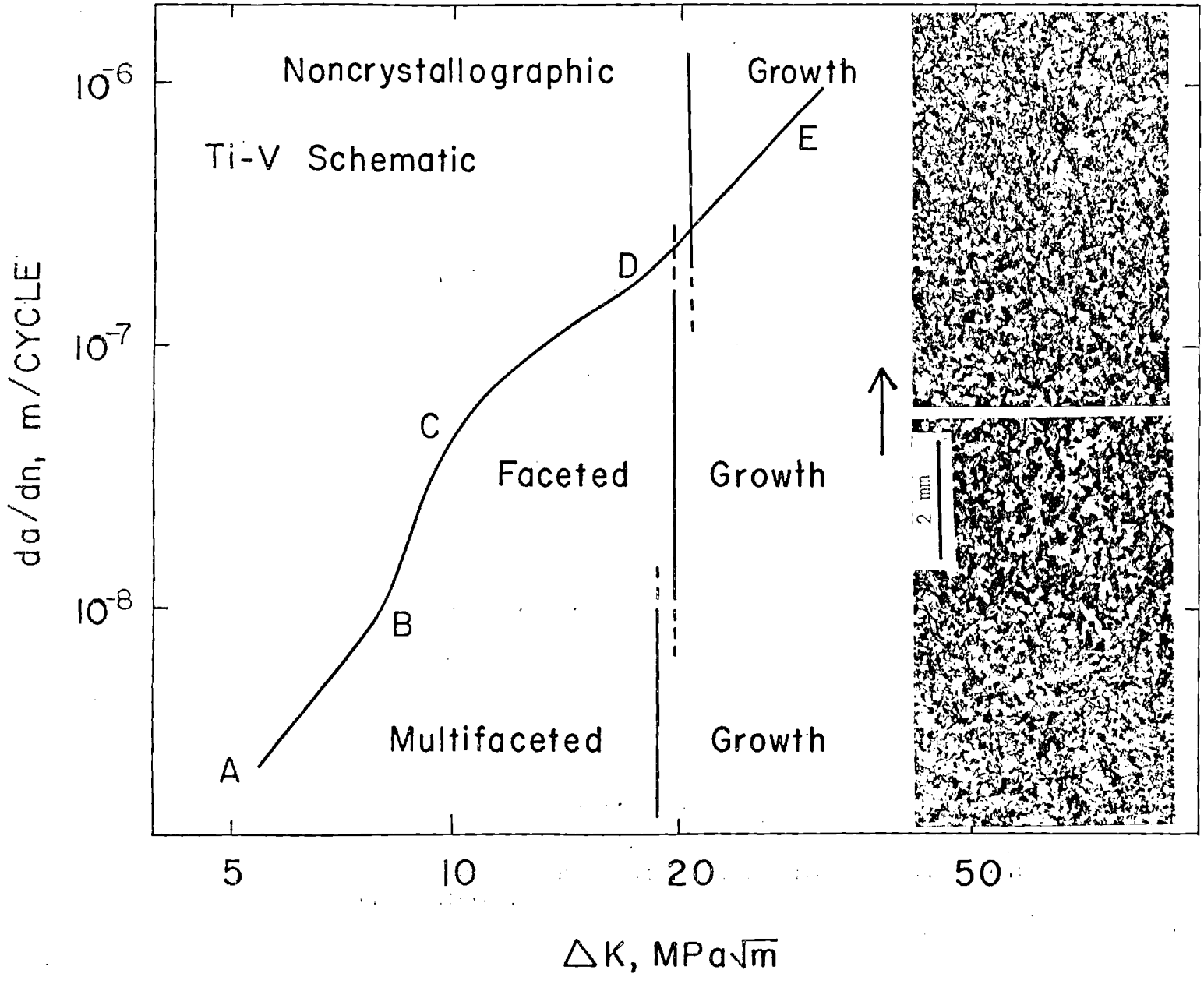

Figure 1 Typical FCGR curve for the Ti-V alloys with the corresponding

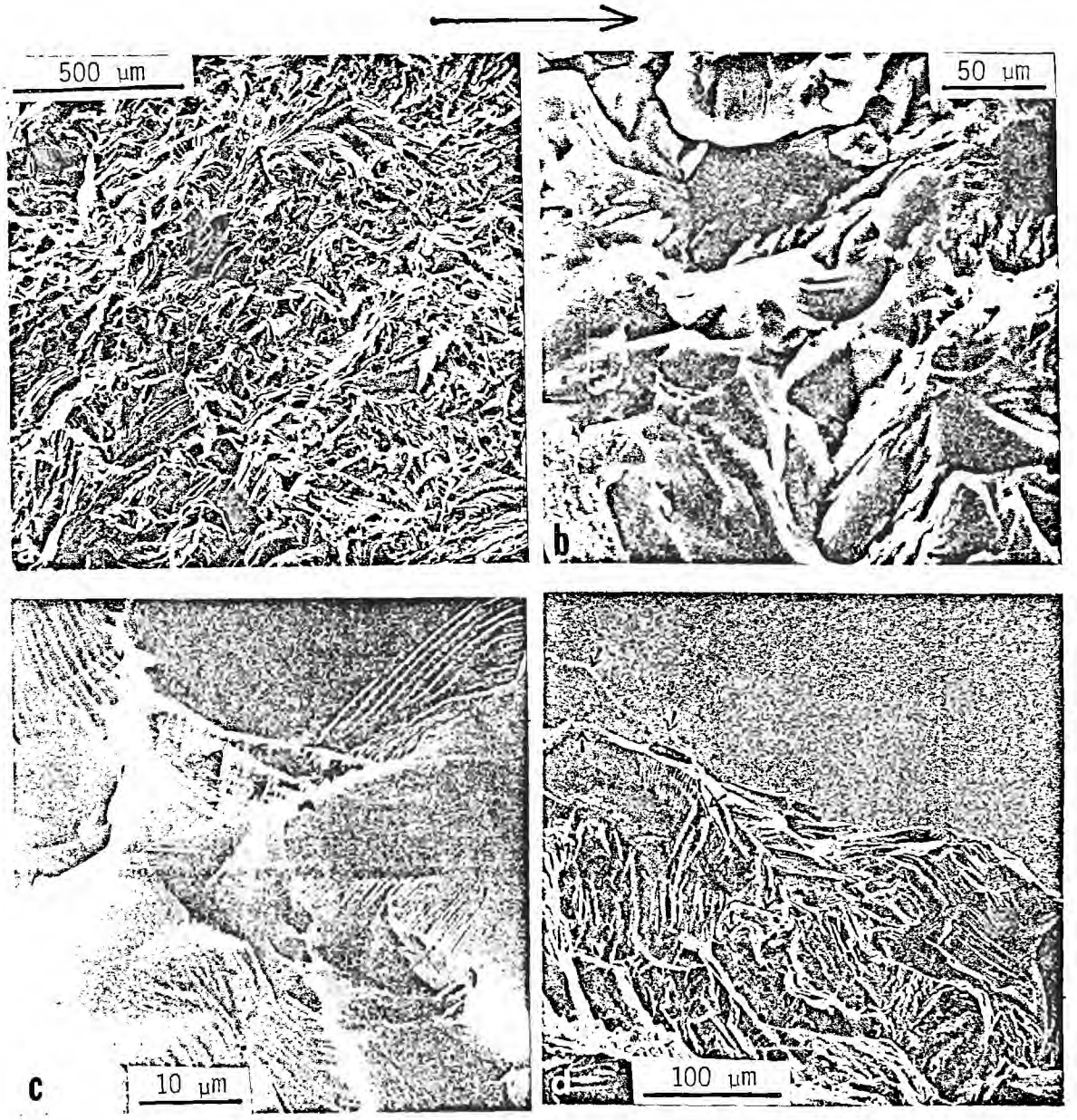

Figure 2. Examples of multifaceted growth features. Ti-28V alloy, as-quenched. $\Delta K \sim 6.5$ MPa$\sqrt{m}$, da/dn $\sim 5X10^{-9}$ m/cycle. Figure 2b is photographed at $\sim 45°$ to both the crack surface and a vertical section. Some secondary cracks are marked with arrows.

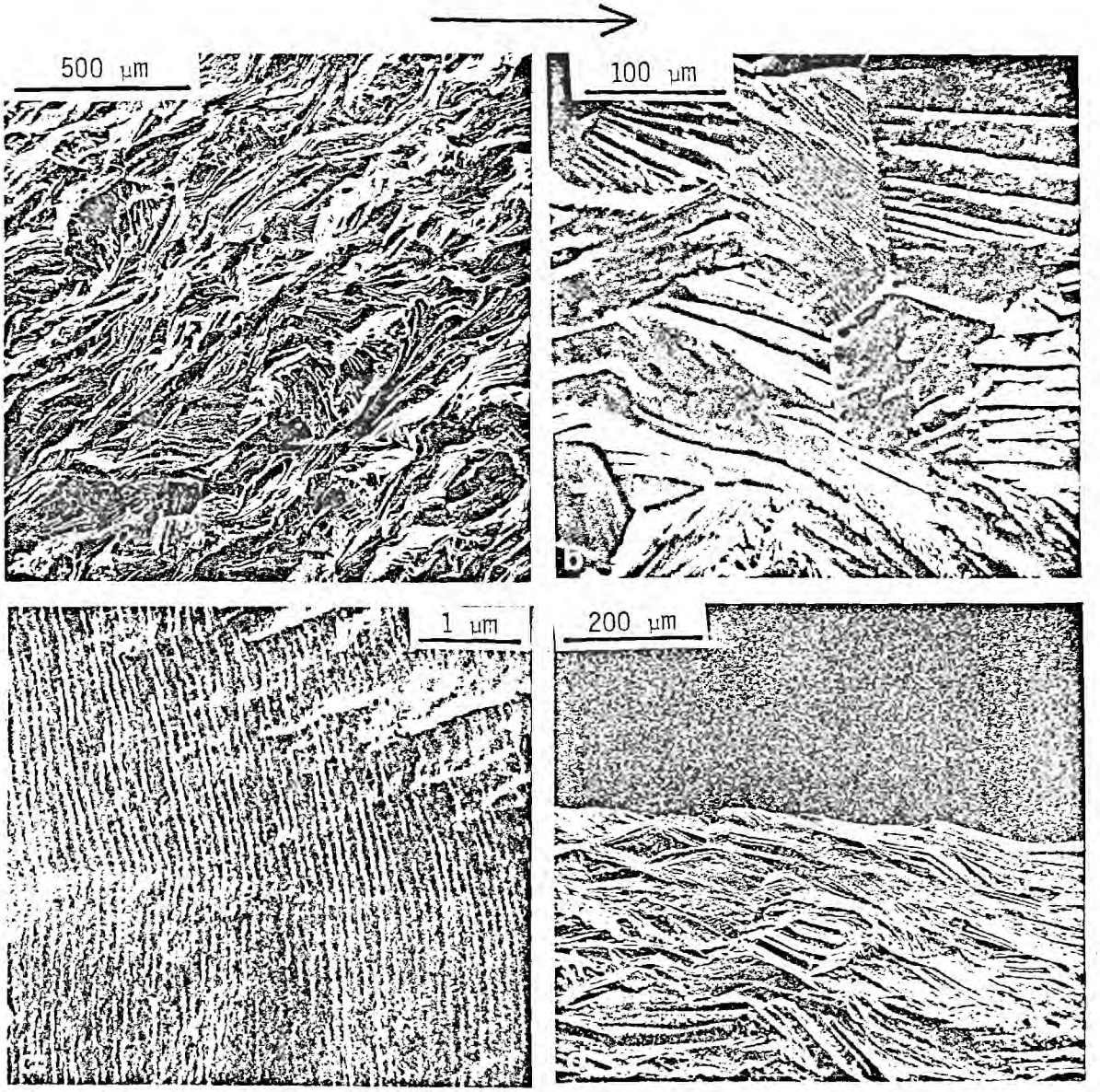

Figure 3. Examples of faceted growth featues. Ti-28V, as-quenched. $\Delta K \sim$ 14.3 MPa$\sqrt{m}$, da/dn $\sim$ 1X10^{-7} m/cycle. Figure 3b is photographed at $\sim$ 45° to both the crack surface and a vertical section.

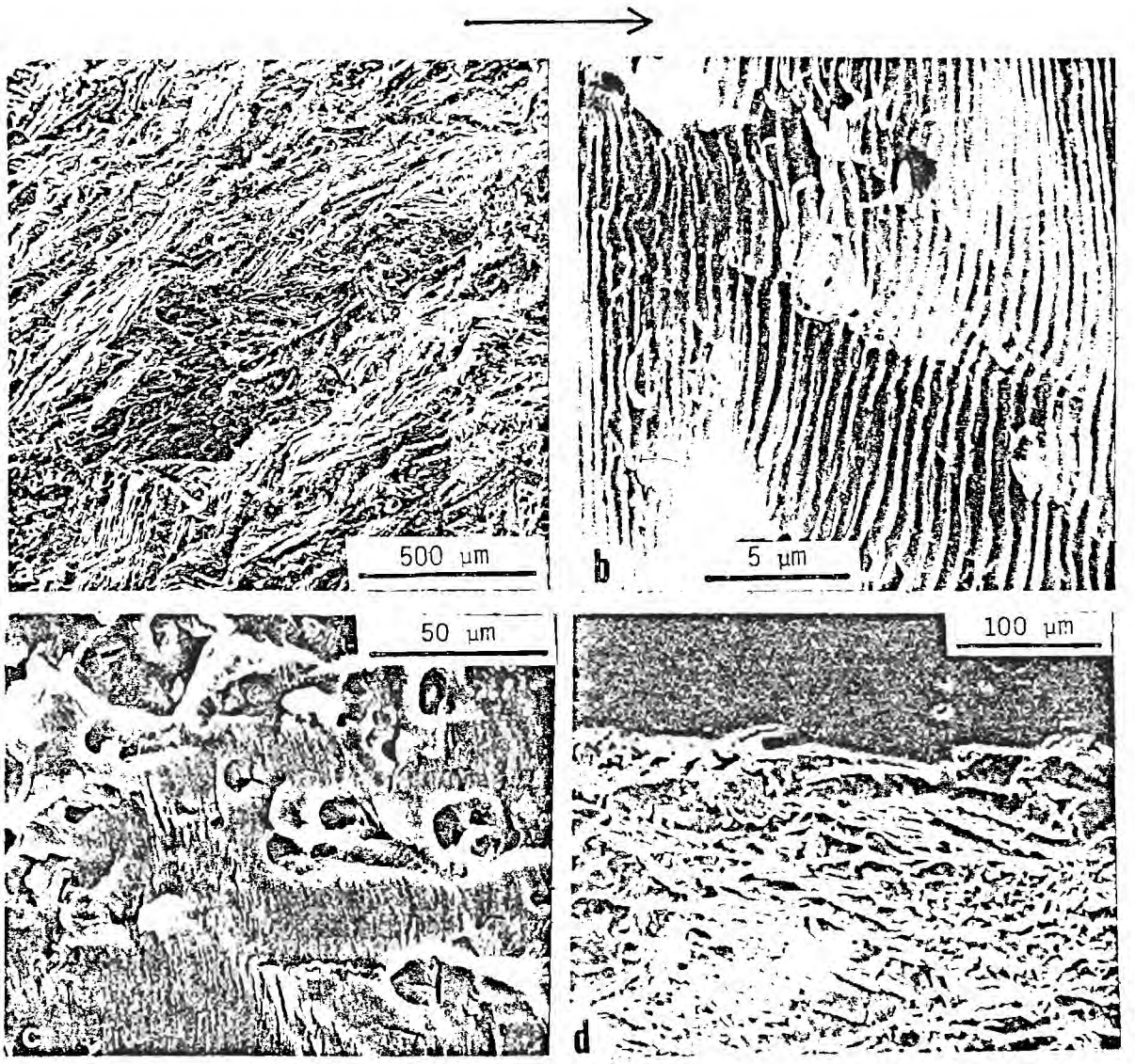

Figure 4. Examples of noncrystallographic growth features. Ti-28V as-quenched. a, b and d- $\Delta K \sim 29$ MPa$\sqrt{m}$, da/dn $\sim 6X10^{-7}$ m/cycle. c.- K $\sim$ 40, da/dn $\sim 1.5X10^{-6}$ m/cycle. Figure 4d is photographed at $\sim$ 45° to both the crack surface and a vertical section.

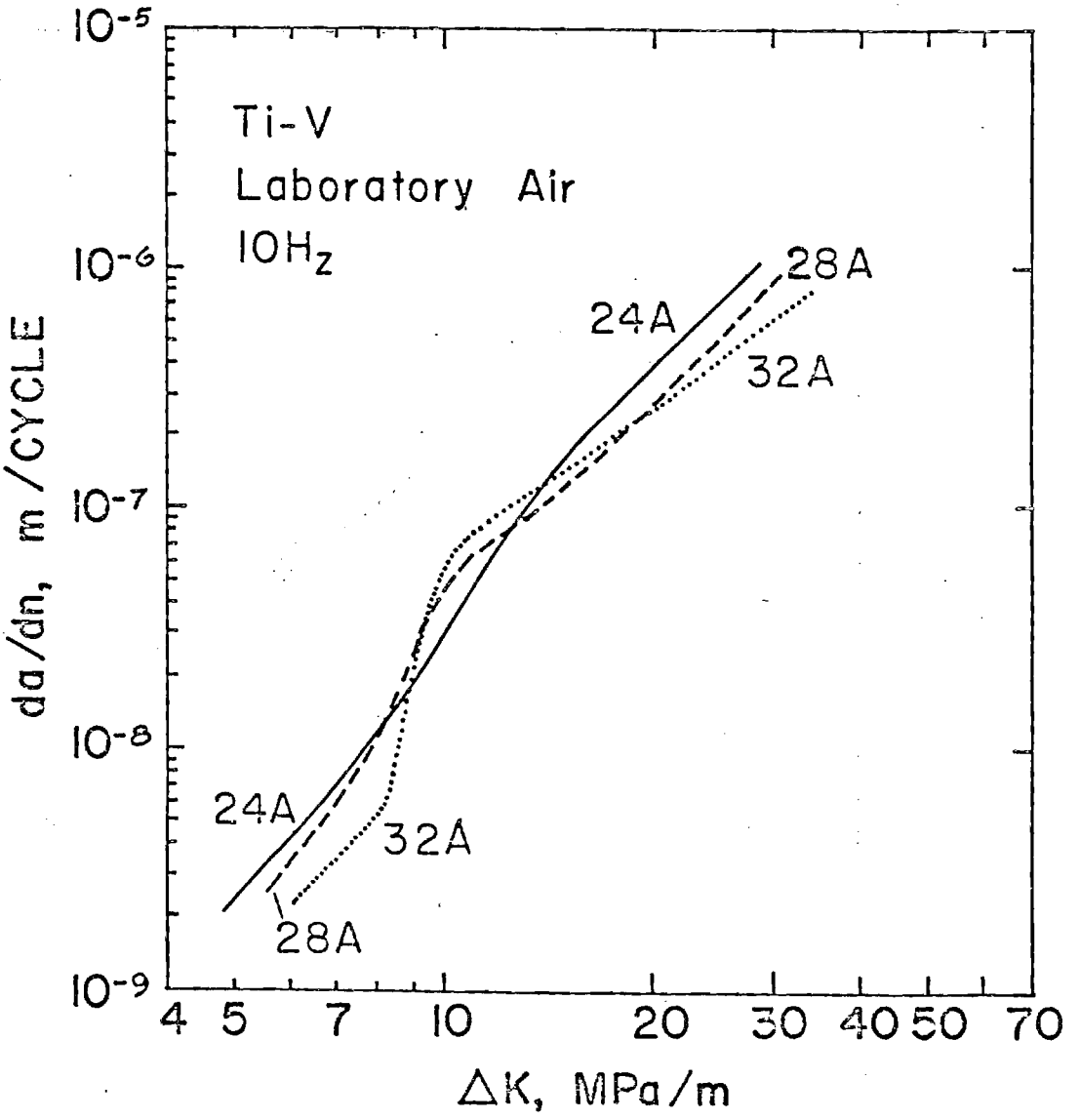

Figure 5. Fatigue crack growth rate versus stress intensity range curves for the Ti-24%V, 28%V and 32%V, as quenched alloys.

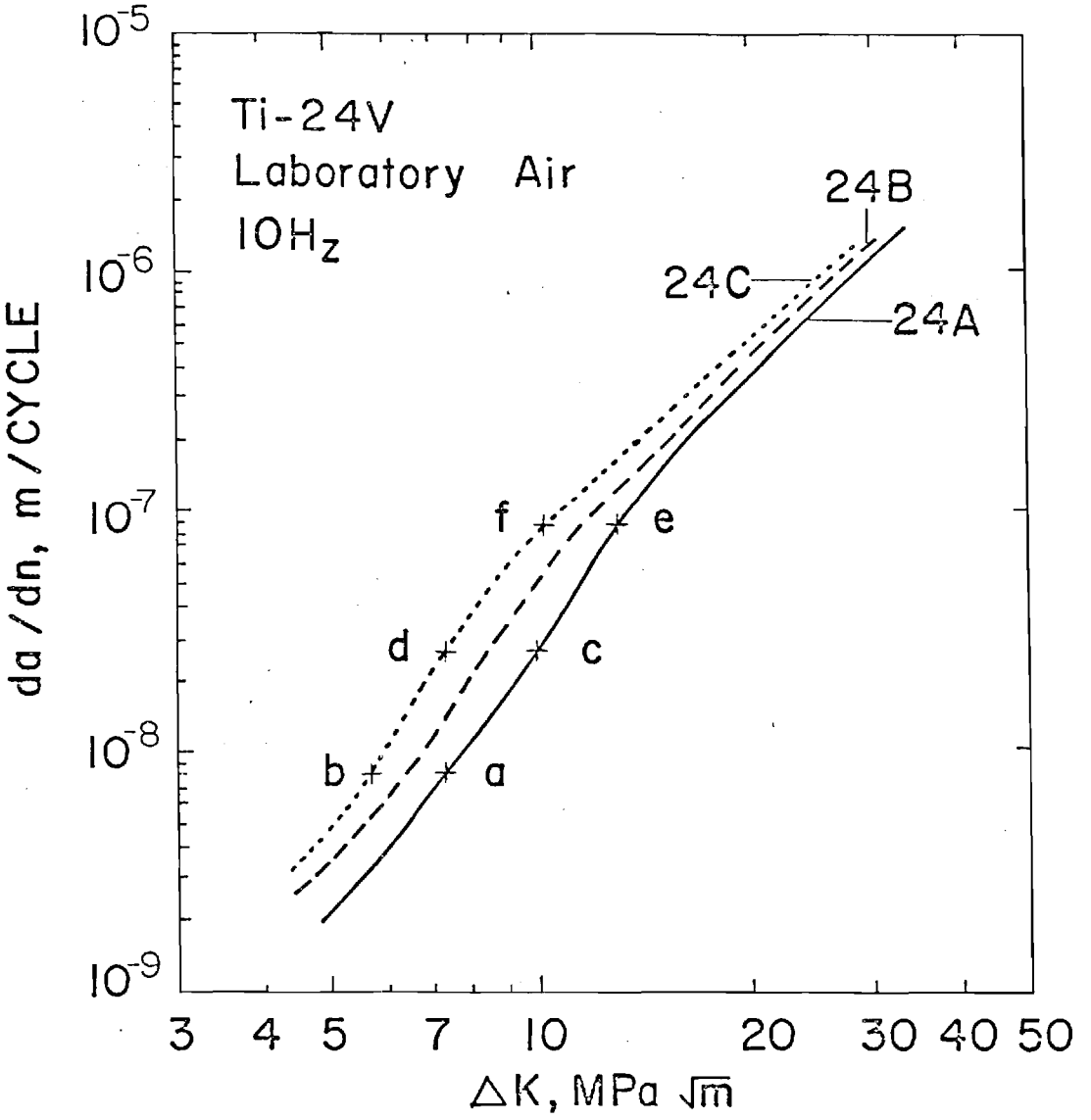

Figure 6. Fatigue crack growth rate versus stress intensity range curves for the Ti-24%V as-quenched and aged alloys.

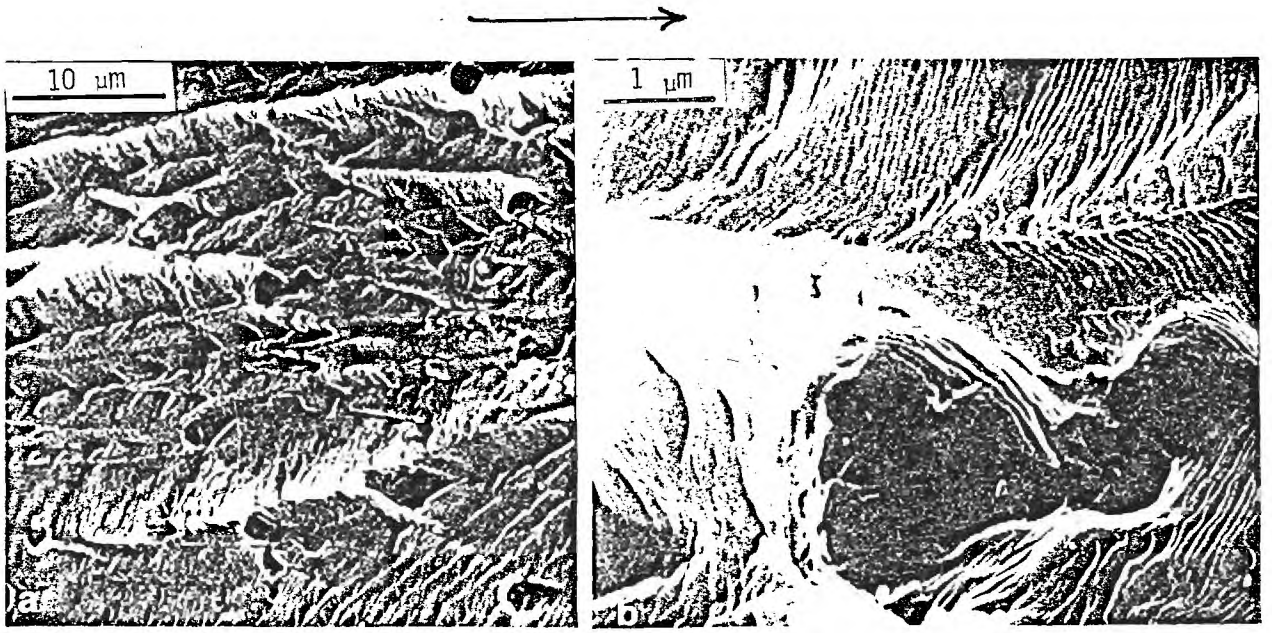

Figure 7. Fractographic features of fatigue crack propagation around the second phase particles of an aged Ti-24%V alloy (24C). $\Delta K \sim 10$ MPA$\sqrt{m}$, da/dn $\sim 8X10^{-8}$ m/cycle.

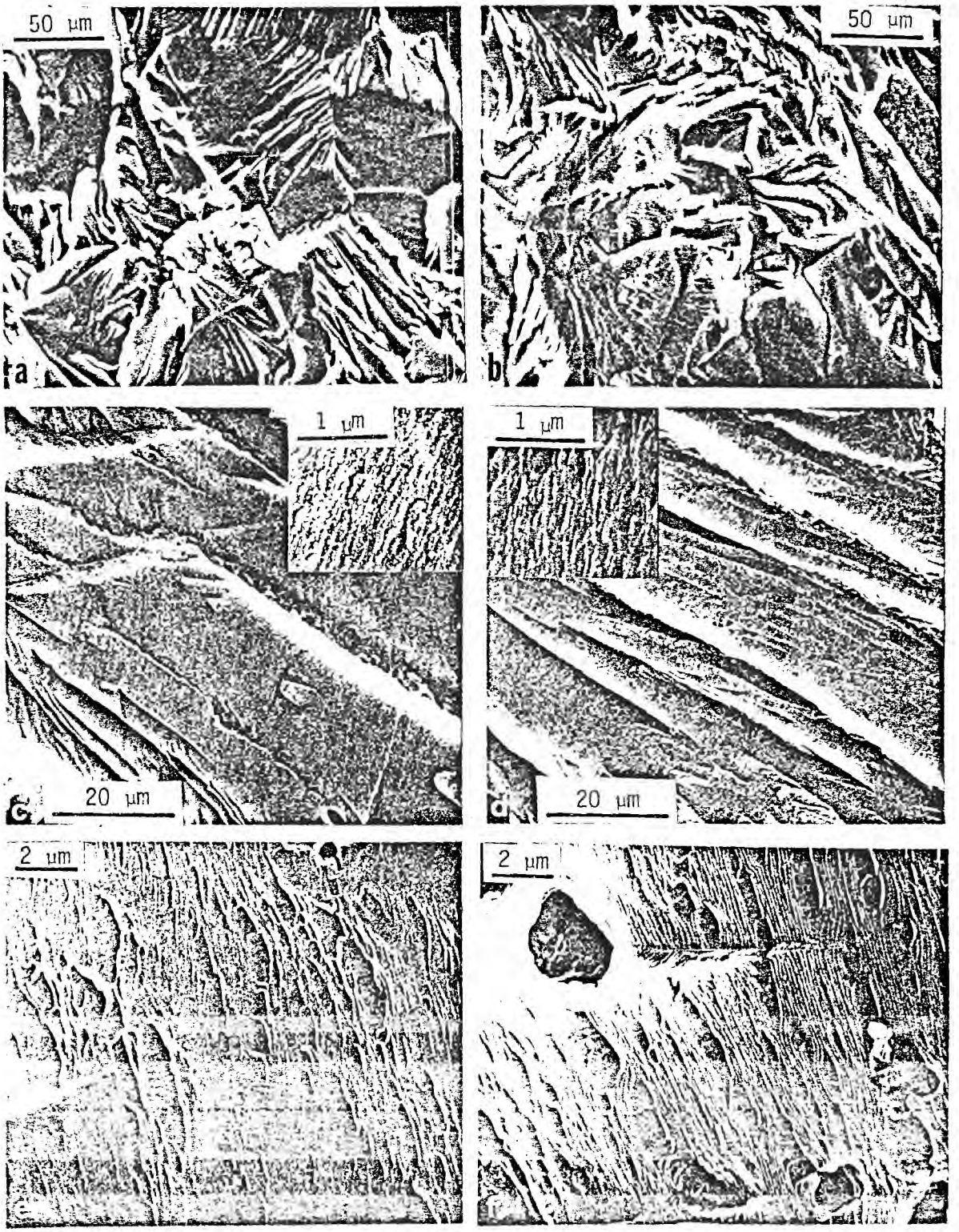

Figure 8. Comparison between the fractographic features of 24A and 24C alloys at various points on the FCGR curves. Figures a, b, c, d, e and f corresponds to the points a, b, c, d, e and f of Figure 6.

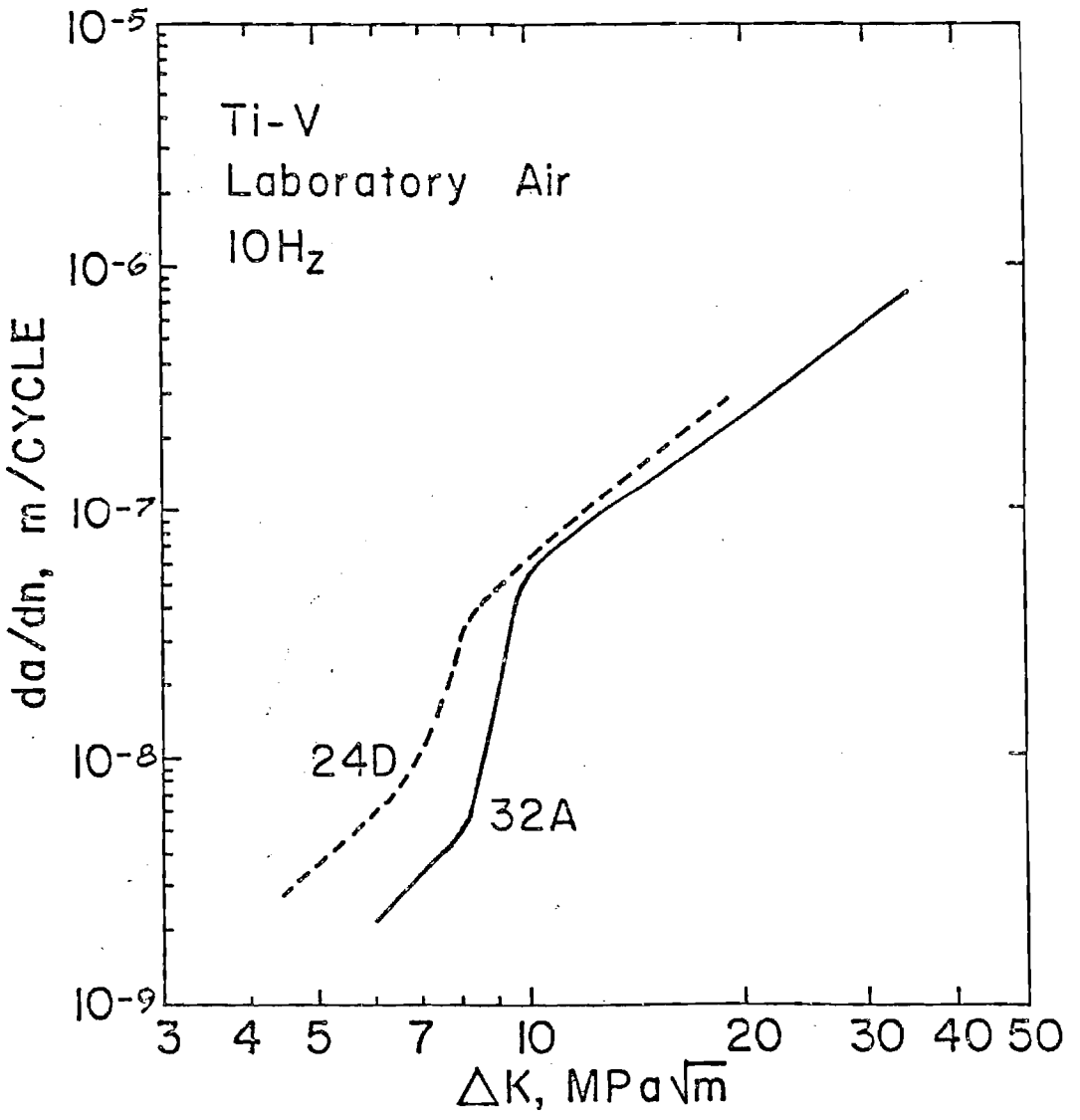

Figure 9. Fatigue crack growth rate versus stress intensity range curves for the 32A and 24D alloys.

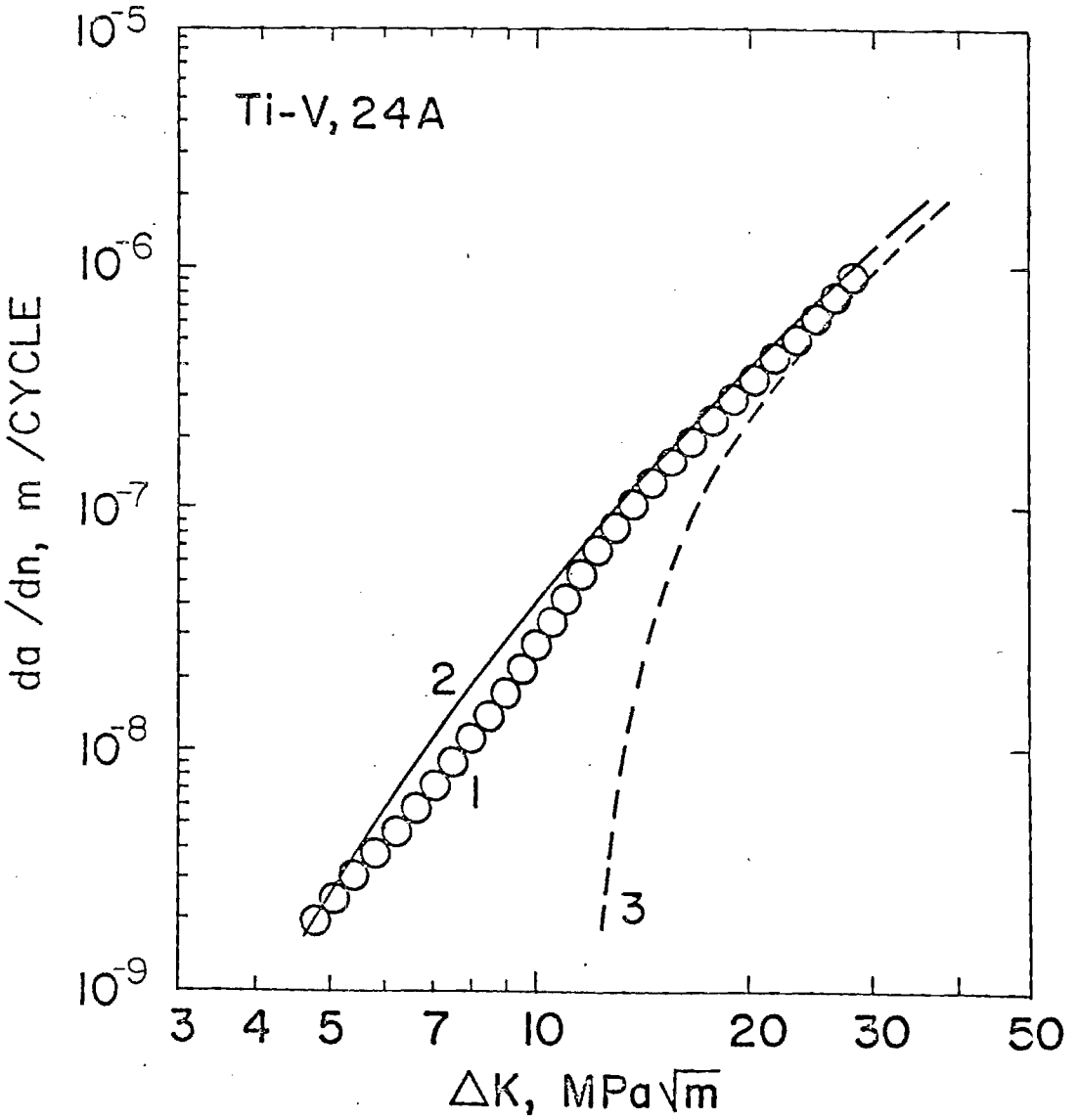

(a)

Figure 10. Comparison between the calculated and experimental fatigue crack growth rate versus stress intensity range curves; (1) Experimental curve, (2) calculated from equation 2, and (3) calculated from equation 1.
(a) for the 24A alloy (λ = 64μ)
(b) for the 24B alloy (λ = 30μ)
(c) for the 24C alloy (λ = 12μ)

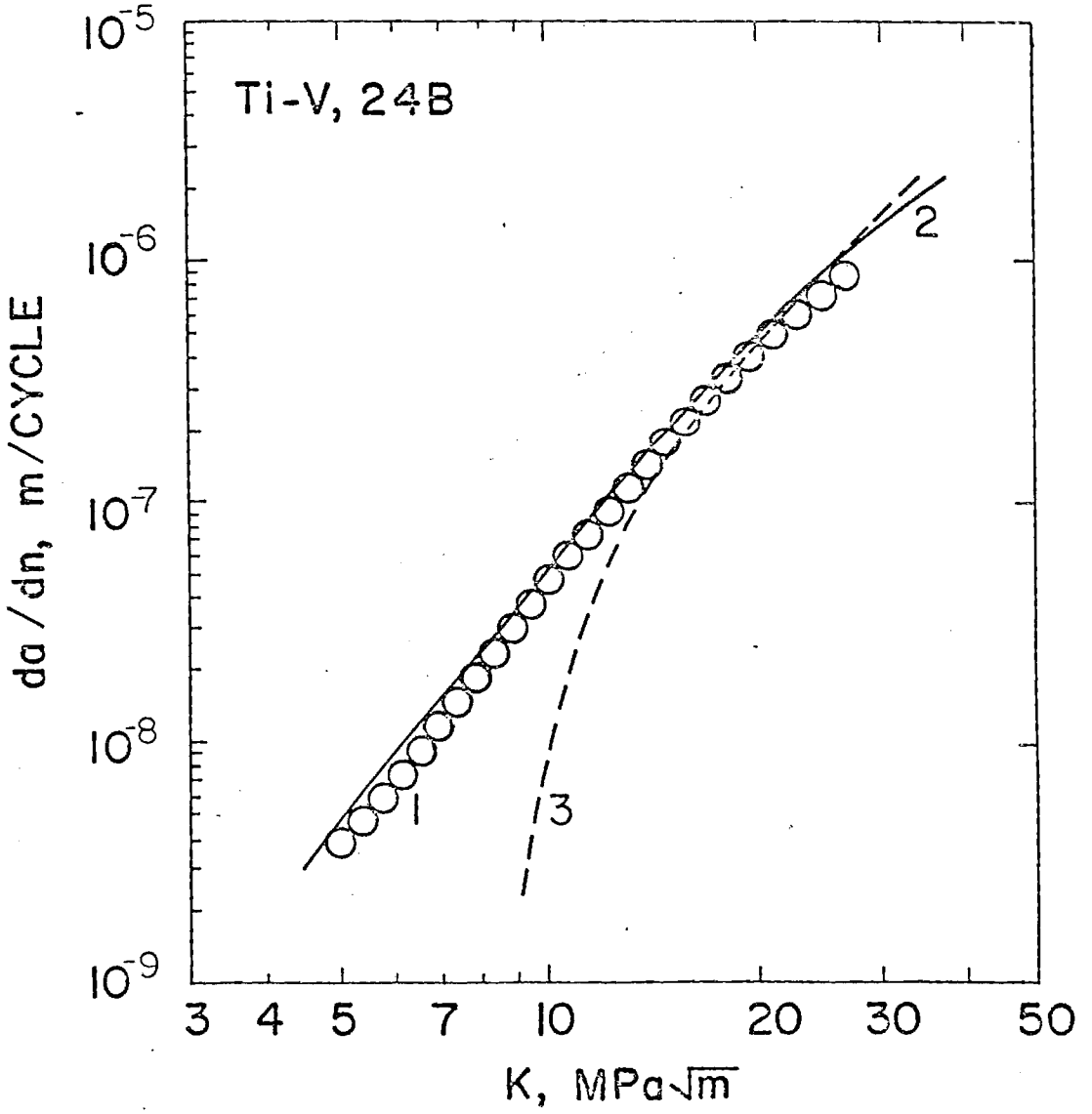
Ti-V, 24B
da/dn, m/CYCLE
K, MPa√m
10^-5
10^-6
10^-7
10^-8
10^-9
3
4
5
7
10
20
30
50
1
2
3

(b)

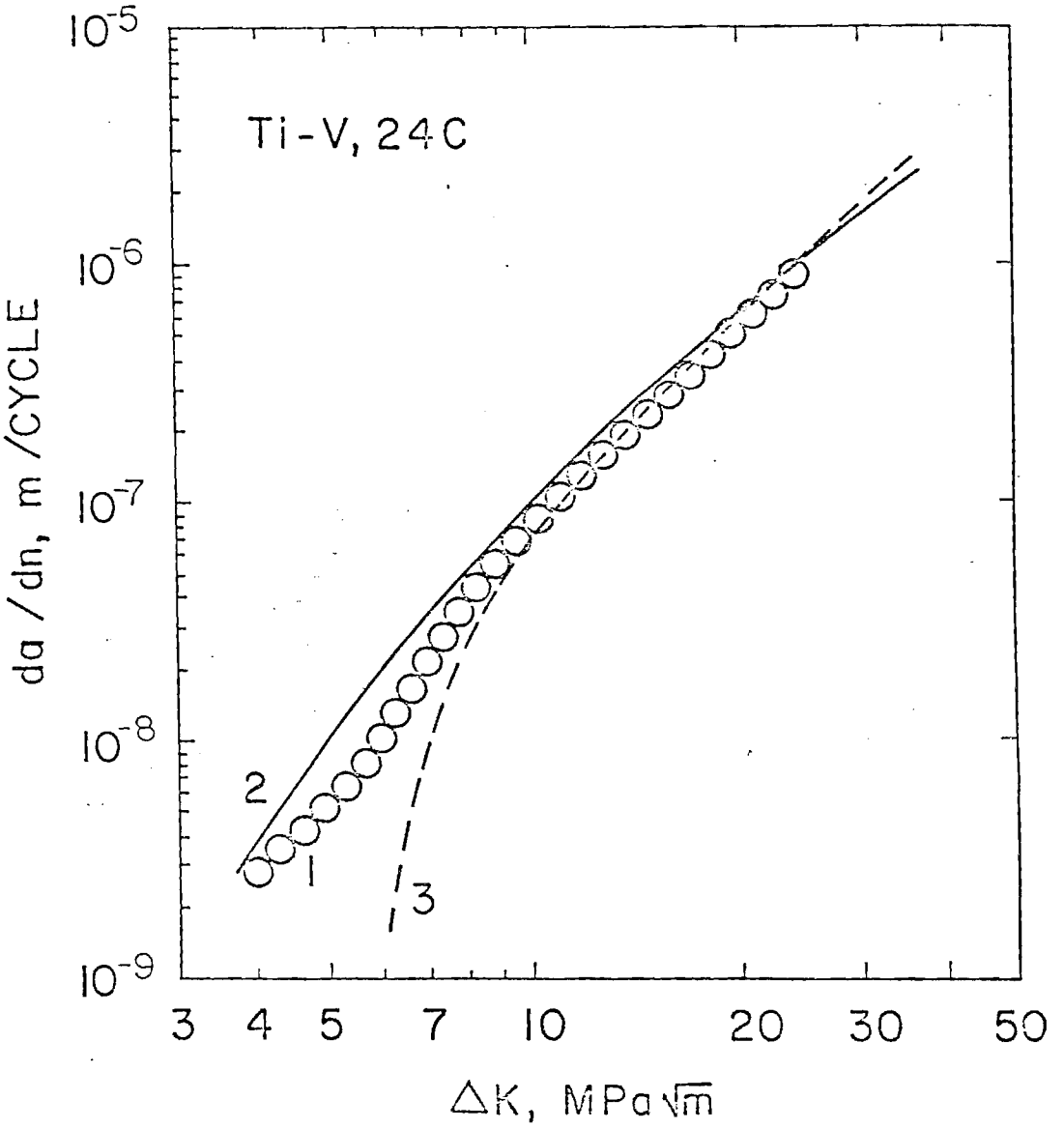
Ti-V, 24C
da / dn, m /CYCLE
ΔK, MPa√m
10-5
10-6
10-7
10-8
10-9
3
4
5
7
10
20
30
50
1
2
3

(c)

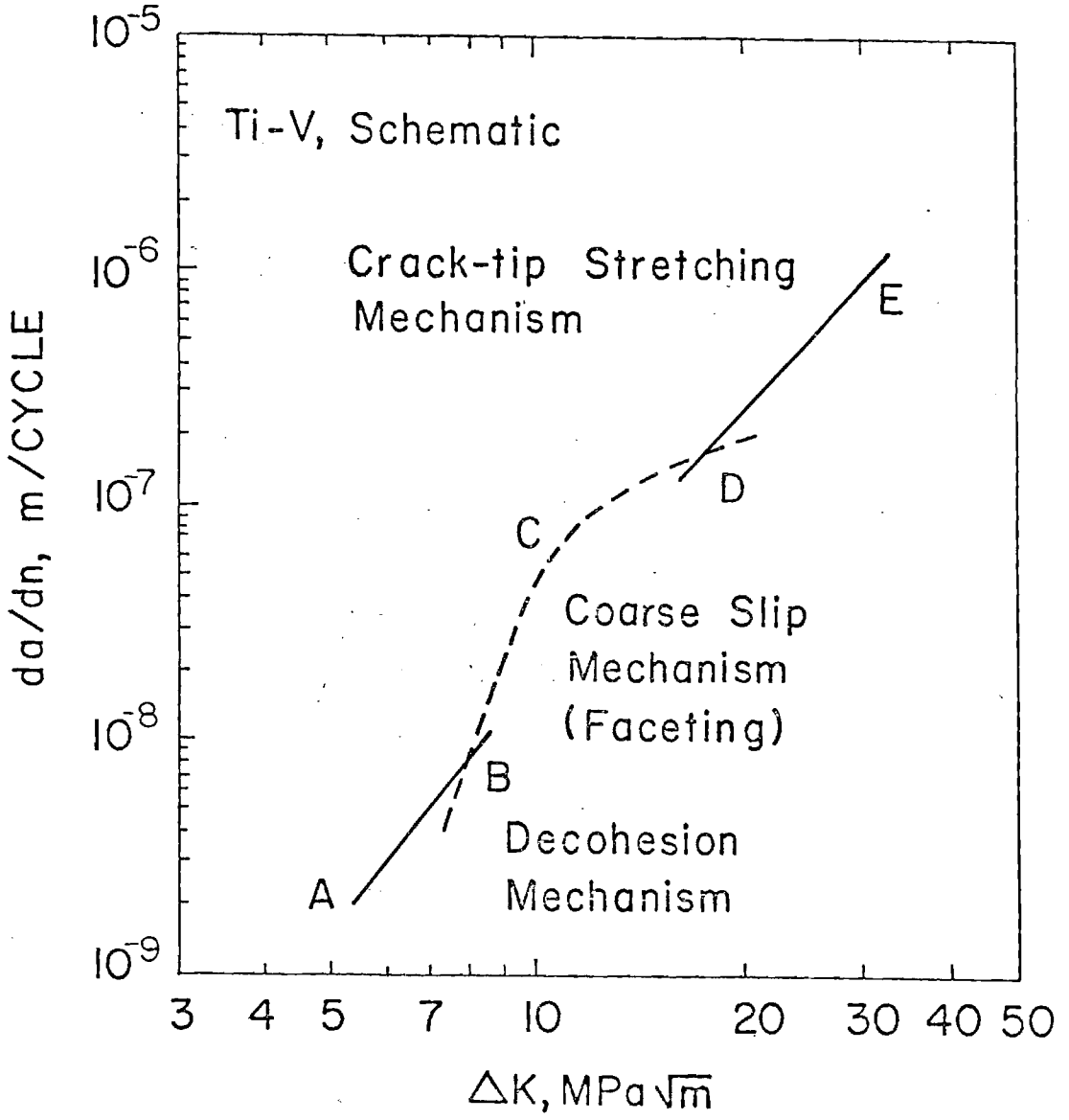

Figure 11: Schematic representation of the FCGR contributions from the three crack growth mechanisms for a typical beta Ti-V alloy.

SECURITY CLASSIFICATION OF THIS PAGE *(When Data Entered)*

REPORT DOCUMENTATION PAGE

READ INSTRUCTIONS BEFORE COMPLETING FORM

1. REPORT NUMBER: 78-3	2. GOVT ACCESSION NO.
3. RECIPIENT'S CATALOG NUMBER	
4. TITLE *(and Subtitle)*: Fatigue Crack Propagation of Metastable Beta Titanium-Vanadium Alloys	5. TYPE OF REPORT & PERIOD COVERED: Technical Report
	6. PERFORMING ORG. REPORT NUMBER
7. AUTHOR(s): Saghana B. Chakrabortty and Edgar A. Starke, Jr.	8. CONTRACT OR GRANT NUMBER(s): N00014-75-C-0349, NR 031-75
9. PERFORMING ORGANIZATION NAME AND ADDRESS: Fracture and Fatigue Research Laboratory, Georgia Institute of Technology, Atlanta, GA 30332	10. PROGRAM ELEMENT, PROJECT, TASK AREA & WORK UNIT NUMBERS
11. CONTROLLING OFFICE NAME AND ADDRESS: Metallurgy Program, Office of Naval Research, 800 North Quincy Street, Arlington, Virginia 22217	12. REPORT DATE: December 7, 1978
	13. NUMBER OF PAGES
14. MONITORING AGENCY NAME & ADDRESS *(if different from Controlling Office)*	15. SECURITY CLASS. *(of this report)*: Unclassified
	15a. DECLASSIFICATION/DOWNGRADING SCHEDULE

16. DISTRIBUTION STATEMENT *(of this Report)*

unlimited

17. DISTRIBUTION STATEMENT *(of the abstract entered in Block 20, if different from Report)*

18. SUPPLEMENTARY NOTES

19. KEY WORDS *(Continue on reverse side if necessary and identify by block number)*

titanium alloys
deformation
microstructure
fatigue

20. ABSTRACT *(Continue on reverse side if necessary and identify by block number)*

The fatigue crack propagation behavior of three titanium-vanadium alloys (24, 28 and 32 wt.% V) which have (tensile) deformation modes ranging from coarse twinning to wavy and planar slip has been measured in laboratory air and correla with their low cycle fatigue properties and microstructure. The fatigue crack growth rate of alloys with similar microstructures but different deformation modes, and of alloys with similar deformation modes but different microstructure have been compared. Increasing the deformation barrier mean free path and improving low cycle fatigue properties has been observed to reduce the fatigue

DD FORM 1 JAN 73 1473 EDITION OF 1 NOV 65 IS OBSOLETE

crack growth rate at low and intermediate ΔK levels. The fatigue crack growth data have been compared with that calculated from equations which use microstructure and low cycle fatigue parameters. The predictive capability of these equations which contain only measurable parameters has been found to be quite adequate.